2009-04-02

Role of molecular chaperones in G protein B5-Regulator of G protein signaling dimer assembly and G protein By dimer specificity

Alyson Cerny Howlett
Brigham Young University - Provo

ROLE OF MOLECULAR CHAPERONES IN G PROTEIN β5-REGULATOR OF G PROTEIN SIGNALING DIMER ASSEMBLY AND G PROTEIN βγ DIMER SPECIFICITY

by

Alyson Cerny Howlett

A dissertation submitted to the faculty of

Brigham Young University

In partial fulfillment of the requirements for the degree of

Doctor of Philosophy

Department of Chemistry and Biochemistry

Brigham Young University

August 2009

BRIGHAM YOUNG UNIVERSITY

GRADUATE COMMITTEE APPROVAL
of a dissertation submitted by
Alyson C. Howlett

This dissertation has been read by each member of the following graduate committee and by majority vote has been found to be satisfactory.

Date	Barry M. Willardson, Chair
Date	Steven W. Graves
Date	Craig D. Thulin
Date	Allen R. Buskirk
Date	Laura C. Bridgewater

BRIGHAM YOUNG UNIVERSITY

As chair of the candidate's graduate committee, I have read the dissertation of Alyson C. Howlett in its final form and have found that (1) its format, citation, and biographical style are consistent and acceptable and fulfill university and department style requirements; (2) its illustrative materials including figures, tables, and charts are in place; and (3) the final manuscript is satisfactory to the graduate committee and is ready for submission to the university library.

Date	Barry M. Willardson Chair, Graduate Committee

Accepted for the Department

Date	David V. Dearden Graduate Coordinator

Accepted for the College

Date	Thomas W. Sederberg Associate Dean College of Physical and Mathematical Science

ABSTRACT

ROLE OF MOLECULAR CHAPERONES IN

G PROTEIN β5-REGULATOR OF G PROTEIN SIGNALING DIMER

ASSEMBLY AND G PROTEIN βγ DIMER SPECIFICITY

Alyson C. Howlett

Department of Chemistry and Biochemistry

Doctor of Philosophy

In order for G protein signaling to occur, the G protein heterotrimer must be assembled from its nascent polypeptides. The most difficult step in this process is the formation of the Gβγ dimer from the free subunits since both are unstable in the absence of the other. Recent studies have shown that phosducin-like protein (PhLP1) works as a co-chaperone with the cytosolic chaperonin complex (CCT) to fold Gβ and mediate its interaction with Gγ. However, these studies did not address questions concerning the scope of PhLP1 and CCT-mediated Gβγ assembly, which are important questions given that there are four Gβs that form various dimers with 12 Gγs and a 5th Gβ that dimerizes with the four regulator of G protein signaling (RGS) proteins of the R7 family. The data presented in Chapter 2 shows that PhLP1 plays a vital role in the assembly of Gγ2 with all four Gβ1-4 subunits and in the assembly of Gβ2 with all twelve Gγ subunits, without affecting the specificity of the Gβγ

interactions. The results of Chapter 3 show that Gβ5-RGS7 assembly is dependent on CCT and PhLP1, but the apparent mechanism is different from that of Gβγ. PhLP1 seems to stabilize the interaction of Gβ5 with CCT until Gβ5 is folded, after which it is released to allow Gβ5 to interact with RGS7. These findings point to a general role for PhLP1 in the assembly of all Gβγ combinations, and suggest a CCT-dependent mechanism for Gβ5-RGS7 assembly that utilizes the co-chaperone activity of PhLP1 in a unique way.

Chapter 4 discusses PhLP2, a recently discovered essential protein, and member of the Pdc family that does not play a role in G protein signaling. Several studies have indicated that PhLP2 acts as a co-chaperone with CCT in the folding of actin, tubulin, and several cell cycle and pro-apoptotic proteins. In a proteomics screen for PhLP2A interacting partners, α-tubulin, 14-3-3, elongation factor 1α, and ribosomal protein L3 were found. Further proteomics studies indicated that PhLP2A is a phosphoprotein that is phosphorylated by CK2 at threonines 47 and 52.

ACKNOWLEDGEMENTS

I wish to acknowledge and thank everyone who contributed to this work. I am especially grateful for my advisor, Dr. Barry Willardson, and his willingness to lead me in this research. I am thankful to have worked with such an outstanding group of people in the Willardson lab, and particularly Amy J. Gray, who contributed directly to this work. I owe deep gratitude to my family and my husband, John D. Howlett, for their love and support. I could not have accomplished this goal without the opportunity granted by the Department of Chemistry and Biochemistry and Brigham Young University. And finally, I am thankful to our Heavenly Father for His abundant blessings and constant care during these years of study.

TABLE OF CONTENTS

LIST OF FIGURES AND TABLES

ABBREVIATIONS

C-	Carboxy-terminus
CCT	Chaperonin containing tailless complex polypeptide 1
DEP	Disheveled, Egl-10, pleckstrin
DRiP78	Dopamine receptor-interacting protein 78
eEF1α	Eukaryotic elongation factor 1α
eEF2	Eukaryotic elongation factor 2
EF-Tu	Elongation factor Tu
G	Heterotrimeric GTP binding protein
GAP	GTPase accelerating protein
GDP	Guanosine diphosphate
GGL	Gγ-like
GPCR	G-protein coupled receptor
GTP	Guanosine triphosphate
Gα	G-protein alpha subunit
Gβ	G-protein beta subunit
Gβγ	G-protein beta and gamma subunit dimer
Gγ	G-protein gamma subunit
HA	Hemagglutinin
HEK-293T cells	Human embryonic kidney 293 cells
LCMSMS	Liquid chromatography coupled to tandem mass spectrometry
MS	Mass spectrometry
MSMS	Tandem mass spectrometry
N-	Amino-terminus
PCR	Polymerase chain reaction
Pdc	Phosducin
PhLP1	Phosducin-like protein 1
PhLP 2A	Phosducin-like protein 2A
PhLP 2B	Phosducin-like protein 2B
PhLP 3	Phosducin-like protein 3
PSI	Phosphorylation site identification
R7BP	R7 binding protein
R9AP	R9 anchoring protein
RGS	Regulator of G protein signaling
siRNA	Short interfering RNA

CHAPTER 1 INTRODUCTION:

FUNCTION OF PHOSDUCIN-LIKE PROTEINS IN G PROTEIN SIGNALING AND CHAPERONE-ASSISTED PROTEIN FOLDING

Summary

Members of the phosducin (Pdc) gene family were initially proposed to act as down-regulators of G protein signaling by binding G protein βγ dimers (Gβγ) and inhibiting their ability to interact with G protein α subunits (Gα) and effectors. However, recent findings have over-turned this hypothesis by showing that most members of the phosducin family act as co-chaperones with the cytosolic chaperonin complex (CCT) to assist in the folding of a variety of proteins from their nascent polypeptides. In fact, rather than inhibiting G protein pathways, phosducin-like protein 1 (PhLP1) has been shown to be essential for G protein signaling by catalyzing the folding and assembly of the Gβγ dimer. PhLP2 and PhLP3 have no role in G protein signaling, but they appear to assist in the folding of proteins essential in regulating cell cycle progression as well as actin and tubulin. Phosducin itself is the only family member that does not participate with CCT in protein folding, but it is believed to have a specific role in visual signal transduction to chaperone Gβγ subunits as they translocate to and from the outer and inner segments of photoreceptor cells during light-adaptation.

Introduction

Eukaryotic cells use G protein signaling systems to mediate a wide array of hormonal, neuronal and sensory signals that control numerous physiological processes ranging from cardiac rhythm (*1*) to psychological behavior (*2*) to vision (*3*). The importance of G protein signaling to cellular physiology is evidenced by the large number of genes encoding GPCRs (~800 in humans (*4*)) and the myriad diseases linked to malfunctions in G protein signaling (*5*). In fact, more than half of all currently prescribed pharmaceuticals target GPCRs and other G protein pathway components (*6*). Consequently, the mechanisms by which G protein signals are propagated has been described in molecular detail (*7*). Signaling is initiated by the binding of a ligand to the extracellular face of a GPCR, resulting in a change in the packing of the seven transmembrane α-helices found in all GPCRs. This conformational change activates the G protein on the intracellular surface of the receptor by initiating an exchange of GDP for GTP on the G protein α subunit (Gα). GTP binding causes Gα to dissociate from the G protein βγ subunit complex (Gβγ). Both Gα-GTP and Gβγ control the activity of effector enzymes such as adenylyl cyclase, cGMP phosphodiesterase, phospholipase Cβ, phosphatidylinositol-3-kinase, Rho guanine nucleotide exchange factors, as well as K^+ and Ca^{2+} ion channels. These effectors regulate the intracellular concentration of second messengers (cyclic nucleotides, inositol phosphates and Ca^{2+}), the actin cytoskeleton (via Rho-GTP) and the plasma membrane electrical potential (via K^+ channels), thereby orchestrating the cellular response to the stimulus.

Controlling such responses is vital to the cell. Hence, G protein pathways are exquisitely regulated and regulatory targets are found at multiple levels within the cascade. At the level of the GPCR, the ability of agonist-bound receptors to activate G proteins is blocked by phosphorylation, arrestin binding and internalization (*2*). Interestingly, this deactivation step with respect to the G protein results in initiation of a β-arrestin signaling pathway that leads to activation of mitogen-activated protein kinase (MAPK) cascades (*9*). At the level of Gα, the lifetime of many Gα-GTP isoforms is decreased by acceleration of GTP hydrolysis by regulators of G protein signaling (RGS) proteins and certain effectors such as phospholipase Cβ (*10*). These GTPase accelerating proteins (GAPs) play a vital role in determining the lifetime of the G protein signal (*11*). At the level

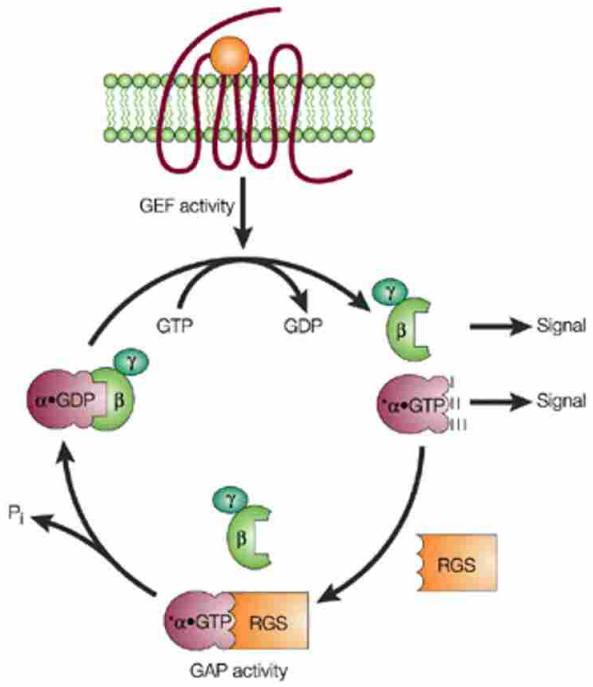

Figure 1-1. Overview of G protein signaling.
Once a ligand binds and activates a GPCR, the GPCR acts as a guanine-nucleotide exchange factor (GEF) for Gα which exchanges GDP for GTP. GTP-bound Gα dissociates from Gβγ and each moiety is free to bind and control the activity of effector enzymes and ion channels. RGS proteins act as GTPase accelerating proteins (GAPs) to greatly accelerate Gα-GTP hydrolysis back to Gα-GDP which associates with Gβγ. Gαβγ can again bind to a GPCR, and if the GPCR is active, undergo another round of signaling. Reprinted by permission from Macmillan Publishers Ltd: [Nat Rev Drug Discov], (*8*) copyright (2002). http://www.nature.com

of Gβγ, the binding of Pdc (*12-15*) and PhLP1 (*16, 17*) to Gβγ has been proposed to control the amount of Gβγ available for interaction with effectors or with Gα-GDP. However, this Gβγ sequestration model for Pdc and PhLP1 function has been brought into serious question by recent findings (*18-20*). This introductory chapter will focus on current understanding of the role of PhLP1 in Gβγ signaling and on the possible functions of the other Pdc family members, PhLP2 and PhLP3.

The Pdc protein family appears to have ancient origins in that its members are widely expressed in organisms varying from yeast to plants to man. The family can be divided into three subgroups (*21*). Subgroup I includes the initial members of the family, Pdc and PhLP1, which have been shown to bind Gβγ subunits with high affinity (*13, 22, 23*). Pdc expression is very restricted, being found at significant levels in only the photoreceptor cells of the retina and in the pineal gland (*13, 24*). This expression pattern suggests a specific role for Pdc in light signaling. In contrast, PhLP1 is broadly expressed in most tissues and cell types (*25, 26*), indicating a more general function. Subgroup II consists of two recently discovered proteins in humans, identified as PhLP2A and PhLP2B (*21, 27, 28*). The yeast ortholog of PhLP2 lacks Gβγ binding ability, but is essential for cell growth in both the yeast *Saccharomyces cerevisiae* (*29*) and the soil amoeba *Dictyostelium discoideum* (*21*), indicating a vital function that is independent of G protein signaling. Subgroup III consists of a single protein, designated PhLP3 (*21*). Again, the yeast ortholog of PhLP3 binds Gβγ poorly (*29*), but its genetic deletion has no obvious phenotype in yeast (*29*) or *Dictyostelium* (*21*). Closer analyses suggest that PhLP3 may participate in actin and β-tubulin folding (*30, 31*). At first glance, these data portray the Pdc protein family

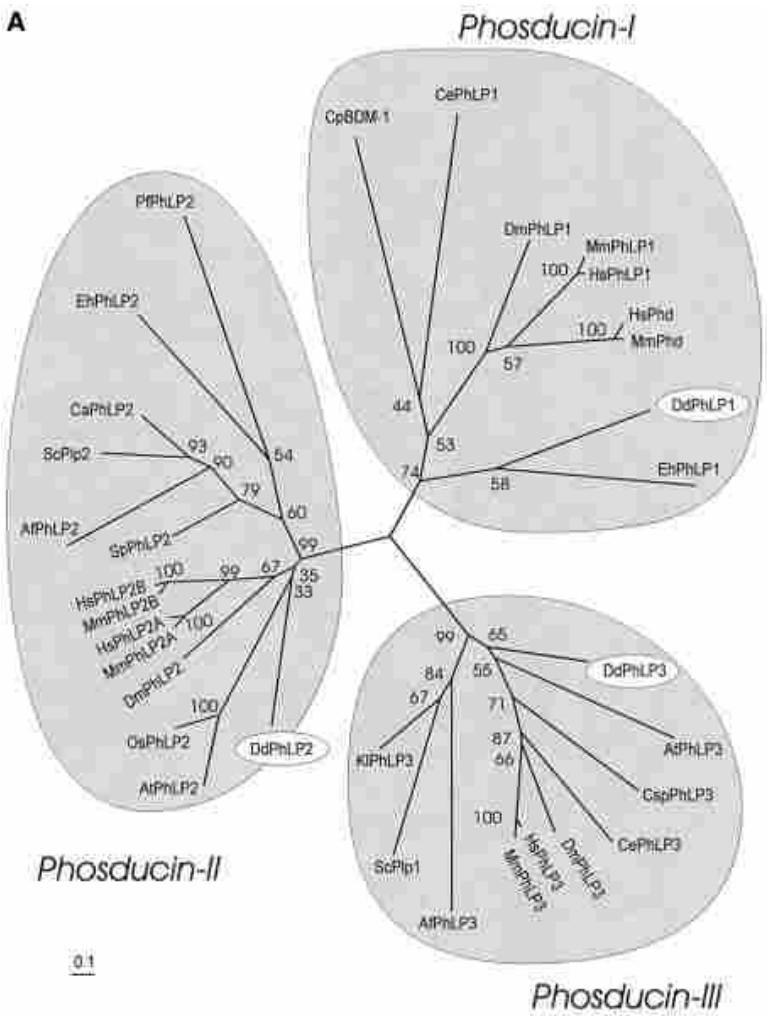

Figure 1-2. The Pdc family phylogenetic tree.
The phosducin family contains three subfamilies. Protein sequences of 33 phosducin homologues were obtained from different organisms. These sequences were aligned then used as input for the Phylip program to create the tree. The numbers indicate bootstrap values. Reprinted by permission from Macmillan Publishers Ltd: [EMBO J], (*21*) copyright 2003. http://www.nature.com/emboj

as one with just a few members whose physiological roles are very diverse, having apparently no single unifying cellular function. However, a common theme appears to be emerging from recent findings which indicate that PhLPs 1-3 may all act as co-chaperones in protein folding while Pdc may have a unique role in Gβγ signaling in photoreceptor cells.

The Physiological Function of PhLP1

Initial hypothesis — PhLP1 as a general inhibitor of G protein signaling

A close homolog of Pdc was discovered in a screen for genes whose expression was induced by ethanol in neuronal cell cultures (*25*). This protein displayed 65% sequence homology to Pdc and was consequently given the name of phosducin-like protein (PhLP) (*25*). Pdc and PhLP make up subgroup I of the Pdc protein family (*21*), and therefore PhLP will be referred to here as PhLP1 to distinguish it from subgroup II and III family members. PhLP1 contains an 11 amino acid sequence corresponding to Helix 1 of Pdc that is perfectly conserved (*25*). In Pdc, this sequence of Helix 1 is a major site of interaction with $G_t\beta\gamma$ (*32*). Accordingly, PhLP1 was shown to bind $G\beta\gamma$ with similar affinity to Pdc (*22*) and to block interactions of $G\beta\gamma$ with $G\alpha$ and GRK2 *in vitro* (*23, 33*). As with Pdc, over-expression of PhLP1 inhibited G protein signaling (*17*), but unlike Pdc, PhLP1 displayed a broad expression pattern, being found in significant levels in most tissues (*25, 26, 34*). These findings led to the hypothesis that it was PhLP1, and not Pdc, that was the general down-regulator of G protein signaling through $G\beta\gamma$ sequestration.

Since these initial observations, several inconsistencies with a PhLP1-mediated $G\beta\gamma$ sequestration hypothesis have been observed. First, the expression levels of PhLP1 were significantly less than those of $G\beta\gamma$ (*26*) and had to be increased to well above endogenous levels to begin to inhibit G protein signaling (*17*), raising questions about the ability of endogenous PhLP1 to sequester much of the $G\beta\gamma$ pool in the cell. This moderate expression level of PhLP1 is in contrast to the high expression level of Pdc in photoreceptors, which matches that of $G\beta\gamma$ (*20, 35*) and

provides sufficient Pdc to bind a large fraction of the Gβγ to exert a major effect on its subcellular localization and signaling. Second, PhLP1 binding to Gβγ was not regulated by phosphorylation (*35, 36*), suggesting that the interaction is more constitutive in nature and less dependent on a phosphorylation-dependent feedback loop like that of Pdc. Third, deletion of the *phlp1* gene in the chestnut blight fungus *Cryphonectria parasitica* (*37*) and in *Dictyostelium discoideum* (*21*) yielded the same phenotypes as deletion of the Gβ gene, the opposite result of that expected if PhLP1 where a negative regulator of G protein signaling. Moreover, G protein signaling in *Dictyostelium* was abolished by the deletion of *phlp1*, confirming a requirement for PhLP1 in G protein function (*21*). Fourth, antisense oligonucleotide-mediated knockdown of PhLP1 in mouse brain significantly prolonged the period of desensitization induced by both acute and chronic expose to morphine (*34*), again suggesting that PhLP1 was not an inhibitor of G protein signaling but rather a promoter of both short and long-term responses to agonists. These inconsistencies raised doubts about the sequestration hypothesis and led to the search for other possible functions of PhLP1.

Overturning the paradigm — PhLP1 as an essential co-chaperone in Gβγ assembly

Clues about other functions of PhLP1 came from a proteomics screen for PhLP1 binding partners in which a high affinity interaction of PhLP1 with the cytosolic chaperonin complex (CCT) was discovered (*38*). This interaction was later confirmed in yeast protein–protein interaction screens (*39, 40*). Interestingly, unlike PhLP1, Pdc does not share the ability to bind CCT (*38*). CCT is an essential chaperone of protein folding found in the cytosol of eukaryotic cells (*41, 42*). It

consists of eight different, but related, subunits of ~60 kDa packed together to form a ring structure (*43*). Two identical rings stack on top of each other to form the holo-CCT complex of sixteen subunits (*43*). Nascent polypeptides and denatured proteins associate in a large cavity formed in the center of each eight-membered ring (*43*). Amino acid residues within the ring make contacts with the unfolded protein and decrease the activation energy required to form the three-dimensional structure of the native protein (*44*). Each CCT subunit binds ATP and uses the energy of ATP hydrolysis to drive the folding process (*45, 46*). Actin and tubulin are major cellular proteins that require CCT to fold, but other substrates have been described. In fact, it has been estimated that 5-15% of cellular proteins are assisted in their folding by CCT (*47, 48*). Among the known substrates of CCT are Gα (*49*) and several proteins with seven β-propeller WD40 structures similar to that of Gβ (*42, 50, 51*). PhLP1 did not bind CCT as a folding substrate, but rather it interacted in its native form, suggesting a regulatory role for PhLP1 in CCT-dependent folding (*38*).

Important insight into the function of the PhLP1-CCT interaction has come from the structure of the complex determined by cryo-electron microscopy (cryo-EM) (*52*). Unlike folding substrates such as actin and tubulin which bind CCT within the folding cavity, PhLP1 bound above the cavity, making contacts with only the tips of the apical domains of the CCT subunits. PhLP1 spanned the folding cavity and constricted the apical domains, effectively occluding the cavity. In many respects, this structure is similar to that of CCT bound to prefoldin, a co-chaperone that delivers actin and tubulin to CCT for folding (*53*). These substrates occupy the folding cavity while prefoldin sits above the cavity with protrusions into the cavity

(*53*). Together, these observations suggested that PhLP1 may act as a co-chaperone for the folding of Gβ subunits by stabilizing an interaction between Gβ, Gγ and CCT until the Gβγ reaches its native state. This idea was consistent with the observation that when *phlp1* was deleted in *Dictyostelium*, Gβ and Gγ no longer associated with the plasma membrane, but exhibited a cytosolic localization that would be expected if the subunits did not associate (*21*).

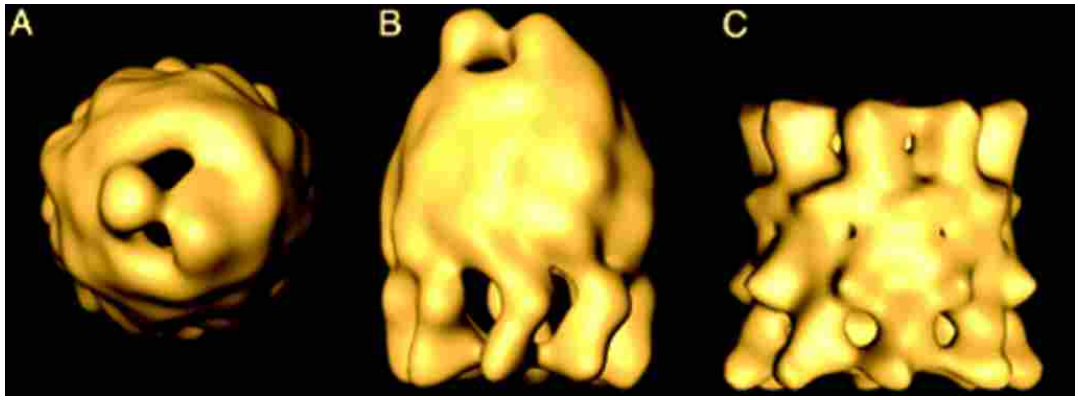

Figure 1-3. Cryo-EM structures of the PhLP1-CCT and apo-CCT complexes. A. Top view of the PhLP1-CCT complex made by cryo-EM and 3-D reconstruction. B. Side view of the PhLP1-CCT complex. C. Side view of apo-CCT. Reproduced with permission from *Proceedings of the National Academy of Sciences USA,* (*52*) copyright 2004. http://www.pnas.org

These findings set the stage for studies that directly measured the role for PhLP1 and CCT in the folding and assembly of Gβγ (*18, 19, 36, 54, 55*). In one such study, siRNA-mediated depletion of PhLP1 in mammalian cells resulted in a significant decrease in Gβ1 expression that led to a corresponding decrease in G protein signaling without affecting Gβ1 mRNA levels (*19*). Pulse-chase experiments measuring Gβ1γ2 assembly in these cells showed that the rate of assembly decreased by five-fold when the cells were depleted of 90% of their PhLP1 and increased by four-fold when PhLP1 was over-expressed (*19*). These results demonstrated that the decrease in Gβ1 expression and G protein signaling upon PhLP1 depletion was

caused by an inability to form Gβγ dimers. Similar data were obtained when the PhLP1 gene was deleted in *Dictyostelium*; cells were completely devoid of Gβγ dimers (*54*). CCT was also strongly implicated in the Gβγ assembly process by the observation that nascent Gβs bound to CCT in translation assays *in vitro* (*55*). Moreover, addition of Gγ subunits significantly decreased Gβ binding to CCT while increasing Gβ binding to Gγ in an ATP-dependent manner (*55*). Together, these observations indicated that PhLP1 and CCT were somehow acting as co-chaperones in the folding and assembly of the Gβγ dimer.

In order to catalyze Gβγ dimer formation, PhLP1 must be phosphorylated by the protein kinase CK2 within a cluster of three consecutive serines at residues 18-20 (S18-20) (*19*). Initially, it was reported that PhLP1 was phosphorylated by CK2 within the S18-20 cluster and that an S18-20A alanine substitution variant was more effective at inhibiting Gβγ signaling than wild-type PhLP1 (*56*). However, it was unclear why the PhLP1 S18-20A variant was a better inhibitor given that CK2 phosphorylation of PhLP1 did not change its binding affinity for Gβγ (*36*). Subsequently, the PhLP1 S18-20A variant was shown to block Gβγ assembly in a striking manner (*19*). Over-expression of PhLP1 S18-20A in HEK-293 cells decreased the rate of assembly by 15-fold compared to wildtype PhLP1 and by 4-fold compared to an empty vector control (*19*). Thus, not only did PhLP1 S18-20A not support Gβγ dimer formation, it was also able to block the ability of endogenous PhLP1 to catalyze assembly in a dominant negative manner. Measuring the effects of various serine to alanine substitutions within the S18-20 sequence on the rate of Gβγ assembly led to the conclusion that at least two of the three serines must be

phosphorylated in order for PhLP1 to effectively support assembly, with S20 phosphorylation being the most important (*36*).

A useful tool in understanding PhLP1-mediated Gβγ assembly was discovered when an N-terminal 75 amino acids truncation of PhLP1 (PhLP1 Δ1-75) was found to be an even more effective dominant negative inhibitor than PhLP1 S18-20A (*19*). Over-expression of PhLP1 Δ1-75 completely blocks the Gβγ assembly process in HEK-293 cells (*19*). This variant lacks both the S18-20 phosphorylation site as well as the conserved Gβγ binding region corresponding to Helix 1 of Pdc. As a result, PhLP1 Δ1-75 could not be phosphorylated and bound Gβγ poorly, yet it maintained its full CCT binding capacity (*19*). Interestingly, the PhLP1 Δ1-75 variant is very similar to a naturally occurring PhLP1 truncation (designated PhLP1s) that is missing the N-terminal 83 amino acids due to alternative mRNA splicing (*25, 56*). When over-expressed, PhLP1s blocked Gβ and Gγ expression and strongly inhibited Gβγ signaling (*18, 56*), as would be predicted by the effects of PhLP1 Δ1-75 on Gβγ assembly.

The data presented thus far establish the need for PhLP1 and CCT in Gβγ dimer formation, but they give little insight into the mechanism by which this process occurs. The cryo-EM structure of PhLP1-CCT suggested that PhLP1 might stabilize the binding of nascent Gβ to CCT by forming a ternary complex with Gβ positioned in the CCT folding cavity and PhLP1 sitting above the cavity (*52*). Contrary to this prediction, overexpression of PhLP1 was found not to increase but rather to decrease the binding of Gβ to CCT (*36*). However, overexpression of the PhLP1 S18-20A and Δ1-75 variants resulted in a large increase in Gβ binding to CCT, indicating that

when PhLP1 is not phosphorylated, a stable PhLP1-Gβ-CCT ternary complex is formed (*36*). Thus, it appears that PhLP1 phosphorylation destabilizes the ternary complex. This idea is supported by the fact that the rate of release of nascent Gβ from CCT was accelerated by PhLP1 but was inhibited by PhLP1 S18-20A (*36*). The inability of PhLP1 S18-20 and Δ1-75 variants to release Gβ from CCT explains their dominant negative effect on Gβγ assembly. These variants would compete with endogenous PhLP1 for binding the Gβ-CCT complex by forming stable ternary complexes that would not release Gβ.

The mechanism of Gβ release may involve steric repulsion between the phosphates in the S18-20 cluster and negatively charged residues on the apical domains of CCT. This repulsion would cause the dissociation of a phosphorylated PhLP-Gβ intermediate that would subsequently associate with Gγ. Support for a PhLP-Gβ intermediate comes from several observations. First, complexes of nascent PhLP1 and Gβ were found that do not contain Gγ (*19*). Second, Gγ did not accelerate the rate of Gβ release from CCT beyond that observed in the presence of PhLP1 (*36*). Third, Gγ did not interact with CCT either directly or in a complex with Gβ (*36, 55*). Interestingly, a separate chaperone for Gγ has very recently been reported to be DRiP78, an ER membrane protein of the Hsp40 chaperone family that participates in GPCR trafficking (*57*). PhLP1 was also shown to interact with DRiP78, suggesting that the PhLP1-Gβ complex may interact with Gγ-bound DRiP78 to facilitate Gβγ dimer formation (*57*). From these observations, a mechanistic model of Gβγ assembly can be proposed as depicted in Fig. 1-4. PhLP1 plays a central role in this model by releasing nascent Gβ from CCT in a PhLP1-Gβ complex that then picks up

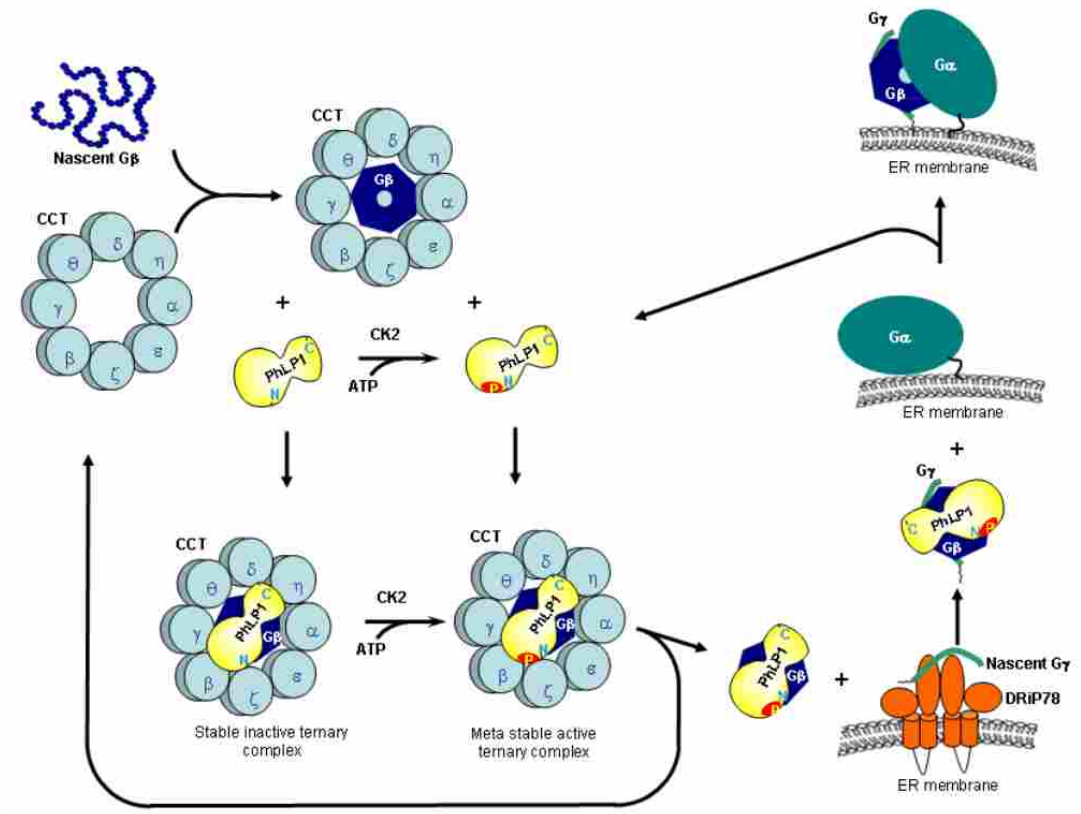

Figure 1-4. Model of PhLP1-mediated Gβγ dimer assembly.
Nascent Gβ binds CCT within the folding cavity and PhLP1 associates above Gβ, forming a ternary complex. If PhLP1 is not phosphorylated within the S18-20 sequence by CK2, the ternary complex is stable and inactive in Gβγ assembly. If PhLP1 is phosphorylated at this site, then a PhLP1-Gβ complex is released from CCT and interacts with Gγ bound to DriP78, forming the Gβγ dimer. PhLP1 is released when Gβγ associates with Gα and the ER membrane, and the G protein heterotrimer is then trafficked to the plasma membrane. PhLP1 is then free to catalyze another round of Gβγ assembly.

nascent Gγ from DRiP78 to form the Gβγ dimer at the ER membrane. Subsequent association of Gα with Gβγ on the membrane would release PhLP1 for additional rounds of dimer formation.

The Emerging Roles of Other Pdc Family Members

Other members of the Pdc family were first identified in a search for Pdc-like proteins in yeast (*29*). They were originally named Plp1 and Plp2, but later

phylogenetic analysis placed Plp1 in subgroup III and Plp2 in subgroup II of the Pdc family, so the current convention is to refer to group II subfamily members as PhLP2 and group III members as PhLP3 (*21*). There is a high degree of sequence homology between all Pdc family members in the C-terminal ~150 amino acids (Fig. 1-5), indicating that all probably retain the thioredoxin fold of the C-terminal domain of Pdc. In contrast, their N-terminal regions differ significantly (*21, 29*). The N-terminal domains of Pdc and PhLP1 both contain a conserved 11-amino acid sequence of Helix 1 which is imperative in binding Gβγ, while PhLP2 and PhLP3 do not have this sequence and they bind Gβγ poorly (Fig. 1-5) (*29*). PhLPs 1-3 all contain an acidic sequence in the loop between Helix 2 and 3 of the Pdc structure that is not well conserved in Pdc (*21*). This acidic region has been shown to play an important role in the binding of PhLP1 to CCT (*19, 52*), and accordingly, PhLPs 1-3 all bind CCT while Pdc does not (*31, 38, 58*). Apart from this loop and the Helix 3 region that follows, there is very little homology in the N-terminal domain between Pdc subfamily members (*21*). PhLP2 and PhLP3 are believed to bind CCT in a manner analogous to PhLP1, as native binding partners and regulators of CCT and not as nascent folding substrates (*31, 38, 58*). These findings suggest that PhLP2 and PhLP3 might function like PhLP1 as co-chaperones with CCT in protein folding.

PhLP2 — an essential gene involved in CCT-dependent protein folding

Phlp2 genes have been found in many eukaryotic genomes including human, mouse, zebrafish, and fly and have been shown to have an essential function in *D. discoideum* and *S. cerevisiae* (*21, 29*). Deletion of the *phlp2* gene in yeast yielded spore products that failed to grow (*29*), while disruption of *phlp2* in *Dictyostelium* led

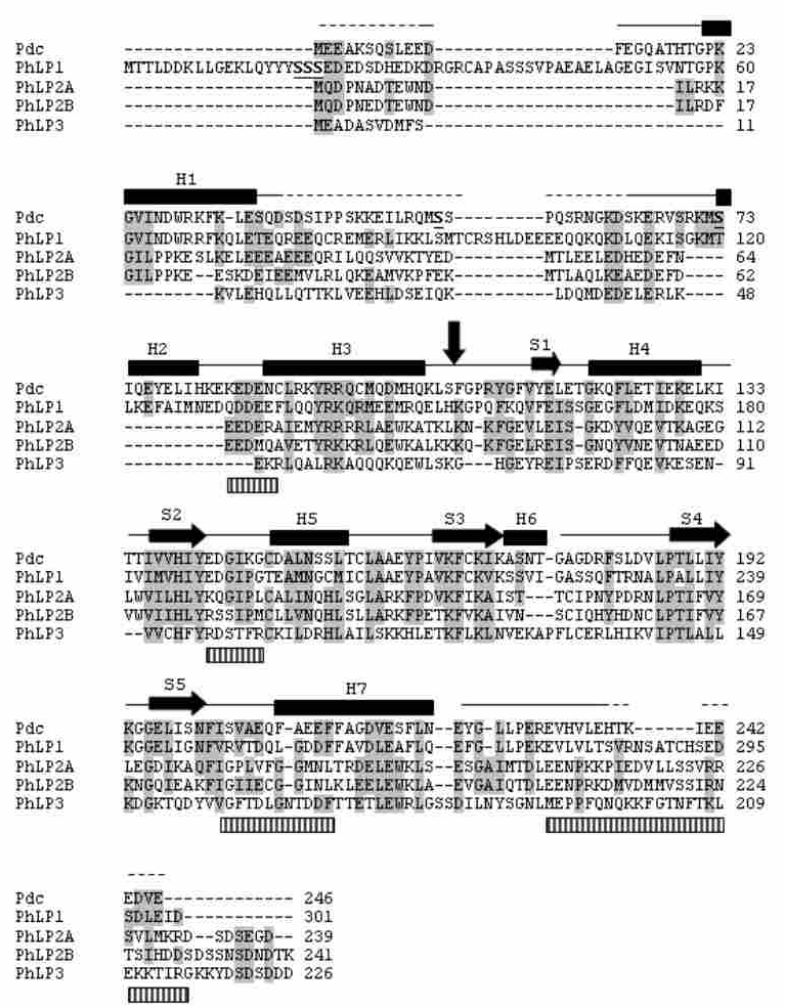

Figure 1-5. Sequence alignment of Pdc family members.
Sequences of the five human Pdc family members were aligned using CLUSTAL W. Regions of homology between sequences are shaded and gaps are represented by dashes. The structural division between the N-terminal domain and the thioredoxin-like C-terminal domain is indicated by the arrow pointing downward, and the secondary structural components of Pdc are indicated above the sequence (bar = helix, arrow = β-sheet, line = loop, dashed line = unstructured region) (*32*). Sites of interaction of PhLP1 with CCT as determined by cryo-EM and mutagenesis are indicated below the sequence (lined bars) (*52*). The S18-20 CK2 phosphorylation site of PhLP1 is in bold and underlined as are the S54 CaMK and S73 PKA phosphorylation sites of Pdc.

to a decreasing growth rate and simultaneous collapse of the cell culture after 16–17 cell divisions (*21*). The essential function of PhLP2 appears to be separate and unrelated to Gβγ signaling as indicated by the lack of effect of PhLP2 and PhLP3 over-expression or *phlp3* deletion on the Gβγ-dependent mating pheromone response

in yeast (*29*). Furthermore, yeast temperature sensitive *phlp2* mutants show no change in sensitivity of their pheromone response at restrictive temperatures (*58*). In humans and mice there are two *phlp2* genes designated as *phlp2A* and *phlp2B* (*21*). These two genes share 57% sequence homology, but differ in expression patterns (*28*). PhLP2A is a broadly-expressed cytosolic phosphoprotein (*28*), while PhLP2B is only expressed in male and female germ cells undergoing meiotic maturation (*27*). As a result of this limited expression in the mouse, PhLP2B was initially referred to as mouse germ cell-specific phosducin-like protein (MgcPhLP) (*27*). Interestingly, PhLP2B expression is able to rescue the lethal phenotype of yeast *phlp2*Δ, indicating an evolutionarily-conserved function. Given their sequence similarity, shared CCT binding capability and distinct expression patterns, it is believed that PhLP2A and PhLP2B have similar, albeit tissue-specific, functions.

Analyses of temperature sensitive *phlp2* mutants in yeast suggest a possible role for PhLP2 in proper cell cycle progression and cytoskeletal function (*58*). A screen to identify genes that partially rescued the lethal defects of *phlp2* mutants at restrictive temperatures revealed several promoters of the G1/S cell cycle transition (*58*). In addition, temperature sensitive *phlp2* mutants exhibited a delay in DNA replication and impeded S-phase entry (*58*). Interestingly, temperature sensitive mutants of *cct* subunits also displayed defects in cell cycle progression (*50, 51*), suggesting a possible co-chaperone role of PhLP2 with CCT in the folding of components essential in regulating cell cycle progression. The temperature sensitive *phlp2* mutants also harbored defects in cytoskeletal function. Growth at semi-permissive temperatures was sensitive to the microfilament disrupting drug

latrunculin and to a lesser extent, the microtubule disrupting drug benomyl (*58*). Moreover, the mutants displayed significantly larger cell sizes and budding defects, which also suggest actin or tubulin deficiencies (*58*). These results point to a role for PhLP2 in the folding of actin and possibly tubulin by CCT. However, *in vitro* experiments show that while human PhLP2A forms a ternary complex with CCT and actin much like PhLP1, CCT and Gβ, this complex is inactive and actin folding is inhibited by PhLP2A (*58*). This discrepancy between the *in vivo* phenotypes and the *in vitro* results could be explained if PhLP2 were not directly required for actin folding, but for the folding of actin-associated proteins necessary for cytoskeletal function. Alternatively, necessary cofactors for PhLP2-mediated actin folding may be missing *in vitro*. The cytoskeletal defects in *phlp2* mutants are probably not responsible for the observed cell cycle defects because genes that partially rescued the cell cycle phenotype did not affect the cytoskeletal phenotype (*58*). Perhaps the best explanation of the *phlp2* temperature sensitive mutant results is that PhLP2 participates with CCT in the folding of several substrates important in cell cycle control and cytoskeletal function (*58*).

Human PhLP2A has also been referred to as viral inhibitor of apoptosis-associated factor (VIAF) because of an interaction between PhLP2A and the baculovirus *Orgyia pseudotsugata* inhibitor of apoptosis protein (Op-IAP) that was discovered in a human B cell yeast two-hybrid screen (*28*). Further investigation proved that PhLP2A does not serve as an antagonist to Op-IAP, but that PhLP2A is ubiquitinated by Op-IAP (*28*). However, PhLP2A was shown to play an essential role in the progression of apoptosis when siRNA knockdown of PhLP2A was found

to completely inhibit the processing of caspase-3 following the initiation of Bax-induced programmed cell death (*28*). Given the apparent role of PhLP2A in CCT-dependent protein folding, these results may best be explained by PhLP2-assisted folding of one or more proapoptotic factors.

PhLP3 — a potential co-chaperone for β-tubulin and other CCT substrates

Despite the high degree of homology in their C-terminal domains and their shared ability to bind CCT, PhLP3 has a physiological function distinct from PhLP2. This conclusion stems from the very different phenotypes of *phlp2* and *phlp3* deletions in yeast and *Dictyostelium*. The *phlp2* deletion in both organisms resulted in a loss of viability whereas *phlp3* deletion had no obvious effect (*21, 29*). Moreover, PhLP3 over-expression did not rescue the lethality of *phlp2* deletion (*29*). Further genetic analyses have suggested a role for PhLP3 in β-tubulin folding. In yeast, deletion of *phlp3* protected cells against the toxic effects of excess free β-tubulin, suggesting that PhLP3 is necessary for β-tubulin folding (*30, 31*). In *C. elegans*, siRNA-mediated knockdown of PhLP3 resulted in defects in microtubule architecture and aberrant cytokinesis, again pointing to a positive role of PhLP3 in tubulin function (*59*). Interestingly, cryo-EM studies have demonstrated the formation of a ternary complex between PhLP3, tubulin and CCT, indicating that PhLP3 interacts directly with CCT to regulate β-tubulin folding (*31*). In contrast to the positive role of PhLP3 predicted from the genetic studies, *in vitro* β-tubulin folding assays showed significant inhibition by PhLP3 (*31*). This same discrepancy between *in vivo* genetic phenotypes and *in vitro* folding measurements was observed

with PhLP2 (*58*). Again, important co-factors for PhLP3-induced tubulin folding may be missing in the *in vitro* assays.

PhLP3 also appears to regulate actin function. Genetic deletion of the *pac10* subunit of prefoldin in yeast results in a marked decrease in F-actin in the cell, while dual *phlp3*Δ and *pac10*Δ deletions restored F-actin to the same level as wild-type (*31*). This finding suggests that PhLP3 may somehow down-regulate actin expression or F-actin formation. In support of this finding, PhLP3 inhibits actin folding in *in vitro* assays (*31*). However, the *phlp3*Δ*pac10*Δ deletions greatly impaired a number of actin dependent functions compared to *pac10*Δ alone or wild-type cells (*31*). These data do not give a clear picture of the role of PhLP3 in actin function possibly as a result of both direct effects on actin folding and indirect effects on actin-associated proteins. Nevertheless, it is clear that PhLP3 does work in concert with prefoldin and CCT to regulate actin function.

Conclusion

The initial view of members of the Pdc gene family as downregulators of G protein signaling through sequestration of Gβγ has been completely reversed in the case of PhLP1, and shown to be irrelevant in the case of PhLPs 2 and 3. PhLPs 1-3 are now more accurately viewed as molecular co-chaperones with CCT in the folding and assembly of different CCT substrates. PhLP1 is an essential component in the assembly of Gβγ dimers, mediating the release of Gβ from CCT to interact with Gγ. PhLP2 is involved with CCT in the folding of yet to be identified cell cycle regulators as well as actin or actin-associated proteins and possibly tubulin. PhLP3 is important

in CCT-dependent folding of β-tubulin and possibly actin. In this manner, PhLP isoforms may broaden the range of substrates that are effectively folded by CCT by each assisting a unique subset of substrates in the folding process.

CHAPTER 2:

SPECIFICITY OF PHOSDUCIN-LIKE PROTEIN 1-MEDIATED G PROTEIN βγ ASSEMBLY

Summary

In order for G protein signaling to occur, the G protein heterotrimer must be assembled from its nascent polypeptides. The most difficult step in this process is the formation of the Gβγ dimer from the free subunits since both are unstable in the absence of the other. Recent studies have shown that phosducin-like protein (PhLP1) works as a co-chaperone with the cytosolic chaperonin complex (CCT) to fold Gβ and mediate its interaction with Gγ. However, these studies did not address questions concerning the scope of PhLP1 and CCT-mediated Gβγ assembly, which are important questions given that there are four Gβs that form various dimers with 12 Gγs and a fifth Gβ that dimerizes with the four regulator of G protein signaling (RGS) proteins of the R7 family. This chapter shows that PhLP1 plays a vital role in the assembly of Gγ2 with all four Gβ1-4 subunits and in the assembly of Gβ2 with all 12 Gγ subunits, without affecting the specificity of the Gβγ interactions. These findings point to a general role for PhLP1 in the assembly of all Gβγ combinations.

Introduction

Eukaryotic cells utilize receptors coupled to heterotrimeric GTP-binding proteins to mediate a vast array of responses ranging from nutrient-induced migration of single-celled organisms to neurotransmitter-regulated neuronal activity in the

human brain (*60*). Ligand binding to a GPCR initiates GTP exchange on the G protein heterotrimer (composed of Gα, Gβ, and Gγ subunits), which in turn causes the release of Gα-GTP from the Gβγ dimer (*61-63*). Both Gα-GTP and Gβγ propagate and amplify the signal by interacting with effector enzymes and ion channels (*7, 60*). The duration and amplitude of the signal is dictated by receptor phosphorylation coupled with arrestin binding and internalization (*64*) and by regulators of G protein signaling (RGS) proteins, which serve as GTPase activating proteins for the GTP-bound Gα subunit (*10, 65*). The G protein signaling cycle is reset as the inactive Gα−GDP reassembles with the Gβγ dimer and Gαβγ reassociates with the GPCR (*7*).

In order to fulfill its essential role in signaling, the G protein heterotrimer must be assembled post-translationally from its nascent polypeptides. Significant progress has been made recently regarding the mechanism by which this process occurs. It has been clear for some time that the Gβγ dimer must assemble first, followed by subsequent association of Gα with Gβγ (*66*). What has not been clear was how Gβγ assembly would occur given the fact that neither Gβ nor Gγ is structurally stable without the other. An important breakthrough was the finding that PhLP1 functions as a co-chaperone with CCT in the folding of nascent Gβ and its association with Gγ (*18, 19, 36, 54, 55, 67*). CCT is an important chaperone that assists in the folding of actin, tubulin, and many other cytosolic proteins including many β-propeller proteins like Gβ (*42*). PhLP1 has been known for some time to interact with Gβγ and was initially believed to inhibit Gβγ function (*17*). However, several recent studies have demonstrated that PhLP1 and CCT work together in a highly orchestrated manner to form the Gβγ dimer (*18, 19, 36, 54, 55, 67*).

Studies on the mechanism of PhLP1-mediated Gβγ assembly have focused on the most common dimer Gβ1γ2 (*18, 19, 36*), leaving open questions about the role of PhLP1 in the assembly of the other Gβγ combinations. These are important considerations given that humans possess 5 Gβ genes and 12 Gγ genes with some important splice variants (*68, 69*), resulting in more than 60 possible combinations of Gβγ dimers. Gβs 1-4 share between 80-90% sequence identity and are broadly expressed (*68, 69*). Gβ5, the more atypical isoform, shares only about 53% identity with Gβ1, carries a longer N-terminal domain, and is only expressed in the central nervous system and retina (*70*). The Gγ protein family is more heterogeneous than the Gβ family. The sequence identity of the 12 Gγ isoforms extends from 10-70% (*71*), and the Gγ family can be separated into 5 subfamilies (*71-73*). All Gγ proteins carry C-terminal isoprenyl modifications which contribute to their association with the cell membrane, GPCRs, Gαs, and effectors (*66*). Subfamily I Gγ isoforms are post-translationally farnesylated while all others are geranylgeranylated (*73, 74*).

There is some inherent selectivity in the assembly of different Gβγ combinations, but in general Gβs 1−4 can form dimers with most Gγ subunits (*75*). The physiological purpose of this large number of Gβγ combinations has intrigued researchers in the field for many years, and a large body of research indicates that GPCRs and effectors couple to a preferred subset of Gβγ combinations based somewhat on specific sequence complementarity, but even more so on cellular expression patterns, subcellular localization, and post-translational modifications (*69*). In contrast to Gβs 1-4, Gβ5 does not interact with Gγ subunits *in vivo*, but it instead forms irreversible dimers with RGS proteins of the R7 family.

It has been recently shown that all Gβ isoforms are able to interact with the CCT complex, but to varying degrees (*55*). Gβ4 and Gβ1 bind CCT better than Gβ2 and Gβ3 while Gβ5 binds CCT poorly (*55*). These results suggest that Gβ1 and Gβ4 might be more dependent on PhLP1 than the other Gβs, given the co-chaperone role of PhLP1 with CCT in Gβ1γ2 assembly. However, another report has indicated that Gγ2 assembly with Gβ1 and Gβ2 is more PhLP1-dependent than with Gβ3 and Gβ4 (*57*). Thus, it is not clear from current information whether PhLP1 plays a general role in Gβγ dimer formation or whether it specifically catalyzes assembly of only a subset of these complexes. This report was designed to systematically address this issue.

Experimental Procedures

Cell culture

HEK 293T cells were cultured in DMEM/F-12 (50/50 mix) growth media containing L-glutamine and 15 mM HEPES supplemented with 10% fetal bovine serum (Sigma-Aldrich). The cells were subcultured regularly to maintain growth, but were not used beyond 25 passages.

Preparation of cDNA constructs

The pcDNA3.1 vectors containing N-terminally Flag-tagged human Gβs 1-4, Gβ5short, and N-terminally HA-tagged Gγs 1-5 and 7-13 were obtained from the Missouri University of Science and Technology cDNA Resource Center (www.cdna.org). Wild type human PhLP1 and the PhLP1 Δ1-75 N-terminal

truncation variant each with a 3′ c-myc and His_6 tag were constructed in pcDNA3.1/myc-His B vector using PCR as described (*19, 76*).

RNA interference experiments

Short interfering RNAs (siRNAs) were chemically synthesized (Dharmacon) to target nucleotides 608-628 of human lamin A/C (*19*) and nucleotides 345-365 of human PhLP1 (*19*). HEK 293T cells were grown in 12-well plates to 50-70% confluency at which point they were transfected with siRNA at 100 nM final concentration using Oligofectamine reagent (Invitrogen) as described previously (*19*). Twenty four hours later, the cells were transfected with 0.5 μg each of Flag-Gβ or HA-Gγ in pcDNA3.1(+) using Lipofectamine 2000 according to the manufacturer's protocol (Invitrogen). The cells were harvested for subsequent immunoprecipitation experiments 72 hours later. Ten μg of cell lysate were immunoblotted with an anti-PhLP1 antibody (*35*) to assess the percent PhLP1 knockdown.

Dominant interfering mutant experiments

HEK 293T cells were plated in 6-well plates and grown to 70-80% confluency. The cells were then transfected with Lipofectamine 2000 (Invitrogen) according to the manufacturer's instructions. Each well was transfected with 1.0 μg of either the empty vector control, wild-type PhLP1-myc, or PhLP1 Δ1-75-myc along with 1.0 μg each of the indicated Flag-Gβ and HA-Gγ cDNAs. The cells were harvested for immunoprecipitation 48 hours after transfection.

Immunoprecipitation experiments

Transfected HEK 293T cells were washed with phosphate-buffered saline (PBS) (Fisher) and solubilized in immunoprecipitation buffer (PBS pH 7.4, 2% NP-

40 (Sigma), 0.6 mM PMSF, 6 µl/ml protease inhibitor cocktail per mL buffer (Sigma P8340)). The lysates were passed through a 25-gauge needle 10 times and centrifuged at maximum speed for 10-12 minutes at 4ºC in an Eppendorf microfuge. The protein concentration for each sample was determined using the DC Protein Assay Kit II (Bio-Rad) and equal amounts of protein were used in the subsequent immunoprecipitations. Approximately 150 µg of total protein were used in immunoprecipitations from cells in 12 well plates and 450 µg from cells in 6 well plates. The clarified lysates were incubated for 30 minutes at 4°C with 2.5 µg anti-Flag antibody (clone M2, Sigma), for lysates from 12-well plates or with 6.25 µg of anti-Flag for lysates from 6-well plates. Next, 30 µl of a 50% slurry of Protein A/G Plus agarose (Santa Cruz Biotechnology) was added, and the mixture was incubated for 30 minutes at 4°C as described (*19*). The immunoprecipitated proteins were solubilized in SDS sample buffer and resolved on a 10% Tris-Glycine-SDS gel or a 16.5% Tris-Tricine-SDS gel for Gγ. The proteins were transferred to nitrocellulose and immunoblotted using an anti-Flag (clone M2, Sigma), anti-c-myc (BioMol), anti-HA (Roche), or an anti-PhLP1 antibody (*19*). Immunoblots were incubated with the appropriate anti-rabbit, anti-mouse, (Li-Cor Biosciences), or anti-rat (Rockland) secondary antibody conjugated with an infrared dye. Blots were scanned using an Odyssey Infrared Imaging System (Li-Cor Biosciences), and protein band intensities were quantified using the Odyssey software. The data are presented as the mean value +/- standard error from at least three experiments.

Results

It has been shown that in order to mediate Gβγ assembly, PhLP1 must bind Gβγ with high affinity (*19, 36*). As a first step toward determining the ability of PhLP1 to catalyze Gβγ dimer formation with the five Gβ subunits, we measured the interaction of PhLP1 with each Gβ subunit in complex with Gγ2 by co-immunoprecipitation. Equal amounts of myc-tagged PhLP1, Gγ2, and each Flag-tagged Gβ 1-5 were over-expressed in HEK-293T cells. After incubation, cells were harvested and immunoprecipitated with an anti-Flag antibody and immunoblotted with anti-myc and anti-Flag antibodies. Protein band intensities were quantified and the ratio of the PhLP1-myc band to each Flag-Gβ band was determined (Fig. 2-1A). The data show that Gβs 1-4 all co-immunoprecipitated similar amounts of PhLP1 while Gβ5 co-immunoprecipitated significantly less, indicating that PhLP1 binds Gβ5 complexes with a lower affinity than it does Gβ1-4 complexes. All five Gβs expressed equally well under these conditions, so the differences in binding can not be attributed to different Gβ expression levels (Fig. 2-1A). These results suggest that PhLP1 may be involved in Gβγ assembly of Gβ1-4, but perhaps not Gβ5.

To directly measure the contribution of PhLP1 to the assembly of the five Gβ isoforms with Gγ, the effect of siRNA-mediated PhLP1 knockdown on Gβγ dimer formation was measured by co-immunoprecipitation of Gγ2 with the Gβs. We chose Gγ2 because it is a common isoform that associates to some extent with all Gβ subunits *in vitro* (*75*). HEK 293T cells were treated with PhLP1 siRNA, a control siRNA to lamin A/C or a mock treatment with no siRNA and then HA-Gγ2 and one of the five Flag-tagged Gβ subunits were coexpressed. Cell lysates were

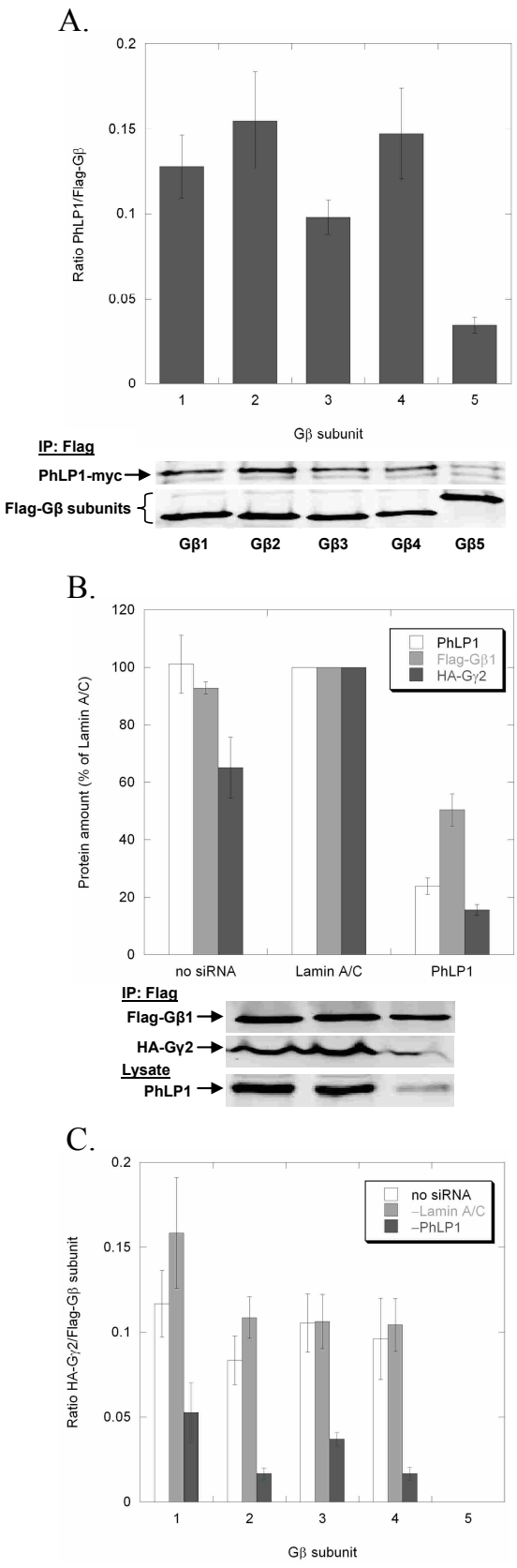

Fig. 2-1. Effects of PhLP1 siRNA knockdown on the assembly of all Gβ subunits with Gγ2. HEK 293T cells were treated as follows: A) Cells were transfected with PhLP1-myc, HA-Gγ2 and the indicated Flag-Gβ cDNAs. After 48 hours, cells were lysed, immunoprecipitated with an anti-Flag antibody and immunoblotted with anti-myc or anti-Flag antibodies. The graph represents the ratio of the PhLP1-myc/Flag-Gβ band intensities for all 5 Gβs. Bars represent the average ± standard error from 3 separate experiments. A representative blot is shown below the graph. B, C) Cells were treated with siRNA against PhLP1, lamin A/C, or no siRNA as indicated. Twenty-four hours later, cells were transfected with the indicated Flag-Gβ subunit and HA-Gγ2 cDNAs. After 72 additional hours, cells were lysed, immunoprecipitated with an anti-Flag antibody and immunoblotted with anti-Flag or anti-HA antibodies. Bands were quantified and expressed as a percentage of the lamin A/C control for Gβ1γ2 in (B) or as the ratio of HA-Gγ2/Flag-Gβ for all five Gβs in (C). PhLP1 knockdown was measured by quantifying the PhLP1 band intensity in immunoblots of 10 μg of whole cell lysate. The average PhLP1 knockdown was between 60-76% compared to the lamin A/C control. Bars represent the average ± standard error from 3-5 separate experiments. If no bar is shown, then no complex was detected for that particular Gβγ species. A representative blot for Gβ1γ2 is shown below the graph in (B).

immunoprecipitated with an anti-Flag antibody and the precipitate was immunoblotted with anti-HA and anti-Flag antibodies to detect the amount of Gγ2 bound to each Gβ subunit. Fig. 2-1B shows the levels of PhLP1 in the cell extract and the amounts of Flag-Gβ1 and HA-Gγ2 in the immunoprecipitate relative to the lamin A/C siRNA control. A 75% knockdown of PhLP1 resulted in a 50% decrease in Gβ1 and a striking 85% decrease in the co-immunoprecipitated Gγ2 compared to the lamin A/C control. This pattern was consistent among all the Gβ subunits except for Gβ5, which had no detectable Gγ2 bound under these conditions (Fig. 2-1C). To more directly compare the effects of PhLP1 knockdown, the Gγ2/Gβ1-4 band intensity ratios in the immunoprecipitates were determined for the three siRNA conditions (Fig. 2-1C). In each case, much less Gγ2 was associated with Gβ when PhLP1 was knocked down. The Gγ2/Gβ ratio decreased between 65-84% compared to the lamin A/C control. These results indicate that PhLP1 does assist in the formation of Gβγ complexes containing Gβs 1-4 with Gγ2.

To further examine the role of PhLP1 in Gβγ assembly with the different Gβ subunits, an alternative method to block PhLP1 function was employed. It has been shown previously that an N-terminally truncated PhLP1 variant in which the first 75 amino acids have been removed (PhLP1 Δ1-75) acts in a dominant interfering manner to block Gβγ assembly by forming a stable PhLP1 Δ1-75-Gβ-CCT ternary complex that does not release Gβ from CCT for association with Gγ (*19, 36*). Co-expression of PhLP1 Δ1-75 with Flag-Gβ1 and HA-Gγ2 resulted in a dramatic reduction in the amount of Gγ2 in the Gβ1 immunoprecipitate compared to wild-type PhLP1 (expressed at comparable levels) or to an empty vector control (Fig. 2-2A). This

pattern was similar among Gβs 1-4. PhLP1 Δ1-75 decreased the Gγ2/Gβ ratios by 75-92% in the Gβ1-4 immunoprecipitates (Fig. 2-2B). For Gβ5, again very little Gγ2 was associated with it under these conditions. Interestingly, co-expression of wildtype PhLP1 increased the amount of both Gβ and Gγ2 in the Flag-Gβ immunoprecipitate by 30-50% for all five Gβ isoforms (Figs. 2-2A, 2-4A and 3-3B). This observation is consistent with a PhLP1-mediated enhancement of Gβγ formation, resulting in a stabilization of Gβ and Gγ expression. Together, these findings confirm the siRNA knockdown results by showing that PhLP1 is important in the assembly of each of the Gβs 1-4 with Gγ2.

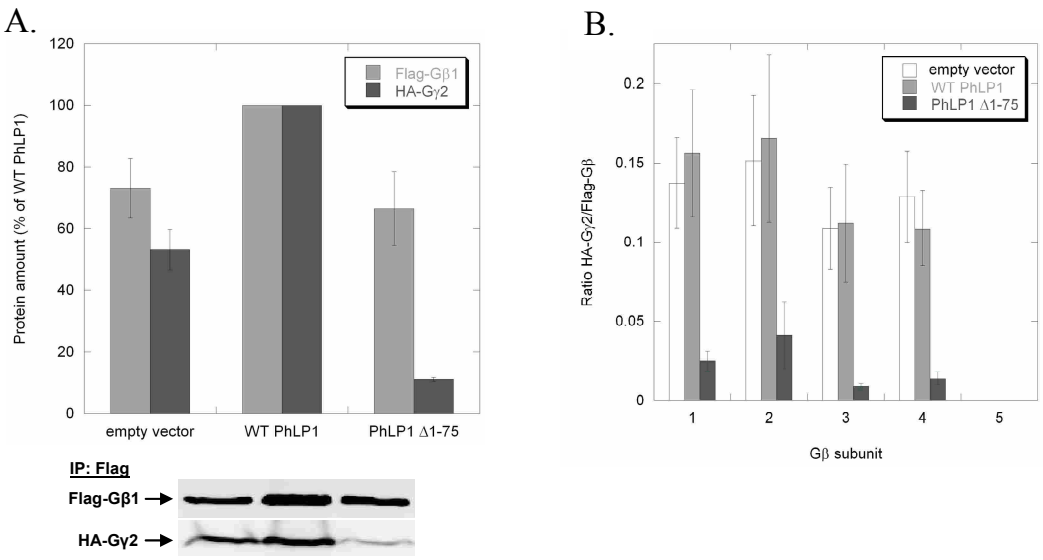

Fig. 2-2. Effects of PhLP1 Δ1-75 expression on the assembly of all Gβ subunits with Gγ2. HEK 293T cells were transfected with either wild-type PhLP1, PhLP1 Δ1-75, or an empty vector control along with the indicated Flag-Gβ subunit and HA-Gγ2 cDNAs. After 48 hours, cells were lysed, immunoprecipitated with an anti-Flag antibody and immunoblotted with anti-Flag or anti-HA antibodies. Bands were quantified and expressed as a percentage of the wild-type PhLP1 control for Gβ1γ2 in (A) or as the ratio of HA-Gγ2/Flag-Gβ for all five Gβs in (B). Bars represent the average ± standard error from 3-5 separate experiments. If no bar is shown, then no complex was detected for that particular Gβγ species. A representative blot for Gβ1γ2 is shown below the graph in (A).

A second question regarding the scope of PhLP1-mediated Gβγ assembly is whether all 12 Gγ subunits or just a subset require PhLP1 to associate with Gβ. To address this question, the effects of siRNA-mediated PhLP1 knockdown and PhLP1 Δ1-75 over-expression on the association of the twelve Gγ subunits with Gβ2 were measured. Gβ2 was chosen because it forms dimers with most Gγ isoforms, yet it shows selectivity between the different Gγs (*75*). The siRNA knockdown experiments followed the same format as those in Fig. 2-1. HEK 293T cells were treated with PhLP1 siRNA, a control siRNA to lamin A/C or no siRNA and then co-expressed with Flag-Gβ2 and each of the 12 HA-tagged Gγ subunits. Cell lysates were immunoprecipitated with an anti-Flag antibody and the precipitate was immunoblotted with anti-HA and anti-Flag antibodies to detect the amount of each Gγ subunit bound to Gβ2. Fig. 2-3A shows the levels of PhLP1 in the cell extract and Flag-Gβ2 and HA-Gγ2 in the immunoprecipitate relative to the lamin A/C siRNA control. The results were similar to the Gβ1γ2 experiment. The PhLP1 knockdown was 80%, which resulted in a 30% decrease in Gβ2 and a 90% decrease in the co-immunoprecipitated Gγ2 compared to the lamin A/C control. This pattern was consistent among all the Gβ2Gγ combinations that formed dimers. Gβ2 decreased by 20-50% while the co-immunoprecipitating Gγs decreased by 80-95% (data not shown). Figure 2-3B compares the Gγ/Gβ2 band intensity ratios for the three siRNA conditions. In each case, much less Gγ was associated with Gβ when PhLP1 was knocked down. The Gγ/Gβ2 ratios decreased between 74-91% compared to the lamin A/C control, except for Gγs 1, 11 and 13 which did not form dimers with Gβ2. These results indicate that all Gβ2Gγ dimers depend upon PhLP1 for their assembly.

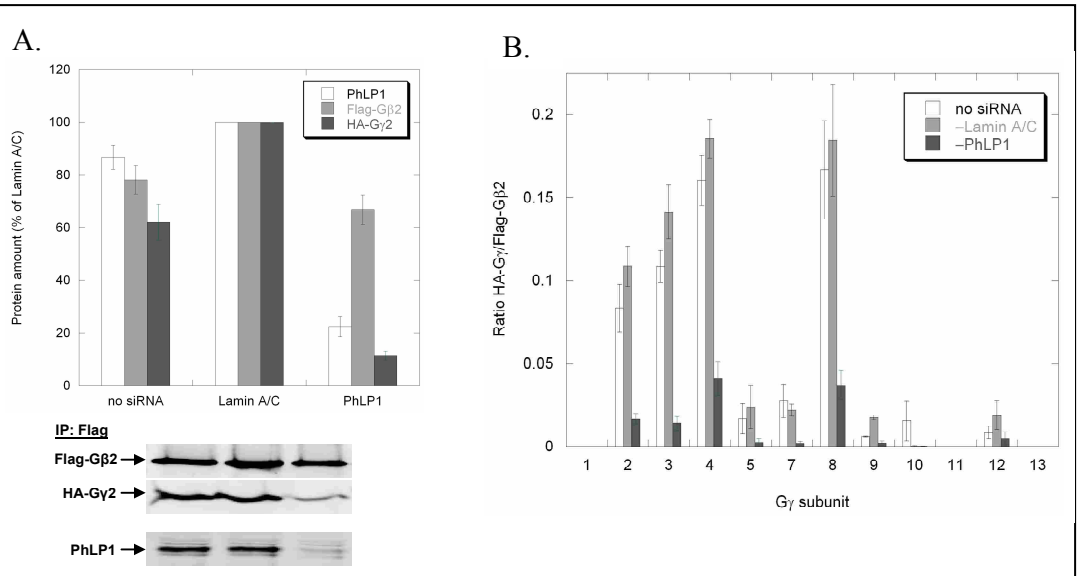

Fig. 2-3. Effects of PhLP1 knockdown on the assembly of all Gγ subunits with Gβ2. HEK 293T cells were treated with siRNA against PhLP1, lamin A/C, or no siRNA as indicated. Twenty-four hours later, cells were transfected with the indicated HA-Gγ subunit and Flag-Gβ2 cDNAs. After 72 additional hours, cells were lysed, immunoprecipitated with an anti-Flag antibody and immunoblotted with anti-Flag or anti-HA antibodies. Bands were quantified and expressed as a percentage of the lamin A/C control for Gβ2γ2 in (A) or as the ratio of HA-Gγ/Flag-Gβ2 for all 12 Gγs in (B). PhLP1 knockdown was measured by quantifying the PhLP1 band intensity in immunoblots of 10 μg of whole cell lysate. The average PhLP1 knockdown was between 66-90% compared to the lamin A/C control. Bars represent the average ± standard error from 3-14 separate experiments. If no bar is shown, then no complex was detected for that particular Gβγ species. A representative blot for Gβ2γ2 is shown below the graph in (A).

The dominant interference experiments with PhLP1 Δ1-75 followed a similar pattern. Coexpression of PhLP1 Δ1-75 with Flag-Gβ2 and HA-Gγ2 resulted in a 50% reduction in the amount of Gβ2 and a 95% reduction in the amount of Gγ2 in the Flag immunoprecipitate when compared to the wild-type PhLP1 control (Fig. 2-4A). Moreover, co-expression of wild-type PhLP1 increased both Gβ2 and Gγ2 levels by 50%, similarly to Gβ1γ2 (Fig. 2-2A). The effect of PhLP1 Δ1-75 on the Gγ/Gβ2 ratio was the same for all the Gγs that formed dimers with Gβ2. The ratios were drastically reduced by amounts ranging from 81-100%. Together with the PhLP1

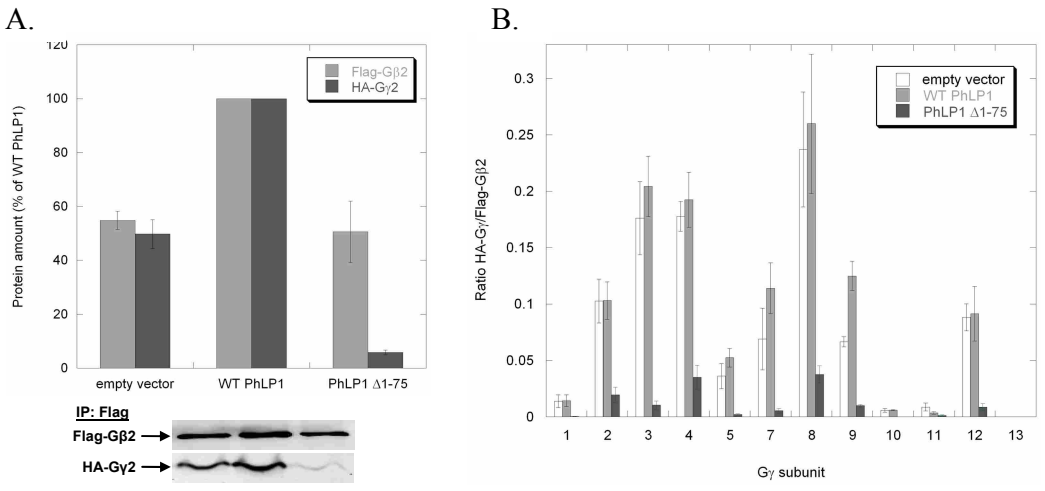

Fig. 2-4. Effects of PhLP1 Δ1-75 expression on the assembly of all Gγ subunits with Gβ2. HEK 293T were transfected with either WT PhLP1, PhLP1 Δ1-75, or an empty vector control along with the indicated HA-Gγ subunit and Flag-Gβ2 cDNAs. After 48 hours, cells were lysed, immunoprecipitated with an anti-Flag antibody and immunoblotted with anti-Flag or anti-HA antibodies. Bands were quantified and expressed as a percentage of the wild-type PhLP1 control for Gβ2γ2 in (A) or as the relative ratio of HA-Gγ/Flag-Gβ2 for all 12 Gγs in (B). Bars represent the average ± standard error from 3-6 separate experiments. If no bar is shown, then no complex was detected for that particular Gβγ species. A representative blot for Gβ2γ2 is shown below the graph in (A).

knockdown data, these results clearly demonstrate that all Gγ subunits that interact with Gβ2 require PhLP1 for dimer formation.

Another interesting observation that can be made from the data in Figures 2-3B and 2-4B concerns the effect of PhLP1 on the specificity of Gβ2γ dimer formation. The Gγ subunits can be divided genetically into five subfamilies as shown in the phylogenetic tree of Fig. 2-5A. Members of subfamily II form dimers with Gβ2 readily, while members of the other subfamilies interact weakly with Gβ2 or not at all (Fig. 2-5B and C). The order of dimer formation of the Gγ subfamilies with Gβ2 is II > III > I, IV with no dimer formation found with subgroup V. This pattern of Gβ2γ dimer specificity is similar to *in vitro* data reported previously (*75*).

Importantly, PhLP1 does not appear to influence the specificity of Gβ2γ dimer formation. The specificity pattern is the same no matter the level of PhLP1 activity. For example, when PhLP1 is siRNA-depleted, Gβ2γ formation with Gγ subfamily II is greater than with subfamilies III, I and IV by a similar factor as when PhLP1 is at endogenous levels. Similarly, when PhLP1 function is blocked by the PhLP1 Δ1-75 variant, Gβ2γ formation with subgroup II is greater than the other subgroups by a similar factor as when PhLP1 is over-expressed (Fig. 2-5B and C). Thus, it appears that PhLP1 has no effect on which Gγ subunit will interact with Gβ2.

Discussion

Post-translational assembly of stable G protein heterotrimers is a fundamental prerequisite for G protein signaling, yet the mechanism by which the assembly process occurs had been an enigma for more than two decades since the G protein heterotrimer was initially discovered. The most puzzling issue has been how the Gβ and Gγ subunits could come together to form a stable dimer when the individual polypeptides were structurally unstable. Recent studies have shed considerable light on the assembly process and have outlined a mechanism by which CCT and PhLP1 work as co-chaperones to fold Gβ and present it to Gγ for dimerization to occur (*18, 19, 36, 38, 52, 54, 55, 67*). Gγ itself appears to be held by another chaperone DRiP78 (*57*) until it can interact with PhLP1-Gβ. Mechanistic studies have thus far focused on the most common Gβ1γ2 dimer combination and have not addressed whether this assembly mechanism was general to the many other Gβγ dimers, or specific to only a subset. All the Gβ subunits have been recently shown to interact with CCT with Gβ5

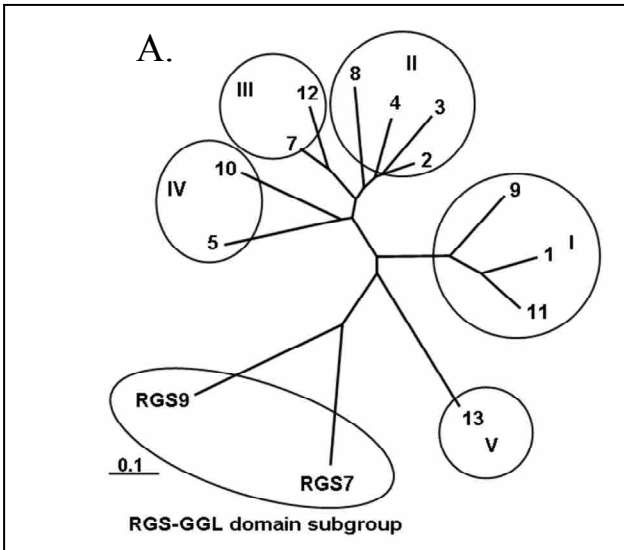

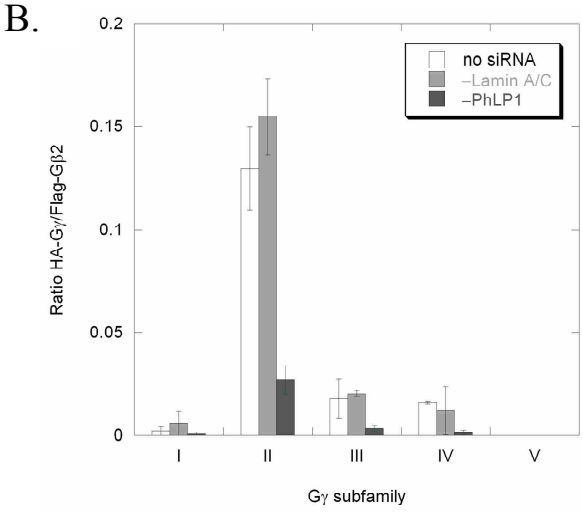

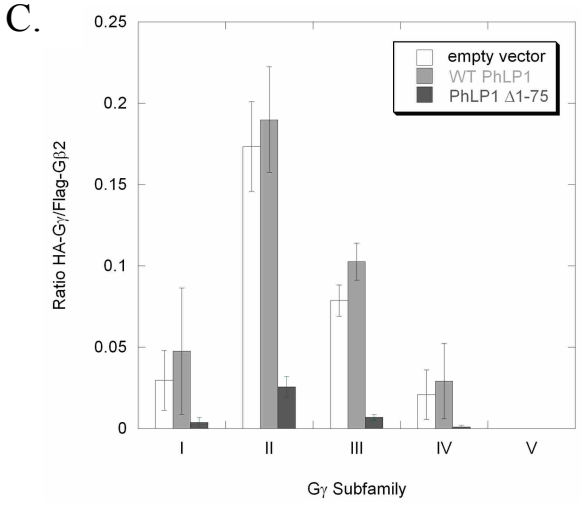

Fig. 2-5. Effects of PhLP1 knockdown on the specificity of Gβ2 dimerization with Gγ subfamilies. A) The phylogenetic relationship between human Gγ subunits and RGS7 and 9 is depicted. An unrooted dendrogram was made using TreeView from a Gγ family sequence alignment created with ClustalX. The Gγ family can be separated into 5 subfamilies as indicated. The scale bar represents a substitution rate of 0.1 per amino acid. B) The Gγ/Gβ2 ratios within each Gγ subfamily under the different siRNA conditions from Fig. 3B were averaged and plotted to show the effects of PhLP1 knockdown on the subfamily specificity of Gβ2Gγ dimer formation. Error bars represent the standard error of the mean within each subfamily. C) A similar average of the Gβ2Gγ ratios for each subfamily under the different PhLP1 over-expression conditions from Fig. 4B was calculated and plotted. If no bar is shown, then no complex was detected for that particular Gβγ species.

interacting weakly relative to the other Gβ subunits (*55*). The current study has addressed the scope of PhLP1-mediated dimer assembly for many Gβγ combinations. The results clearly show that PhLP1 is a general co-chaperone for Gβγ assembly. All Gβ subunits required PhLP1 for association with Gγ2 (Figs. 2-1 and 2-2) and all Gγ subunits that form dimers with Gβ2 required PhLP1 for association with Gβ2 (Figs. 2-3 and 2-4). It seems very likely that the other possible Gβγ dimer combinations would also require PhLP1 for their assembly as well. Thus, it appears that all Gβγs follow a similar mechanism of dimer formation.

Understanding the reasons why some Gβγ combinations form dimers and others do not has been of interest in the field for some time (*69*). Apparent differences in Gβγ specificity between *in vitro* assays and cell-based assays have suggested that cellular factors that are involved in the assembly process such as PhLP1 might influence Gβγ specificity (*75*). However, this does not appear to be the case. As noted above, the specificity of Gβγ dimer formation was not changed by increases or decreases in PhLP1 activity. Thus, it appears that PhLP1 is acting as a true catalyst in Gβγ assembly by not influencing which Gβ can bind which Gγs but simply facilitating the association of Gβγ combinations that are intrinsically stable. In the case of the Gβ2γ combinations investigated here, dimer stability appears to be determined by sequence specificity since Gγ binding segregated along subfamily lines according to sequence homology (Fig. 2-5). Hence, the major factors that determine Gβ2γ specificity appear to be limited to complementarity of the binding surfaces as determined by specific amino acid interactions, the expression of the complementary

Gβγ combinations in the same cell types, and the subcellular localization within the cell (*69*).

It is interesting to note that inhibition of PhLP1 activity through siRNA-mediated knockdown or over-expression of the PhLP1 Δ1-75 dominant negative variant resulted in a surprisingly small decrease in Gβ expression (~ 50%), despite the fact that very little of this residual Gβ was associated with Gγ (Figs. 2-1 through 2-4). This finding indicates that Gβ can exist in the cell unassociated with Gγ. It is likely that this pool of undimerized Gβ is associated with CCT because it has been previously shown that Gβ-CCT complexes are relatively stable in the absence of PhLP1 and Gγ (*36*). Thus, it appears that the role of CCT is to fold Gβ and protect it from aggregation or proteolytic degradation until it can be released by PhLP1 to interact with Gγ.

In conclusion, this work expands the role of PhLP1 as an essential co-chaperone in the assembly of all Gβγ combinations. The data provide additional insight into the broad role PhLP1 assumes to bring the unstable β-propeller fold of Gβ subunits together with their complementary Gγ to create stable Gβγ dimers in order to perform their vital functions in G protein signaling.

CHAPTER 3:

MECHANISM OF PHOSDUCIN-LIKE PROTEIN 1-MEDIATED Gβ5-R7 RGS ASSEMBLY

Summary

Recent studies have shown that PhLP1 works as a co-chaperone with CCT to fold Gβ and mediate its interaction with Gγ. However, these studies did not address the question concerning the role of PhLP1 or CCT in the folding of Gβ5 and its assembly with R7 RGS proteins. The results show that Gβ5 folding and Gβ5-RGS7 assembly is dependent on CCT and PhLP1, but the apparent mechanism is different from that of Gβγ. PhLP1 seems to stabilize the interaction of Gβ5 with CCT until Gβ5 is folded, after which, PhLP1 is released to allow Gβ5 to interact with RGS7. These findings suggest a CCT-dependent mechanism for Gβ5 folding and Gβ5-RGS7 assembly that utilizes the co-chaperone activity of PhLP1.

Introduction

Once triggered by a ligand-bound GPCR, the G protein Gα subunit exchanges GDP for GTP causing a decrease in the binding affinity between Gα and Gβγ to the extent that Gα and Gβγ dissociate from each other. Gα bound to GTP has a higher affinity for effectors, while the free Gβγ subunit has an exposed effector binding surface capable of interacting with effector enzymes and ion channels. Formerly, it was thought that the duration of the G protein signal was dictated by the slow intrinsic GTPase activity of the Gα subunit. However, this hypothesis could not

explain the large timing discrepancy between the fast GPCR-mediated physiological responses measured *in vivo* and the slow GTPase activity of the Gα subunit *in vitro* (*77*). Theses observations were reconciled when a new family of GTPase accelerating proteins (GAPs) was identified that were able to bind Gα and dramatically enhance its intrinsic GTP hydrolysis rate (*78, 79*). Subsequently, these proteins were named regulators of G protein signaling (RGS) proteins (*78, 79*), and to date, at least 37 RGS proteins have been identified in humans (*80*). All RGS proteins contain a distinctive ~120 amino acid sequence through which they bind Gα and stabilize its switch regions. In the binding process, the position of a key Gα glutamine residue found in the switch II region is stabilized in a manner that fixes the catalytic domain in the GTP hydrolysis transition state (*81*) and orients the nucleophilic water molecule required for GTP hydrolysis.(*82*)

Four RGS proteins (6, 7, 9, and 11) contain a central domain similar to the G protein γ subunit, and as such, this domain has come to be known as the Gγ-like (GGL) domain. It is through this domain that R7 RGS proteins interact with Gβ5 in a manner similar to other Gβγ associations (*83, 84*). Like other Gβγs, Gβ5 and R7 RGS proteins form obligate dimers required for their mutual stability (*85*), and without their partner, Gβ5 and R7 RGS proteins are rapidly degraded in cells (*85, 86*). Besides the GGL domain, R7 RGS proteins contain an N-terminal DEP (disheveled, Egl-10, pleckstrin) homology domain and a C-terminal RGS domain (*65, 85*). The DEP domain interacts with the membrane anchoring/nuclear shuttling R7 binding protein (R7BP), or in the case of RGS9, the R9 anchoring protein (R9AP). Through the RGS domain, Gβ5-R7 RGS complexes act as GAPs for Gi/o_a, Gq_a and $G\alpha_t$

subunits in neuronal cells, some immune cells, and in the retina (*75*). In addition, the Gβ5-RGS7 complexes and may also serve to couple inactive Gα subunits to particular GPCRs (*80*).

R7 RGS proteins are abundantly expressed in the retina and central nervous system with RGS9 existing as RGS9-1 in the retina and RGS9-2 in the nervous system. Because of their mutual dependence, Gβ5 and R7 RGS proteins are expressed in the same tissues with Gβ5 also found in two alternately spliced forms (*7*). The photoreceptor-specific Gβ5-Long ($G\beta5_L$) complexes with RGS9-1 in the retina, and the more widely expressed Gβ5-short ($G\beta5_S$), forms complexes with RGS9-2 and other R7 RGS proteins in the nervous system (*70*).

The physiological function of RGS9-1 has been described in the phototransduction cascade of mice and humans. In *rgs9-1* knockout mice, initial flash response rates and amplitudes are normal, but the recovery response is much slower than in the control mice. This is explained by the fact that the *rgs9-1* knockout mice showed a significant reduction in GTP hydrolysis in their rod outer segments leading to a prolonged lifetime of GTP-bound $G\alpha_t$ (*86*). In humans, it appears that loss-of-function mutations in either RGS9-1, or its membrane anchoring protein, R9AP are found in people with bradyopsia, a condition in which photoresponse recovery is abnormally low. Symptoms of bradyopsia include an inability to see moving objects which becomes more severe in low lighting, and difficulty adjusting to changes in light intensity (*87*). The knockout mice and human observations are due to an inability of RGS9-1 to properly act as a GAP for Gα-transducin in the phototransduction cascade leading to detrimentally long $G\alpha_t$

signaling. Likewise, RGS9-2 operates as a GAP for $G\alpha_i$ to turn off dopaminergic and opiod signaling in a timely manner. RGS9-2 overexpression in rat brain nucleus accumbens reduced the response to the dopamine agonist cocaine, while *rgs9-2* knockout mice showed a heightened response to the drug (*88*). In another study, *rgs9-2* knockout mice showed a 10-fold increase in response to the opiate morphine (*88*). These results emphasize the necessity of R7-RGS proteins in the precise control of the duration and amplitude of G protein signaling. The physiological function of Gβ5, other than stabilizing R7 RGS proteins, is less understood. It is possible that Gβ5 is needed to keep the RGS protein close to Gα in signaling events that are extremely fast or sensitive. In this hypothesis, the GDP-bound Gα would bind to Gβ5, but once in its GTP-bound form, Gα would dissociate from Gβ5, and hydrolyze its GTP quickly with help from the awaiting R7 RGS protein (*74*).

In order to understand the molecular mechanisms responsible for the mentioned physiological responses, the crystal structure of the Gβ5-RGS9 complex was solved (*89*) which provides a model for the interaction of Gβ5 with all R7 RGS proteins. Even though Gβ5 shares only ~50% sequence identity with Gβs 1-4, it was shown to fold into an almost identical 7-bladed β-propeller structure and bind RGS9 most extensively across the side in a coiled coil analogous to Gβγ binding (*32, 89*). Additionally, residues along the top and bottom of the Gβ5 propeller were found in contact with RGS9 (*89*). The Gβ5 residues that interact with the GGL domain along the side of the propeller are conserved between Gβ5 and other Gβs, but the residues that interact with RGS9 along the top and bottom of the propeller are not. These divergent residues help explain why Gβ5 is the only Gβ that is able to associate with

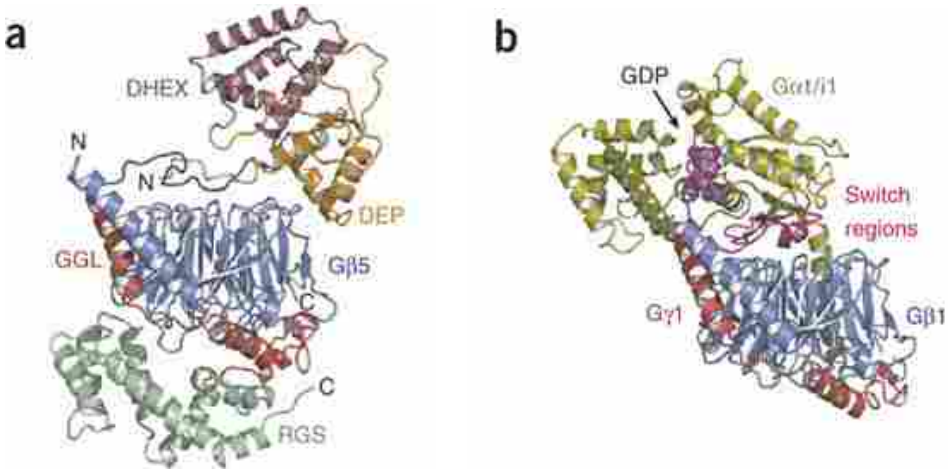

Figure 3-1. Structures of Gβ5-RGS9 and Gαβγ.
Ribbon diagrams of: A) Gβ5 (blue) in complex with RGS9. RGS9 is shown with its N-terminal (light gray), DEP (orange),DHEX (maroon) DHEX-GGL linker (dark gray) GGL (red), and RGS (green) regions. The RGS9 N-terminal region, DEP domain, and DHEX-GGL linker regions bind to the top of the Gβ5 propeller and act as a cap. B) Gαβγ transducin with Gβ (blue), Gγ (red), Gα (gold), Gα switch regions (magenta), and GDP (purple). Both the Gα and N-terminal RGS9 binding surfaces overlap on Gβ5. The RGS N-terminal domains may function as a hinge to allow Gβ5 to simultaneously interact with Gα and RGS9. Reprinted by permission from Macmillan Publishers Ltd: [Nat Struct Mol Biol.] (*89*), copyright 2008. http://www.nature.com/nsmb/index.html

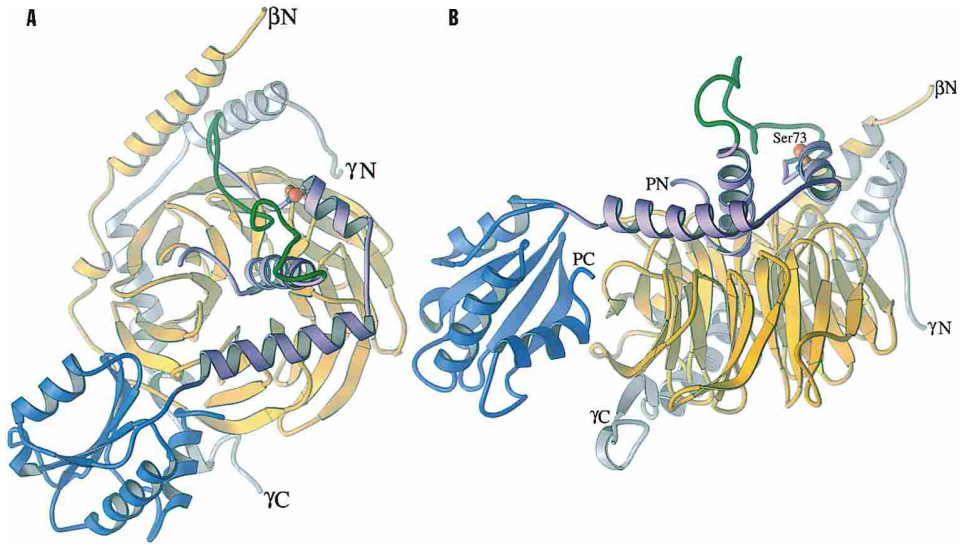

Figure 3-2. Structure of Pdc-G_tβγ.
Ribbon diagrams showing the A) top, and B) side views of Pdc (N-term purple, and C-term blue) in complex with Gβ1 (gold) and Gγ1 (silver). It is proposed that N-terminal regions of Pdc and PhLP1 interact similarly with Gβ. As a result, the PhLP1, N-term RGS9, and Gα binding surfaces on the top of the Gβ propeller overlap. Reprinted by permission from Elsevier: [Cell] (*32*), copyright 1996. http://www.cell.com.

R7 RGS proteins. Structurally, the Gβγ interactions are almost identical to the Gβ5-GGL domain associations, but Gγ subunits are not able to form stable complexes with Gβ5 due to the collective effect of several individually minor residue changes found in Gβ5. Interestingly, the Gβ residues shown to interact with Gα are conserved in Gβ5, but RGS9 inhibits the Gα-Gβ5 interaction by capping the top side of the Gβ5 propeller where Gα binds to Gβ. Thus, it is proposed that *in vivo* several N-terminal RGS9 residues may act like a hinge, and when opened, uncover the Gβ5 residues required for interaction with Gα. In addition, the way in which RGS9 caps the top of the Gβ5 propeller poses a major structural problem for possible Gβ5-PhLP1 interactions because, based on the Pdc-Gβγ crystal structure, PhLP1 is also proposed to interact with the top of the Gβ5 propeller. In all, it appears that the N-terminal region of RGS9, Gα, and PhLP1 all share the same Gβ5 binding surface with only one of these entities able to interact with Gβ5 at a time.

The Gβ5-R7 RGS complex must be folded and assembled in order to carry out its physiologically important function. The overlapping PhLP1 and RGS9 binding site on Gβ, as well as a weak ability of Gβ5 to bind CCT relative to other Gβs (*55*), led to questions concerning the folding and assembly of Gβ5-R7 RGS proteins. It was unknown whether Gβ5-R7 RGS assembly could follow the same PhLP1 and CCT-dependent assembly mechanism as Gβγ dimers (*19*). PhLP1 and CCT are absolutely essential in Gβ subunit folding and subsequent Gβγ assembly. How could Gβ5 fold when it interacted so weakly with CCT, or subsequently associate with an R7 RGS protein if the association was hindered by PhLP1? Thus, it was not clear from the available information whether CCT or PhLP1 play a role in Gβ5-R7 RGS

dimer formation. This report was designed to address this issue using the $G\beta5_S$-RGS7 dimer as a model for the assembly of all Gβ5-R7 RGS dimers.

Experimental Procedures

Cell culture

HEK 293T cells were cultured in DMEM/F-12 (50/50 mix) growth media containing L-glutamine and 15 mM HEPES supplemented with 10% fetal bovine serum (Sigma-Aldrich). The cells were subcultured regularly to maintain growth, but were not used beyond 25 passages.

Preparation of cDNA constructs

The pcDNA3.1 vectors containing N-terminally Flag-tagged human Gβs 1 and 5short, N-terminally HA-tagged Gγ2 and 3x HA-tagged RGS7 (S2), were obtained from the Missouri University of Science and Technology cDNA Resource Center (www.cdna.org). Wild type human PhLP1 and the PhLP1 Δ1-75 N-terminal truncation variant each with a 3′ c-myc and His_6 tag were constructed in pcDNA3.1/myc-His B vector using PCR as described (*19, 76*).

RNA interference experiments

Short interfering RNAs (siRNAs) were chemically synthesized (Dharmacon) to target nucleotides 608-628 of human lamin A/C (*19*), nucleotides 345-365 of human PhLP1 (*19*), and nucleotides 172-192 of human CCTζ-1 (*90*). HEK 293T cells were grown in 12-well plates to 50-70% confluency at which point they were transfected with siRNA at 100 nM final concentration using Oligofectamine reagent (Invitrogen) as described previously (*19*). Twenty four hours later, the cells were

transfected with 0.5 μg each of Flag-Gβ1 or Flag-Gβ5 and HA-Gγ2 or HA-RGS7 in pcDNA3.1(+) using Lipofectamine 2000 according to the manufacturer's protocol (Invitrogen). The cells were harvested for subsequent immunoprecipitation experiments 72 hours later. Ten μg of cell lysate were immunoblotted with an anti-PhLP1 antibody (*35*) to assess the percent PhLP1 knockdown, and 20 μg were immunoblotted with anti-CCTζ and anti-CCTε antibodies (Santa Cruz Biotechnology) to determine the percent CCT knockdown.

Dominant interfering mutant experiments

HEK 293T cells were plated in 6-well plates and grown to 70-80% confluency. The cells were then transfected with Lipofectamine 2000 (Invitrogen) according to the manufacturer's instructions. Each well was transfected with 1.0 μg of either the empty vector control, wild-type PhLP1-myc, or PhLP1 Δ1-75-myc along with 1.0 μg each of the Flag-Gβ5 and HA-RGS7 cDNAs. The cells were harvested for immunoprecipitation 48 hours after transfection.

Immunoprecipitation experiments

Transfected HEK 293T cells were washed with phosphate-buffered saline (PBS) (Fisher) and solubilized in immunoprecipitation buffer (PBS pH 7.4, 2% NP-40 (Sigma), 0.6 mM PMSF, 6 μl/ml protease inhibitor cocktail per mL buffer (Sigma P8340). The lysates were passed through a 25-gauge needle 10 times and centrifuged at maximum speed for 10-12 minutes at 4ºC in an Eppendorf microfuge. The protein concentration for each sample was determined using the DC Protein Assay Kit II (Bio-Rad) and equal amounts of protein were used in the subsequent immunoprecipitations. Approximately 150 μg of total protein were used in

immunoprecipitations from cells in 12 well plates and 450 μg from cells in 6 well plates. The clarified lysates were incubated for 30 minutes at 4°C with 2.5 μg anti-Flag antibody (clone M2, Sigma), 1 μg anti-CCTε (clone PK/29/23/8d Serotec), 1.75 μg anti-myc (clone 9E10, BioMol), or 1.5 μg anti-HA (clone 3F10 Roche) for lysates from 12-well plates or with 6.25 μg of anti-Flag for lysates from 6-well plates. Next, 30 μl of a 50% slurry of Protein A/G Plus agarose (Santa Cruz Biotechnology) was added, and the mixture was incubated for 30 minutes at 4°C as described (*19*). The immunoprecipitated proteins were solubilized in SDS sample buffer and resolved on a 10% Tris-Glycine-SDS gel or a 16.5% Tris-Tricine-SDS gel for Gβ1γ2. The proteins were transferred to nitrocellulose and immunoblotted using an anti-Flag (clone M2, Sigma), anti-c-myc (BioMol), anti-HA (Roche), or an anti-PhLP1 antibody (*19*). Immunoblots were incubated with the appropriate anti-rabbit, anti-mouse, anti-goat (Li-Cor Biosciences), or anti-rat (Rockland) secondary antibody conjugated with an infrared dye. Blots were scanned using an Odyssey Infrared Imaging System (Li-Cor Biosciences), and protein band intensities were quantified using the Odyssey software. The data are presented as the mean value +/- standard error from at least three experiments.

Radiolabel pulse-chase assays

Radiolabel pulse-chase assays were preformed as previously described (*19*). Briefly, siRNA-treated or transfected HEK 293T cells in 12-well plates were washed once with 1.5 ml of methionine-free DMEM media (Mediatech) and then incubated in 1 ml of this same media at 37°C for 1 hour. The media was discarded and 400 μl of media supplemented with 200 μCi/ml radiolabeled L-[^{35}S] methionine (Perkin-Elmer)

was added. The cells were incubated in the radiolabeled media for 10 minutes at 23°C. Subsequently, the cells were washed once with 1.6 ml of DMEM media supplemented with 4 mM nonradiolabeled L-methionine (Sigma) and 4 μM cycloheximide to remove the radiolabeled media and then incubated in 0.8 ml of this same media at 23°C for the chase times indicated. After the chase periods, the cells were harvested for immunoprecipitation. Radiolabeled gels were visualized with a Storm 860 phosphorimager, and the band intensities were quantified using Image Quant software (GE Healthcare). The molar ratios were determined by normalizing the band intensities to the number of methionine residues found in Flag-Gβ1, HA-Gγ2, Flag-Gβ5, or HA-RGS7 and then calculating the ratios. The molar ratios were consistently substoichiometric, with the HA-Gγ2/Flag-Gβ1 ratio reaching ~ 0.4 by 60 minutes of chase (Fig. 3-6C) and the HA-RGS7/Gβ5 ratio reaching ~ 0.1 by 60 minutes of chase (Figs. 3-5A and 3-6B). The lower HA-RGS7/Gβ5 ratio probably results from less efficient synthesis and folding of the nascent RGS7 compared to nascent Gβ5. In addition, non-complexed Gβ5 may be more stable than other non-complexed Gβs. *In vitro* experiments have shown that Gβ5 is more stable in solution than other Gβs when neither are complexed with Gγ (*7*). The rate data for Gβγ and Gβ5-RGS7 assembly were fit to a first-order rate equation with background correction to determine the rate constant for assembly.

Protein purifications

Gβ1γ2, Gβ5γ2 and Gβ5-RGS9-1 were expressed and purified from insect cells. Recombinant baculovirus constructs were generously provided by Narasimhan Gautam of Washington University (Gβ1 (*91*)), James Garrison from the University of

Virginia (Gβ5 and Gγ2 (*92*)) and Ching-Kang Chen from Virginia Commonwealth University (RGS9-1 (*93*)). The Gγ2 subunit contained both a His_6 tag and a Flag epitope tag on the N-terminus. The RGS9-1 subunit contained only a Flag epitope tag on the C-terminus. Sf9 cells (GIBCO) were grown to a density of 2 x 10^6 cell/ml and then co-infected with a Gβ and Gγ2 or RGS9-1 baculovirus at an MOI of 5 for each virus type. Cells were grown in shaker culture for ~ 60 hours and were pelleted by centrifugation at 250 x g for 10 min. at 4°C. The supernatant was discarded and the cell pellet was snap frozen in liquid nitrogen and stored at -80°C.

Gβ1γ2 and Gβ5γ2 were purified by a modification of a previously described protocols (*92, 94*). The cell pellet from 1 L of cells was thawed and resuspended in 100 mL of Homogenization Buffer (20 mM HEPES pH 7.5, 3 mM $MgCl_2$, 150 mM NaCl, 2 μg/mL aprotinin, 2 μg/mL leupeptin, 2 μg/mL pepstatin, 20 μg/mL benzamidine and 0.1 mM PMSF). The suspension was sonicated with a tip sonicator on ice and centrifuged at 100,000 x g for 1 hour. The pellet was homogenized in 100 mL of Extraction Buffer (Homogenization Buffer + 0.1% polyoxyethylene 10 laurel ether) using a Dounce homogenizer and stirred on ice for 1 hour. The suspension was centrifuged again at 100,000 x g for 1 hour. The supernatant was collected and applied to a 5 mL M2 Flag agarose column (Sigma Aldrich) equilibrated in Extraction Buffer. The column was washed with 30 mL of Extraction Buffer and the Gβγ dimers were eluted with 15 mL of Flag Elution Buffer (Extraction Buffer plus 250 μg/mL Flag peptide). Fractions containing the purified dimers were combined and applied to a 2 mL Ni^{2+} NTA column (Novagen) equilibrated in Extraction Buffer plus 30 mM imidazole. The column was washed with 20 mL of this buffer and the

eluted with 10 mL of Extraction Buffer plus 500 mM imidazole. Fractions containing Gβγ were combined and dialyzed in Extraction Buffer plus 50% glycerol, which caused a 4-fold increase in protein concentration. Gβ5-RGS9-1 was purified the same way except the Ni^{2+} NTA column was skipped because the RGS9-1 protein did not contain a His_6 tag. This procedure generally resulted in ~ 1 mL of ~ 1 mg/mL protein that was 90% pure.

Metabolically labeled ^{35}S-PhLP1 was prepared by transforming DE3 *E. coli* cells with a PhLP1 pET15b vector (*22*) and inoculating 100 mL of M9 minimal media with a single colony of cells. The culture was incubated ~ 20 hours at 37°C until the absorbance at 600 nm reached 0.6-0.7. The cells were collected by centrifugation and resuspended in 100 mL of reduced Na_2SO_4 M9 minimal media. At this point, 12 mg of isopropyl-β-D-thiogalactopyranoside was added along with 500 μL of 2 mCi/mL [^{35}S]-H_2S0_4. The culture was grown for 3.5 hours at 37°C to an absorbance at 600 nm of ~1.0. The labeled PhLP1 was then purified as described previously (*22*).

In vitro binding assays

The binding of ^{35}S-PhLP1 to Gβγ or Gβ5-RGS9-1 dimers was determined by mixing 35 μL of a 50% slurry of M2 Flag agarose beads equilibrated in Assay Buffer (Extraction buffer without protease inhibitors) with purified Gβγ or Gβ5-RGS9-1 (final concentration 0.5 μM). The ^{35}S-PhLP1 was then added to the reaction mixture at final concentrations ranging from 0.01 μM to 2 μM in a total reaction volume of 150 μL. The reaction mixture was incubated on a rotator at 4°C for 1 hour. Each reaction was briefly vortexed and 50 μL of the mixture was counted in a scintillation counter to obtain the total amount of PhLP1 added. Each reaction was then

centrifuged for 1 min. at 1000 x g to separate the bound from the free ^{35}S-PhLP1. A 50 µL aliquot of the supernatant was then counted as described above to obtain the free counts. The free counts were subtracted from the total counts to determine the counts of bound ^{35}S-PhLP1. Non-specific binding was determined by running the assay in parallel with Flag-glutathione-S-transferase in place of Gβγ or Gβ5-RGS9-1. The specific binding was determined by subtracting the non-specific binding from the total binding. Counts were converted into concentration units using the specific activity of the ^{35}S-PhLP1. The concentration of specifically bound ^{35}S-PhLP1 was then plotted verses the free PhLP1 concentration, and the K_d for the interaction was determined by fitting the data to a one-to-one binding equation: $B = B_{max}/(1+K_d/[PhLP1])$; where B is the amount of PhLP1 bound to the beads, B_{max} is the maximal binding of PhLP1 and K_d is the dissociation constant for the interaction.

Results

An important question regarding the scope of PhLP1-mediated dimer assembly is whether PhLP1 assists in the formation of Gβ5-R7 RGS protein complexes. Gβ5 binds both CCT (*55*) and PhLP1 (Fig. 2-1) weakly compared to the other Gβ subunits, suggesting that CCT and PhLP1 may not be required for Gβ5-R7 RGS dimer assembly. To begin to address this issue, the effects of PhLP1 knockdown and PhLP1 Δ1-75 over-expression on the interaction of Gβ5 with RGS7 were assessed by co-immunoprecipitation as in Fig. 2-1. PhLP1 knockdown decreased both Gβ5 expression and RGS7 co-immunoprecipitation with Gβ5 by 40% (Fig. 3-3A). This result is in contrast to the Gβγ co-immunoprecipitation data which

showed a similar 40% decrease in Gβ1 and Gβ2 expression, but exhibited a much greater decrease (80-90%) in the amount of Gγ co-immunoprecipitating with Gβ upon PhLP1 knockdown (Figs. 2-1B and 2-3A). The results were similar in the dominant interference experiments (Fig. 3-3B). Over-expression of wildtype PhLP1 increased Gβ5 expression by ~2-fold over the empty vector control, as was observed with Gβ1 and Gβ2 (Figs. 2-2A and 2-4A). However, the proportional increase in co-immunoprecipitation seen with Gγ2 (Fig. 2-2A and 2-4A) was not observed with

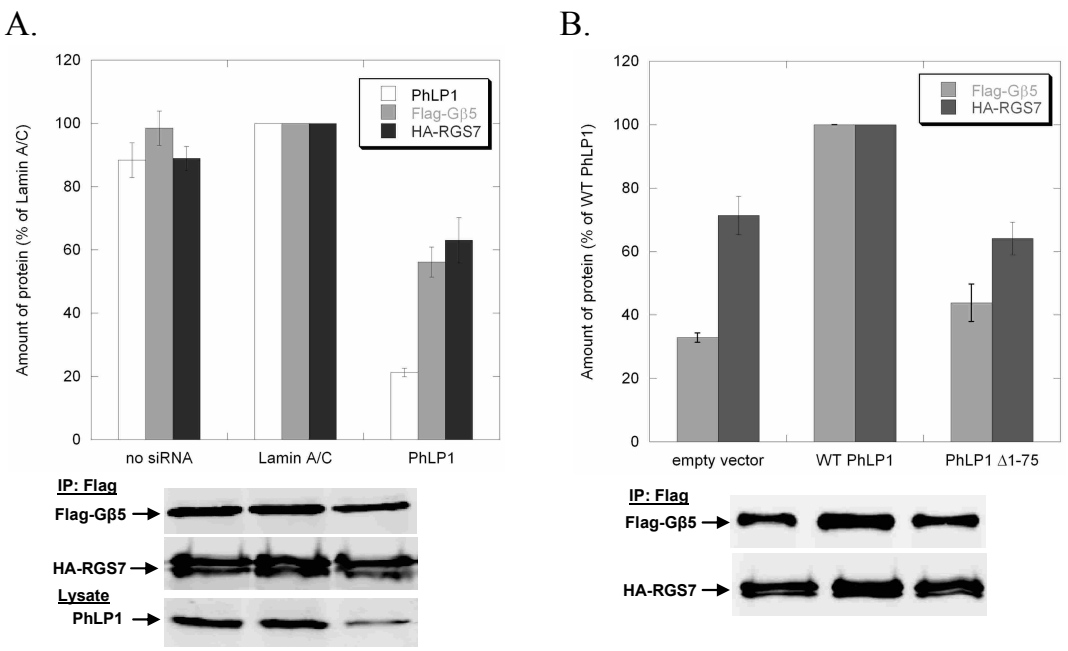

Fig. 3-3. Effects of PhLP1 on the assembly of RGS7 with Gβ5.
A) HEK 293T cells were treated with siRNA against PhLP1, lamin A/C, or no siRNA as indicated. Twenty-four hours later, cells were transfected with HA-RGS7 and Flag-Gβ5 cDNAs. After 72 additional hours, cells were lysed, immunoprecipitated with an anti-Flag antibody and immunoblotted with anti-Flag or anti-HA antibodies. Bands were quantified and expressed as a percentage of the lamin A/C control. PhLP1 knockdown was measured by quantifying the PhLP1 band intensity in immunoblots of 10 μg of whole cell lysate. B**)** Cells were transfected with either WT PhLP1, PhLP1 Δ1-75, or an empty vector control along with HA-RGS7 and Flag-Gβ5 cDNAs. After 48 hours, cells were lysed, immunoprecipitated with an anti-Flag antibody and immunoblotted with anti-Flag or anti-HA antibodies. Bands were quantified and expressed as a percentage of the wild-type PhLP1 control. Bars represent the average ± standard error from 3 separate experiments. Representative blots are shown below the graphs.

RGS7, which showed a much smaller increase. Moreover, overexpression of PhLP1 Δ1-75 did not cause the dramatic decrease in RGS7 co-immunoprecipitation that was observed with Gγ2 (Fig. 3-3B). These findings suggest that the effect of PhLP1 on the expression of Gβ5 is similar to the other Gβs but that PhLP1 may not be as important in Gβ5-RGS7 assembly as it is in Gβγ assembly.

The findings of Fig. 3-3 point to potentially significant differences between the mechanisms of Gβ5-RGS7 assembly and Gβγ assembly. Gβ5-RGS7 assembly was further investigated to better understand the role of PhLP1 and CCT in this process. If CCT were involved in Gβ5 folding, the two would have to interact, yet Gβ5 has been reported to bind CCT poorly *in vitro* (*55*). To further test the ability of Gβ5 to interact with CCT, the co-immunoprecipitation of overexpressed Gβ5 with endogenous CCT in HEK-293T cells was measured. Gβ5 was readily detected in the CCT immunoprecipitate, but the amount was 20-fold less than that of Gβ1 (Fig. 3-4A), confirming the finding that Gβ5 binds CCT much less than other Gβs. Importantly, coexpression of PhLP1 increased Gβ5 binding to CCT by nearly 10-fold (Fig. 3-4B), indicating that PhLP1 stabilizes the interaction of Gβ5 with CCT considerably. In contrast, co-expression of RGS7 had no effect on Gβ5 binding to CCT. These results are very different from the effect of PhLP1 and Gγ2 on Gβ1 binding to CCT in which both PhLP1 and Gγ2 contributed significantly to the release of Gβ1 from the CCT complex (*36*). Thus, it appears that the role of PhLP1 in the binding of Gβ1 and Gβ5 to CCT are opposite – with PhLP1 assisting in the release of a tightly binding Gβ1 while stabilizing the weak interaction of Gβ5.

To complete the investigation of CCT interacting partners in the Gβ5-RGS7 dimer, the binding of RGS7 was also measured by co-immunoprecipitation with CCT. No RGS7 bound CCT when RGS7 was over-expressed alone, but co-expression of Gβ5 caused a detectible amount of RGS7 to co-immunoprecipitate with CCT (Fig. 3-4C). In contrast, co-expression of PhLP1 with RGS7 did not cause RGS7 to bind CCT and coexpression of PhLP1 together with Gβ5 and RGS7 did not increase RGS7 co-immunoprecipitation with CCT. The total amount of RGS7 in the cell lysate also increased significantly upon Gβ5 coexpression, consistent with the fact that R7 RGS proteins require Gβ5 for stable expression in the cell (*86*). These results suggest that in the process of Gβ5-RGS7 assembly Gβ5 recruits RGS7 to CCT. The lack of effect of PhLP1 on RGS7 binding to CCT suggests that PhLP1 does not play a role in this recruitment. To further test this notion, RGS7 and PhLP1 were co-expressed with and without Gβ5 and their ability to co-immunoprecipitate each other was measured. Neither protein was found in the immunoprecipitate of the other in the presence or absence of Gβ5 (Fig. 3-4D), indicating that RGS7 and PhLP1 do not exist in any complexes together. From these binding experiments, it appears that PhLP1 stabilizes the interaction of Gβ5 with CCT and that Gβ5 recruits RGS7 to CCT, but only after PhLP1 has been released from the complex. The data from Figures 3-3 and 3-4 suggest that PhLP1 may be involved in the folding of Gβ5 by stabilizing its interaction with CCT but that PhLP1 may not participate in Gβ5-RGS7 assembly. This concept was further tested by measuring the effect of PhLP1 knockdown or over-expression on the rate of Gβ5-RGS7 dimerization. In these experiments, PhLP1 was either siRNA-depleted or over- expressed in HEK-293T

cells and the rate of Gβ5-RGS7 dimer formation was measured in a pulse chase experimental format (*19*). PhLP1 knockdown resulted in a two-fold decrease in the rate of Gβ5-RGS7 dimerization compared to a control siRNA (Fig. 3-5A), which is somewhat less than the five-fold decrease in the rate of Gβ1γ2 dimerization observed with a similar PhLP1 knockdown (*19*). In contrast, the effects of PhLP1 over-

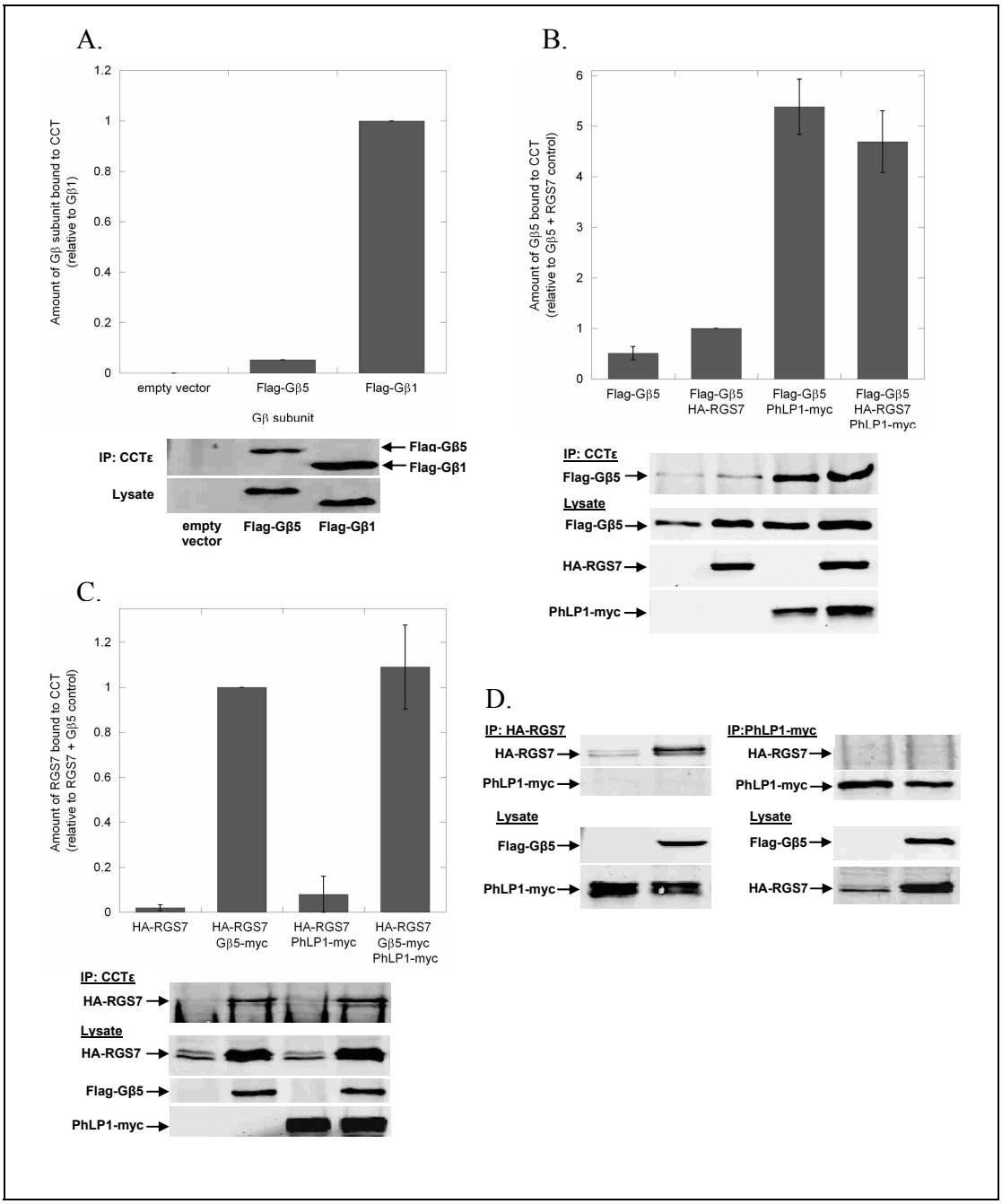

Fig. 3-4. Effects of PhLP1 and RGS7 on the binding of Gβ5 to CCT.
A) Binding of Gβ5 to CCT was compared to that of Gβ1 by co-immunoprecipitation. HEK 293T cells were transfected with cDNAs for Flag-Gβ1, Flag-Gβ5 or an empty vector control as indicated. After 48 hours, cells were lysed, immunoprecipitated with an anti-CCTε antibody and immunoblotted with anti-Flag antibodies. Bands were quantified and the binding of Gβ5 to CCT was expressed relative to that of Gβ1. Bars represent the average ± standard error from 3 separate experiments and representative blots are shown below the graphs. (The Gβ5 error bar is very small.) For all experiments A-D, the expression of each transfected cDNA was confirmed by immunoblotting 5 μg of whole cell lysate with the antibodies indicated. B) The effect of PhLP1 and RGS7 on the binding of Gβ5 to CCT was measured by co-immunoprecipitation as in panel A. Cells were transfected with the indicated cDNAs, and CCT was immunoprecipitated and immunoblotted for Flag-Gβ5. Bands were quantified and expressed relative to the Flag-Gβ5/HA-RGS7 sample. Data are from 8 separate experiments. C) The effects of PhLP1 and Gβ5 on RGS7 binding to CCT was measured by co-immunoprecipitation as in panel A. Cells were transfected with the indicated cDNAs and CCT was immunoprecipitated and immunoblotted for HA-RGS7. Bands were quantified and expressed relative to the Flag-Gβ5/HA-RGS7 sample. Data are from 3 separate experiments. D) The ability of PhLP1 and RGS7 to co-exist in CCT or other complexes was tested by co-immunoprecipitation. Cells were transfected with cDNAs to PhLP1-myc and HA-RGS7 with or without Flag-Gβ5, immunoprecipitated with anti-myc or anti-HA antibodies and immunoblotted with these same antibodies as indicated. The resulting blots are shown.

expression on the rate of Gβ5-RGS7 assembly were strikingly different than what was observed for Gβ1γ2 assembly. PhLP1 overexpression actually caused a small decrease in the rate of Gβ5-RGS7 assembly (Fig. 3-5B), while it resulted in a 4-fold increase in the rate of Gβ1γ2 assembly (*19*). Interestingly, PhLP1 overexpression increased the amount of Gβ5 produced during the 10 min. pulse by 40%, which in turn caused a small increase in RGS7 co-immunoprecipitation. However, the net effect was a decrease in the RGS7/Gβ5 ratio, indicating an inhibition of RGS7/Gβ5 dimer formation despite the fact that more Gβ5 was available for assembly. It is clear from these results that the role of PhLP1 in Gβ5-RGS7 assembly is much different than its role in Gβγ assembly. It appears that endogenous levels of PhLP1 may contribute to Gβ5-RGS7 assembly by stabilizing the interaction of Gβ5 with CCT,

but that excess PhLP1 inhibits Gβ5-RGS7 assembly, possibly by interfering with the Gβ5-RGS7 interaction.

The recently published structure of the Gβ5-RGS9 complex (*89*) suggests a possible reason for the observed inhibition of Gβ5-RGS7 assembly by excess PhLP1. In the structure, the Gγ-like domain interacts along the expected Gγ binding surface of Gβ5, opposite the predicted PhLP1 binding site (*89*). However, the N-terminal lobe of RGS9 interacts with Gβ5 on the same surface as PhLP1 (*32, 89*). This overlap may preclude the formation of a PhLP1-Gβ5-RGS7 complex analogous to the

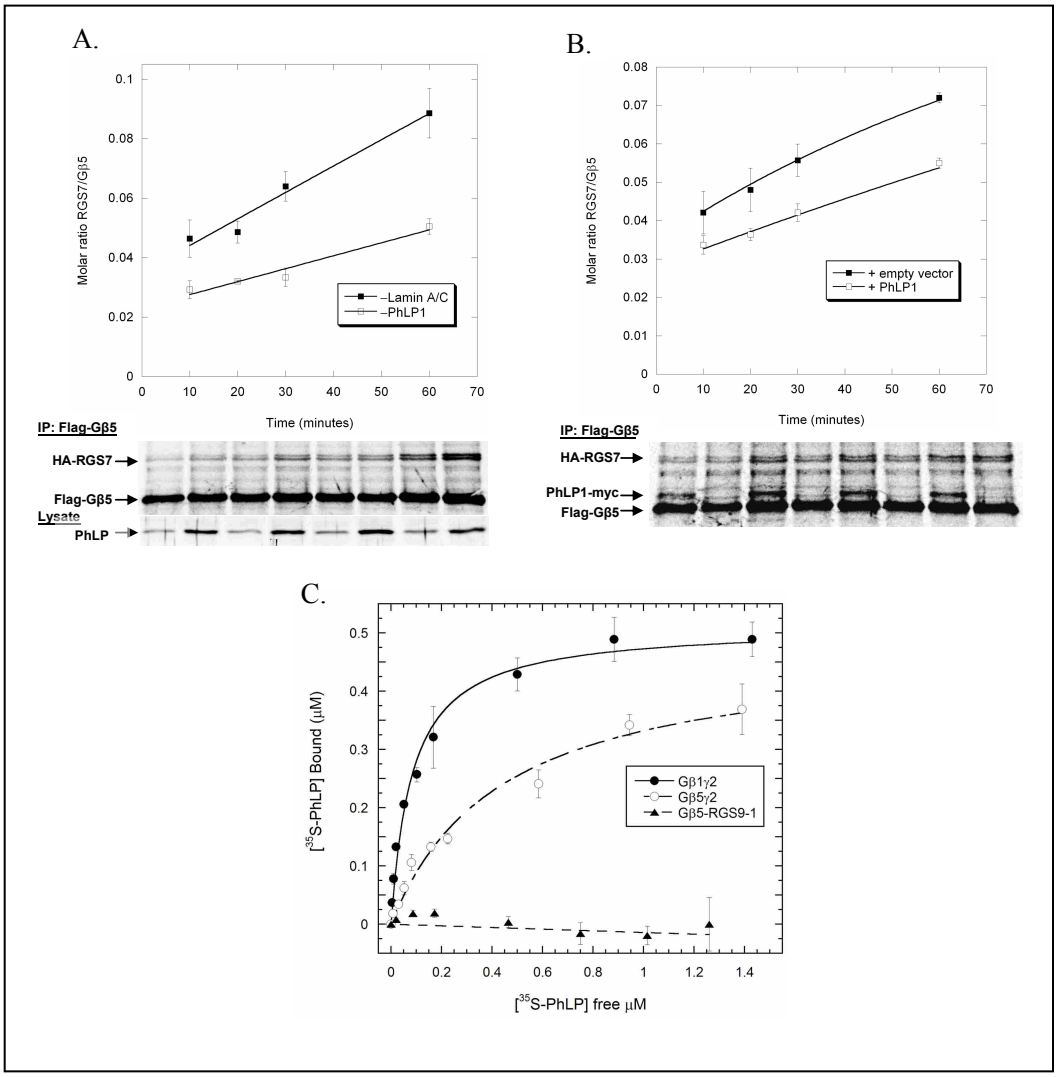

Fig. 3-5. Effects of PhLP1 on the rate of Gβ5-RGS7 dimer formation. A) The rate of Gβ5-RGS7 dimer assembly was measured in HEK-293T cells with or without PhLP1 knockdown. Cells were treated with PhLP1 or lamin A/C siRNAs as indicated. Twenty-four hours later, the cells were transfected with Flag-Gβ5 and HA-RGS7 cDNAs. After 72 additional hrs, nascent polypeptides were labeled for 10 min with [^{35}S] methionine and then chased with unlabeled methionine and cycloheximide. At the chase times indicated, the Flag-Gβ5 was immunoprecipitated and the proteins were separated by SDS-PAGE. The radioactive bands were visualized and quantified using a phosphorimager and the molar ratio of Gβ5 to RGS7 was calculated. The data points represent the average ± standard error from 3 separate experiments, and lines represent fits of the data to a first order rate equation. A representative gel is shown below the graph as is a PhLP1 immunoblot of 10 μg of whole cell lysate showing the degree of siRNA knockdown. B) HEK-293 cells were transfected with Flag-Gβ5 and HA-RGS7 with and without PhLP1-myc cDNAs for 48 hrs and the rate of Gβ5-RGS7 assembly was measured using the pulse-chase assay as in panel A. The data are from 3 separate experiments. C) The binding of the indicated concentrations of ^{35}S-PhLP1 to 0.5 μM purified Gβ1γ2 (●), Gβ5γ2 (○) or Gβ5-RGS9-1 (▲) was measured by *in vitro* co-immunoprecipitation (see Experimental Procedures). Symbols represent the average ± standard error from 3 separate experiments. Lines represent non-linear least squares fits of the data to a one-to-one binding equation. The fits yielded K_d values of 83 ± 13 nM for Gβ1γ2, 440 ± 70 nM for Gβ5γ2 and no measurable value for Gβ5-RGS9-1.

PhLP1-Gβγ complex that is believed to be an intermediate in Gβγ assembly (*19, 36*). To test this possibility, the binding of PhLP1 to the Gβ5-RGS9-1 complex was measured. An *in vitro* assay was preformed in which Gβ5-RGS9-1 was immobilized on Flag antibody-linked agarose beads via a Flag tag on the RGS9-1. Increasing concentrations of metabolically labeled ^{35}S-PhLP1 were added to the beads and allowed to reach equilibrium. The beads were pelleted and the amount of bound and free ^{35}S-PhLP1 was determined. The results show that indeed there was no measurable binding of PhLP1 to Gβ5-RGS9-1 (Fig. 3-5C). In contrast, PhLP1 readily bound Gβ1γ2 and to a lesser extent Gβ5γ2 in this assay. The dissociation constants for the interactions were 83 ± 13 nM for Gβ1γ2 and 440 ± 72 nM for Gβ5γ2. The K_d for Gβ1γ2 binding is similar to the 107 nM K_d reported previously for the PhLP1-Gβ1γ1 interaction using surface plasmon resonance methods (*22*), so the assay appears to be measuring the binding accurately. The inability of Gβ5-

RGS9-1 to bind PhLP1 suggests that excess PhLP1 interferes with Gβ5-RGS7 dimer formation because it binds Gβ5 in a manner that does not allow RGS7 to simultaneously interact.

The binding of Gβ5 to CCT and the Gβ5-dependent recruitment of RGS7 to CCT suggest an important role for CCT in the Gβ5-RGS7 assembly process. This possibility was tested further by measuring the effect of CCT knockdown on the rate of Gβ5-RGS7 dimerization using the pulse/chase assay. An siRNA to CCTζ that results in a substantial knockdown of CCT complexes has been reported (*90, 95*). Using this siRNA, CCTζ expression was decreased by 50% in HEK-293T cells (Fig. 3-6A). In addition, expression of the CCTε subunit was also decreased by a similar amount (Fig. 3-6A), indicating that expression of the entire CCT complex was reduced by 50%. This reduction in CCT resulted in a proportional decrease in the rate of Gβ5-RGS7 assembly of 50% (Fig. 3-6B), suggesting that Gβ5-RGS7 assembly is very dependent on CCT. For comparison, the effect of this CCT knockdown on Gβγ assembly, which is expected to be CCT-dependent (*36, 55*), was also measured. The 50% reduction in CCT caused a similar 50% decrease in the rate of Gβγ assembly (Fig. 3-6C), confirming the importance of CCT in Gβγ formation. The striking similarity of these effects of CCT knockdown on the rates of both Gβ5-RGS7 and Gβγ dimerization show that Gβ5-RGS7 assembly is just as dependent on CCT as Gβγ assembly. Together, the data in Figs. 3-5 and 3-6 indicate a similar role for CCT in both Gβ5-RGS7 and Gβγ assembly, but a much less critical role for PhLP1 in Gβ5-RGS7 assembly compared to its essential role in Gβγ assembly.

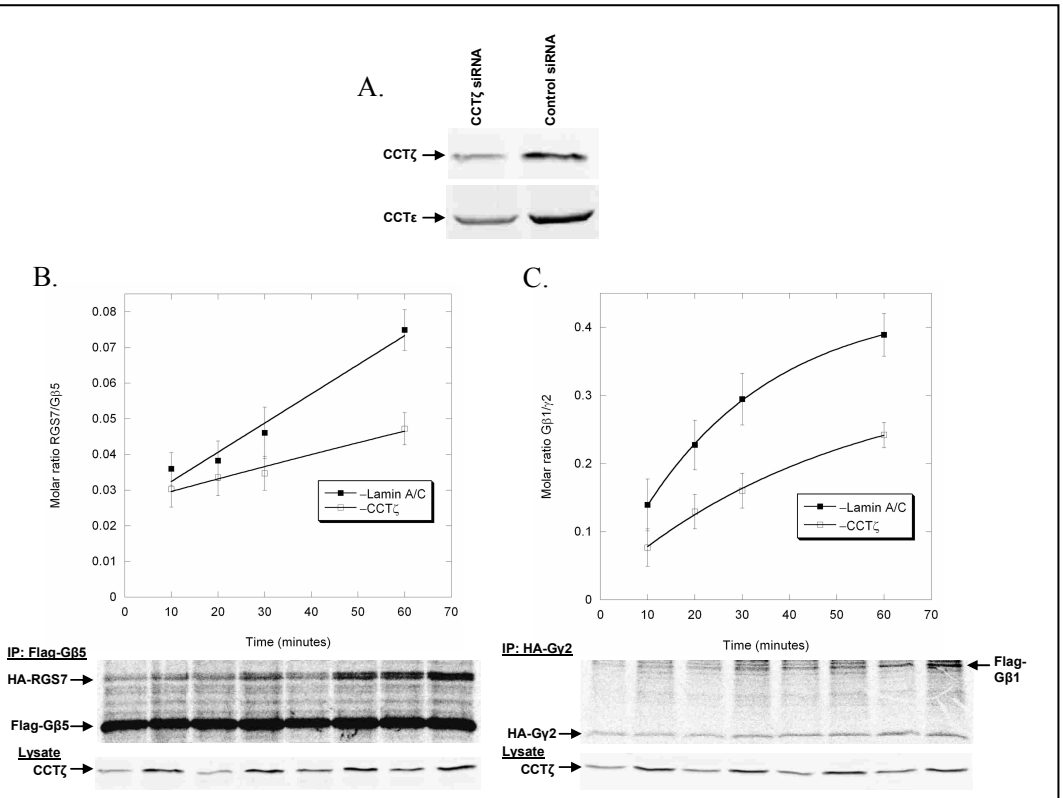

Fig. 3-6. Effects of CCT on the rate of Gβ5-RGS7 dimer formation.
A) HEK-293T cells were treated with CCTζ or lamin A/C siRNA for 96 hrs and the expression of CCTζ and CCTε was measured by immunoblotting 20 μg of whole cell lysate. Representative blots are shown. B) The rate of Gβ5-RGS7 dimer assembly was measured in HEK-293T cells with or without CCTζ knockdown as in Fig. 8A. The data are from 3 separate experiments. C) The rate of Gβ1γ2 dimer assembly was measured in HEK-293T cells with or without CCTζ knockdown as in Fig. 8A. The data are from 3 separate experiments.

Discussion

Mechanistic studies have thus far focused on the most common Gβ1γ2 dimer combination and have not addressed whether this assembly mechanism applies to Gβ5-RGS dimmer formation. The data presented here suggest a very different assembly mechanism for Gβ5-RGS7 dimers than that of Gβγ. An outline of a possible mechanism for Gβ5-RGS7 assembly that is consistent with the data

presented is depicted in Fig. 3-7. The decrease in the rate of Gβ5-RGS7 assembly upon siRNA mediated CCT knockdown (Fig. 3-6B) indicates that CCT is involved in the assembly process, most likely by folding the nascent Gβ5 despite the weak interaction of Gβ5 with CCT. Likewise, the decrease in the rate of Gβ5-RGS7 assembly upon PhLP1 knockdown (Fig. 3-5A) shows that PhLP1 also contributes to the assembly process, possibly by increasing the efficiency of Gβ5 folding by increasing the binding of Gβ5 to CCT through the formation of a stable PhLP1-Gβ5-CCT ternary complex (Fig. 3-4B). However, the decrease in the rate of Gβ5-RGS7 assembly upon over-expression of PhLP1 (Fig. 3-5B) indicates that excess PhLP1 interferes with the assembly process. A logical explanation of this effect is that PhLP1 must be released from Gβ5 prior to its interaction with RGS7 and that excess PhLP1 blocks the association of RGS7 with Gβ5. Once PhLP1 is released, it appears that RGS7 can associate with Gβ5 while still bound to CCT, given the fact that Gβ5 initiates the co-immunoprecipitation of RGS7 with CCT (Fig. 3-4C). Once formed, the Gβ5-RGS7 complex would be expected to readily release from CCT because of the relatively weak interaction of the complex with CCT (Fig. 3-4B and C). The folded and assembled Gβ5-RGS7 complex would then be able to interact with its R7 anchoring protein and with its Gα targets.

The unique roles for PhLP1 in Gβ5-RGS7 verses Gβγ dimer formation can be understood by examining the structures of the complexes. In the case of Gβγ, the Gγ binding surface is on the opposite side of Gβ from the principle PhLP1 binding surface (*32*), allowing PhLP1 and Gγ to interact with Gβ simultaneously. It has been proposed that this configuration allows nascent Gγ to associate with Gβ while the Gβ

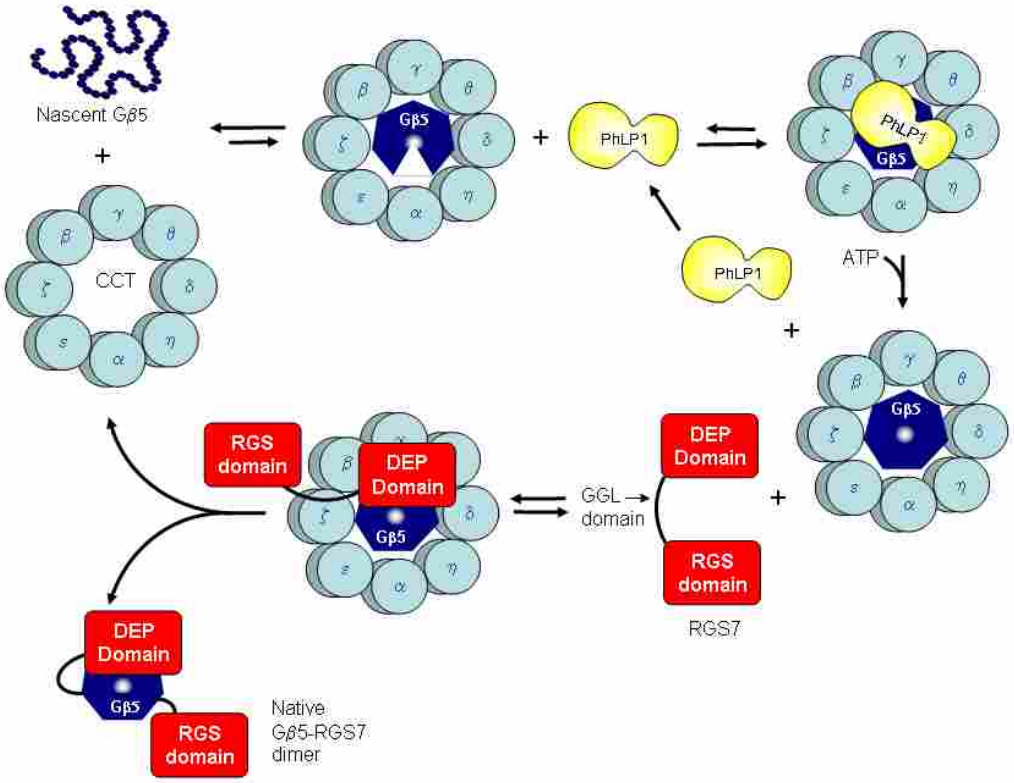

Fig. 3-7. Proposed Model of Gβ5-RGS7 assembly.
A speculative model of the mechanism of Gβ5-RGS7 assembly that is consistent with current data is depicted. In this model, Gβ5 binds CCT, but is unable to fold into its seven-bladed β-propeller structure (illustrated by the gap in the Gβ5 heptagon) without PhLP1. PhLP1 binding increases the interaction of Gβ5 with CCT, allowing folding to occur (Fig. 7B). PhLP1 is then released, perhaps by ATP binding to CCT. The folded Gβ5 is then able to interact with RGS7 on CCT. The initial interaction is most likely via its N-terminal DEP/DHEX domain because this domain binds the same face of Gβ5 as PhLP1 (*89*). Once formed, the Gβ5-RGS7 can release from CCT as a functionally active dimer.

β-propeller is being stabilized by PhLP1 (*36*). In the case of Gβ5-RGS9, the N-terminal lobe of RGS9 covers a 2600 Å2 area on the same face of Gβ5 (*89*) predicted to bind PhLP1, based on the phosducin-Gβ1γ1 structure (*32*). In fact, several residues of Gβ5 that contact the N-terminal lobe of RGS9 are also expected to contact PhLP1 (*32, 89*). Because of this overlap, assembly of the Gβ5-RGS complex apparently can not proceed through a PhLP1-Gβ5-RGS intermediate. A question that is not clear

from the structures is how PhLP1 assists in the release of Gβ1 from CCT, while it stabilizes the binding of Gβ5 to CCT. More structural information on the PhLP1-Gβ-CCT complexes for both the Gβ1 and Gβ5 complexes would be required to understand the underling molecular basis for these disparate binding properties. Perhaps the differences lie more in the interactions of the Gβ subunits with CCT, with Gβ1 making high-affinity contacts and Gβ5 making only low-affinity contacts in the absence of PhLP1. Upon PhLP1 binding, it is possible that both Gβ1 and Gβ5 form a similar complex with CCT in which the high-affinity contacts of Gβ1 have been lost but indirect contacts with CCT through PhLP1 have been gained, thereby increasing the binding of Gβ5 to CCT.

In conclusion, this work expands the role of PhLP1 and CCT as essential chaperones in the folding and assembly of the Gβ5-RGS7 dimer. The Gβ5-RGS7 assembly mechanism is similar to Gβγ assembly in its CCT dependence but differs significantly in its PhLP1 dependence. The data provide additional insight into the intricate means by which the cell utilizes its molecular chaperones to bring the unstable β-propeller fold of the Gβ5 subunit together with the complementary RGS protein to create stable Gβ5-RGS7 dimers to perform their vital functions in G protein signaling.

CHAPTER 4:

PhLP2 FUNCTION AND PHOSPHORYLATION

Introduction

PhLP2, an essential protein, is a member of the Pdc family

Proteins in the phosducin II subfamily were revealed in an analysis of 33 phosducin family protein sequences from different organisms. Pdc and PhLP1 were classified as subfamily I proteins, while PhLP2 and PhLP3 were assigned to subfamilies II and III, respectively (*21*). All Pdc family proteins contain a central thioredoxin-like domain and a charged C-terminus, but differ in their N-terminal regions (*21*). Strikingly, PhLP2 proteins were found to be essential in *Saccharomyces cerevisiae* (*29*) and *Dictyostelium discoideum* (*21*). Deletion of *phlp2* in yeast yielded spore products which failed to grow while disruption of the gene in *Dictyostelium* caused a decreasing growth rate and simultaneous collapse of the cell culture after 16-17 cell divisions (*21, 29*). A unique function for PhLP2A in comparison to other members of the Pdc family was confirmed when overexpression of yeast PhLP3 was not able to complement the *phlp2*Δ mutation (*29*), and deletion of *phlp1* in *Dictyostelium* led to a phenotype similar to Gβ deletion rather than inviability (*21*). Conversely, expression of a mouse *phlp2* gene was able to complement the defects of the *phlp2*Δ mutant in yeast, indicating an evolutionarily conserved function from yeast to mammals (*27*).

PhLP2 does not participate in G protein signaling

When PhLP2 was first discovered, it was unknown whether or not it would play a role in G protein signaling because unlike like Pdc or PhLP1, PhLP2 does not contain an 11-amino acid Gβγ binding sequence in its N-terminal domain (*21*). Additionally, of the 32 total Pdc amino acids known to bind Gβγ in *Dictyostelium*, only 10 of these are conserved in PhLP2 (*21*). Accordingly, initial empirical results proved that PhLP2 bound Gβγ very weakly in yeast (*29*). Further evidence for a distinctive PhLP2 function was found when it was revealed that PhLP2 was not involved in the pheromone-induced G protein mating response in yeast. Upon pheromone induced GPCR activation, Gα and Gβγ dissociate and Gβγ activates a downstream MAP kinase signaling cascade in which the MAP kinase kinase Ste7 is involved. Many cellular responses ensue and among them is a cell cycle arrest in the G1 phase which is required to synchronize the cell cycles of the two mating partners (*96*). Normally, the G1 arrest is short lived and the cell cycle resumes as the mating process completes. However, if Gα is mutated so that it cannot bind and inhibit Gβγ signaling, constitutive G1 arrest occurs due to sustained Gβγ activation of the MAP kinase pathway. This type of arrest can be rescued by a loss-of-function mutation in the *ste7* gene which stops downstream activation (*96*). When PhLP2 was overexpressed in yeast, there was no defective or heightened G protein-dependent mating response seen in response to pheromone (*29*), and similarly, yeast *phlp2* temperature sensitive mutants showed no change in their sensitivity to pheromone response at restrictive temperature (*58*). G1-S growth arrest was observed in *phlp2*Δ mutants before death, but was unrelated to the growth arrest seen in response to

pheromone-induced G protein activation since *phlp2* Δ arrested cells could not be rescued by a *ste7* loss-of-function mutation (*29*). Altogether, these results led to the hypothesis that PhLP2 has a separate function from Pdc or PhLP1 in that it does not participate in G protein signaling.

PhLP2 is a co-chaperone with CCT in the folding of essential proteins

Nevertheless, like PhLP1, PhLP2 is capable of binding to CCT (*58, 97, 98*). CCT is an essential cytosolic chaperonin which folds two well characterized substrates, actin and tubulin, and other substrates with some containing high β-sheet content which are difficult to fold (*48, 50, 51, 53, 99*). It is hypothesized that PhLP2 binds CCT in a manner analogous to PhLP1 or prefoldin, that is, as a co-chaperone in its native form, and not as a folding substrate (*38, 52, 53, 58*). Due to its essential function, it was thought that PhLP2 could act as a co-chaperone with CCT in the folding of one or more essential proteins. However, since no function for PhLP2 in G protein signaling was found, it is unknown which essential proteins could be PhLP2 folding substrates. Recently, evidence for a role in folding actin, tubulin, some cell cycle proteins, and possibly even apoptotic proteins was established using temperature sensitive yeast mutants and siRNA mediated PhLP2 knockdown (*28, 58*).

Because PhLP2 is essential in yeast, its function was studied by way of temperature sensitive mutants (*phlp2-ts*) (*58*). The molecular basis for the temperature sensitivity was unknown, but these mutants grew well at permissible temperatures with normal PhLP2 function but began to show PhLP2-related defects at higher, non-permissible temperatures. Among the defects were a heightened sensitivity to the microfilament disrupting drug latrunculin, and a modest sensitivity

to the microtubule disrupting drug benomyl, indicating that the *phlp2-ts* mutants had predisposed defects in actin and possibly tubulin organization (*58*). Disrupted actin function or polymerization was again suggested by the observation that the *phlp2-ts* mutant cells were significantly larger than wild type cells at both the permissible and non-permissible temperatures, and furthermore, the *phlp2-ts* cells displayed budding defects, improper nucleus segregation, multi-nucleated and anucleated cells, and the abolishment of actin cables at the non-permissible temperatures (*58*). Thus, the *phlp2-ts* mutant defects gave strong evidence for a PhLP2 role in actin folding, and some evidence for a role in tubulin folding. *In vitro*, human PhLP2A bound actin and tubulin, but was shown to only bind actin indirectly. PhLP2A only associated with actin when it was found in a PhLP2A-actin-CCT ternary complex (*58*). Strangely, *in vitro* actin folding was inhibited by the addition of PhLP2 to the complex, even though PhLP2 increased the amount of actin bound to CCT and prefoldin (*58*). The discrepancies between *in vivo* and *in vitro* observations are probably due an overabundance of PhLP2 which may lead to an inhibitory role as an overabundance of PhLP1 is able to inhibit Gβγ assembly (*17*). The PhLP2:CCT ratio was 100:1 in the *in vitro* experiments whereas a global analysis of protein expression in yeast revealed that the ratio is about 1:1 *in vivo* (*58, 100*). A lack of folding cofactors, or PhLP2A phosphorylation not present in the *in vitro* system may have also led to actin folding inhibition.

In addition to actin defects, the yeast *phlp2-ts* mutants were inhibited at the G1-S cell cycle transition with a significant delay in DNA replication at non-permissible temperatures (*58, 100*). The G1-S delay seen in the *phlp2-ts* mutants was

rescued by overexpression of several genes known to promote G1-S transition thus showing that driving cells through G1-S helped to relieve the *phlp2-ts* cell cycle defects (*58*). This finding, along with the fact that entry into S phase occurs independent of actin function (*101*), led to the belief that PhLP2 is involved in the folding of proteins involved in yeast cell cycle progression such as CDC20, CDH1, CDC55 (*58*). Interestingly, PhLP2 was shown in two separate yeast-two hybrid assays to bind to the bait protein CSM1, which is involved in DNA replication and binds several members of the mini chromosome maintenance (MCM) prereplicative complex. (*102, 103*). The MCM complex forms a ring structure and possesses DNA helicase activity required for the initiation of eukaryotic DNA replication (*103*). The reason for the PhLP2-CSM1 interaction was not determined, but it may link PhLP2 to DNA replication. And finally, PhLP2 was implicated in apoptosis when PhLP2 was shown to be ubiquitinated by an inhibitor of apoptosis protein (IAP) and siRNA-mediated PhLP2 knockdown in HEK 293T cells led to an inability to process caspase-3 following Bax-induced cell death (*28*).

PhLP2A and CCT mutants display similar phenotypes

Temperature sensitive cct (*cct-ts*) or *phlp2-ts* mutants exhibit similar phenotypes in yeast indicating that their functions are cooperative. Like *phlp2-ts* mutants, *cct-ts* mutants showed cytoskeletal disorganization at restrictive temperatures (*58, 104*). Specific CCT subunits are responsible for binding certain substrates, and therefore, mutations in different CCT subunits produced different abnormalities in actin and microtubule organization. Yeast harboring a temperature sensitive mutation separately to each CCT subunit exhibited phenotypes with

differing severities in actin and tubulin malfunction (*104*). Interestingly, like *phlp2-ts* mutants, the *cctδ-ts* mutants exhibited phenotypes indicative of altered actin assembly, but were nearly normal in their microtubule organization with only a small percentage of cells showing signs of abnormal microtubule organization (*104*). PhLP2 and CCT are both necessary for normal progression through the G1-S transition of the cell cycle and significant CCT activity is required for cell cycle progression as indicated by the observation that maximal CCT protein and mRNA levels were observed at the G1-S transition (*90, 105*). Moreover, when CCT holocomplex levels were reduced via siRNA, or CCT-substrate interactions were slowed by the addition of an anti-CCT monoclonal antibody, progression through G1-S was severely impaired (*90*). This data provides evidence for a model in which PhLP2 participates in the folding of several essential CCT substrates especially actin, tubulin, and proteins necessary for the G1-S transition.

PhLP2B binds 14-3-3 proteins

In mammals, there are two PhLP2 proteins, PhLP2A and PhLP2B, which share 57% sequence homology, but differ in expression patterns (*21, 27*). PhLP2A is ubiquitously expressed, but PhLP2B is only found in male and female germ-cells undergoing meiotic maturation (*27*). The sequence similarities and spacial expression differences led to the belief that PhLP2A and PhLP2B have parallel, albeit tissue-specific functions. PhLP2B was found to co-immunoprecipitate with 14-3-3 proteins from mouse testicular protein extracts (*27*). 14-3-3 binding usually occurs at consensus binding sites such as RSXS*XP, RX(Y/F)XS*XP (S* denotes a phophoserine and X is any amino acid), or other similar sites (*106*). Therefore, it was

proposed that 14-3-3 bound to the RSSVP motif, amino acids 119-123, of mouse PhLP2B (*27*). In human PhLP2B, the 14-3-3 binding sequence is conserved as RSSIP, amino acids 119-123, but human PhLP2A only retains the last two residues of this sequence with no preceding serines so its ability to bind 14-3-3 was unknown.

Evidence for phosphorylation sites on PhLP2A

PhLP2A is an established phosphoprotein (*28*). Because it is a member of the Pdc family, and Pdc activity is regulated by phosphorylation (*36, 107*), it was hypothesized that PhLP2A folding function might also be regulated by phosphorylation. The kinase CK2 phosphorylates serine or threonine residues that are N-terminal to acidic amino acids usually found in the consensus sequence S*/T*XXE/D. Several putative CK2 phosphorylation sites were identified in PhLP2A using a ProSite scan. These sites are: S25, T47, T52, S98, T190, T206, S234, and S236. A mouse proteome phosphorylation site database developed by Steven Gygi and his lab found three empirical phosphorylation sites on mouse PhLP2A: S65, S235, and S237 (*108*). The S65 site is not conserved in human PhLP2 proteins, but S235 and S237 are conserved as S234 and S236 in human PhLP2A and PhLP2B.

This chapter explains how immunoprecipitation and mass spectrometry were used to identify possible PhLP2A folding substrates and identify PhLP2A phosphorylation sites. The immunoprecipitations shown in Figure 4-3 were done by Amy J. Gray, and the phosphorylation site identification by mass spectrometry work was done by Zhaoyuan Chen in collaboration with the laboratory of Dr. Craig Thulin.

Experimental Procedures

Cell Culture

HEK 293T cells were cultured in Dulbecco's modified Eagle's medium/F-12 (50/50 mix) growth media with L-Glutamine and 15mM HEPES, supplemented with 10% fetal bovine serum (Sigma). The cells were subcultured regularly to maintain active growth but were not used beyond 20-25 passages.

Preparation of cDNA Constructs

Human PhLP1, PhLP1-TEV, PhLP2A, PhLP2A-TEV, PhLP2B, PhLP3, 14-3-3-Flag, rat Pdc, and Pdc-TEV with 3′ c-myc and His_6 tags were cloned into pcDNA3.1/myc-His B vector (Invitrogen). The PhLP1 and rat Pdc constructs were made as described (*19*). A TEV cleavage sequence (Glu-Asn-Leu-Tyr-Phe-Gln-Gly) was added to the 3′ end of Pdc, PhLP1 and PhLP2A using PCR, and the sequences were cloned into the pcDNA3.1/myc-His B vector's multiple cloning site using the 5′ EcoRI and 3′ XbaI restriction sites for Pdc and PhLP1, and the 5′ BamHI and 3′ XbaI sites for PhLP2A. Both the PhLP2B and PhLP3 sequences (Open Biosystems) were cloned into the pcDNA3.1/myc-His B vector using the 5′ EcoRI and 3′ XbaI sites. All Pdc family genes were cloned into the pcDNA3.1/myc-His B vector in frame with the 3′ myc-His_6 vector sequence. A Flag-tag was added to 3′ end of the human 14-3-3ε sequence (Open Biosystems) by PCR and the sequence was cloned into pcDNA3.1/myc-His B via the 5′ EcoRI and 3′ XbaI sites. The human PhLP2A gene was cloned into the pETDuet-1 vector (Novagen) at multiple cloning site 1 via the 5′ BamHI and 3′ HindIII sites in frame with the 5′ His_6 tag. The integrity of each construct was validated by automated DNA sequencing and analysis.

Transient Transfections

HEK 293T cells were plated in 6-well plates so that they were 70-80% confluent the next day. The cells were then separately transfected with 1.0 μg of empty vector, Pdc, PhLP1, PhLP2A, PhLP2B, or PhLP3 in pcDNA3.1/myc-His B using Lipofectamine Plus Reagent according to the manufacturer's protocol (Invitrogen). For co-transfections involving 14-3-3ε and PhLP2A or transfections involving 14-3-3ε or empty vector, 1.0 μg 14-3-3ε and 1.0 μg PhLP2A, or 1.0 μg 14-3-3ε or the empty vector each in pcDNA3.1/myc-His B were transfected using Lipofectamine 2000 Reagent (Invitrogen) according to the manufacturer's directions.

For transfections that were subsequently used for mass spec analysis, HEK 293T cells were plated in 60-mm dishes so that they were 70-80% confluent on the next day. The cells were transfected with 2.5 μg each of empty vector, Pdc-TEV, PhLP1-TEV, or PhLP2A-TEV in pcDNA3.1/myc-His B using Lipofectamine Plus Reagent (Invitrogen). Twenty-four hours later, 2 ml of fresh media was added to each well of the 6-well plate and 5 ml of media was added to each 60-mm dish. For all transfections, the cells were used in subsequent immunoprecipitations 48 hours after transfection.

Immunoprecipitation Experiments

Transfected HEK-293T cells were washed twice with phosphate-buffered saline (PBS, Fisher) and solubilized in immunoprecipitation buffer (PBS, pH 7.4, 2% Igepal (Sigma), 0.6 mM PMSF, and 6 μl mammalian protease inhibitor cocktail (Sigma)/ml of buffer. The lysates were triterated 10-12 times through a 25 gauge needle and centrifuged at maximum speed in an Eppendorf microfuge for 10 minutes

at 4°C. The clarified lysates were incubated for 30 minutes at 4°C with 3.5 µg of anti-c-myc (clone 9E10, BioMol), or 7.5 µg anti-Flag (clone M2, Sigma), or 2.0 µg anti-CCTε (PK/29/23/8d, AbD Serotec) antibody for lysates from a 6-well plate, and 8.75 µg of the same anti-myc antibody for lysates from a 60-mm dish. Twenty µl (6-well plate) or 30 µl (60-mm dish) of a 50% slurry of Protein A/G Plus agarose (Santa Cruz Biotechnology) was added to each sample and then incubated for an additional 30 minutes at 4°C. For immunoprecipitations used for immunoblotting, the precipitate was solubilized in undiluted 4X SDS sample buffer, resolved on a 10% Tris-Glycine-SDS gel, and then blotted onto nitrocellulose. The blots were probed using the anti-c-myc, anti-Flag, or anti-CCTε antibodies described above, or a rabbit polyclonal anti-Gβ1 antibody. Immunoblots were developed with the ECL Plus chemiluminescence reagent (Amersham) and visualized with a Storm 860 phosphorimager or incubated with a secondary antibody conjugated to an infrared dye and visualized using the Li-Cor Odyssey Infrared Imaging System.

Mass spec sample preparation

For immunoprecipitations used for mass spec analysis, the washed protein A/G beads were resuspended in 150 µl AcTEV protease cleavage buffer with 30 units AcTEV protease (Invitrogen) and incubated for 16 hours at 4°C to cleave PhLP2A and co-immunoprecipitating proteins off the beads. Next, each supernatant was reduced with DTT at a final concentration of 4 mM at 60°C for 15 minutes. After the samples had cooled to room temperature, the proteins were alkylated by addition of iodoacetamide at a final concentration of 10 mM and incubated at room temperature for 15 minutes in the dark. The proteins were then acetone precipitated with Acetone-

HCL (one drop HCL in 10 ml acetone) at a ratio of 9 parts Acetone-HCl to 1 part sample and incubated at -80°C for 16 hours. The precipitated proteins were pelleted at maximum speed in an Eppendorf microfuge for 20 minutes at 4°C. The supernatant was removed, and the pelleted proteins dried at room temperature for 20 minutes with the tube lying on its side to prevent dust contamination. The pellet was rehydrated in 20 µl of 8M urea and an additional 73 µl of 25 mM ammonium bicarbonate and 7 µg sequencing grade modified trypsin (Promega) were added. The trypsin digest was incubated for 20 hours at 37°C in a rocking oven and the reaction was quenched by the addition of 1 µl 88% formic acid followed by water bath sonication for 20 minutes. The samples were stored at -20°C until they were used for mass spec analysis.

Protein Expression and Purification

His_6-PhLP2A in pETDuet-1 was transformed into *Escherichia coli* DE3 cells by heat shock. The cells were grown overnight at 37°C in a shaker-incubator and then His_6-PhLP2A protein expression was induced by the addition of isopropyl β-D-1-thiogalactopyranoside (IPTG) at a final concentration of 500 µM and cells were grown for another 3 hours at 37°C. The expressed protein was purified using a Pro-bond nickel chelate column (Invitrogen). The resulting purified protein was exchanged into 20 mM HEPES, pH 7.2, 150 mM NaCl buffer using an Amicon Ultra centrifuge concentrator (Millipore) and protein concentration was assayed using the Coomassie Plus protein assay reagent (Pierce). The protein was stored with 50% glycerol at -20°C.

CK2 Phosphorylation of PhLP2A

PhLP2A was prepared as a non-phosphorylated sample and a CK2 phosphorylated sample. To phosphorylate PhLP2A, a 300 µg amount of purified protein was phosphorylated by CK2 (10 units/µl, Calbiochem) in 20 mM HEPES, pH 7.5, 100 mM KCl, 20 mM NaCl, 5mM $MgCl_2$, 5 mM dithiothreitol, and 1 mM ATP for 1 hour at 37°C (*36*). The non-phosphorylated sample was treated with calf intestinal alkaline phosphatase (1 unit/µl, Invitrogen) according to the manufacturer's instructions for 1 hour at 37°C to make sure that the non-phosphorylated sample protein was completely non-phosphorylated. Both protein samples were digested with sequencing grade modified trypsin for 20 hours at 37°C in a rocking oven.

TiO_2 phosphopeptide enrichment

The phosphorylated PhLP2A peptides were enriched by running 10 µg of the peptides through a MonoTip TiO Pipette Tip (GL Sciences) according to the manufacturer's instructions. The TiO_2 microtip was preconditioned in acetonitrile, conditioned in 0.2 M phosphate buffer, pH 7.0, and equilibrated in a 50% aqueous acetonitrile solution with 1% formic acid. The phosphopeptides were adsorbed to the matrix by pipeting 20 times through the tip. Non-phosphorylated peptides were rinsed off the matrix using a 50% aqueous acetonitrile solution with 0.1% formic acid and 0.1 M KCl, and phosphopeptides were eluted with 0.2 M phosphate buffer, pH 7.0.

Mass Spectrometric Analyses

Tryptic peptides from the Pdc family co-immunoprecipitations and *in vitro* CK2 phosphorylated PhLP2A and non-phosphorylated samples were analyzed by LCMSMS using an Applied Biosystems API Qstar Pulsar i quadrapole orthogonal time-of –flight mass spectrometer with an online LC Packings (Dionex) UltiMaste

Plus Capillary LC System and ionspray source. Tryptic digests of each protein sample were run through a 15 cm x 250 μm-i.d. column hand-packed with Jupiter C18 10 μm reverse phase resin (Phenomenex). An initial gradient of 2.2%/min to a concentration of 60% acetonitrile in 0.1% formic acid was applied to the column, followed by a 3.5%/minute gradient up to a concentration of 95% organic phase. The HPLC was controlled by the mass spectrometer software (Analyst, Applied Biosystems) and incorporated into a FamOC autosampler (Dionex). The column effluent was analyzed in an information-dependant acquisition (IDA) mode on the mass spectrometer. In this mode, a survey scan (full MS scan) is performed and then the three most intense peaks from the survey scan are automatically chosen for collision-induced dissociation fragmentation to obtain an MSMS spectra, as long as they have not been chosen for fragmentation in the last 2 min (time exclusion). Data were collected over the 1 hour time course of the chromatogram and data collection and processing were prepared using the Analyst QS software package (Applied Biosystems). For the Pdc family binding-partner search, protein identifications were assigned using MASCOT software found at www.matrixscience.com (Matrix Science) which searched both the NCBInr and Swissprot databases. For phosphorylation site identification, the reconstructed IDA spectra were searched in the MASCOT database with and without an extra 80 Da or 98 Da corresponding respectively to phosphorylation or a neutral loss of phosphoric acid. Molecular ions of m/z predicted for possible phosphorylation sites were selected as parent ions in manual selection LCMSMS experiments. CID spectra were compared with theoretical peptide fragments to deduce specific phosphorylation sites.

Results

PhLP2 proteins do not co-immunoprecipitate endogenous Gβ1 in human cells

Pdc and PhLP1 each contain an N-terminal Gβγ binding domain, but there are no Gβγ binding domains present in PhLP2 proteins (*21, 28*). Flanary et al. showed that PhLP2 may be able to bind very weakly to Gβγ in yeast, but the results were questionable due to the extremely long exposure time needed to identify Gβ in the immunoblot (*29*). In order to investigate the Gβ1 binding capability of human PhLP2 proteins, myc-tagged Pdc, PhLP1, PhLP2A, or PhLP2B were singly expressed with a C-terminal myc tag in HEK 293T cells. Each Pdc family protein was immunoprecipitated with an anti-myc antibody, and then immunoblotted with an anti-Gβ1 antibody. A representative immunoblot is shown in Figure 4-1. As expected, both Pdc-myc and PhLP1-myc co-immunoprecipitated endogenous Gβ1 very well (*107*), but neither PhLP2 proteins were able to bind endogenous Gβ1 at all. This data indicates that the function of the PhLP2 proteins is separate and unrelated to Gβγ signaling in human cells.

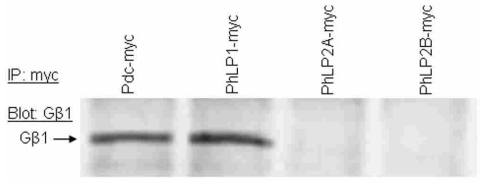

Figure 4-1. PhLP2 proteins do not bind endogenous amounts of Gβ1. HEK 293T cells were transfected with 1μg of each indicated myc-tagged Pdc family genes in pcDNA3.1 B+. After 48 hours, cell lysates were immunoprecipitated with an anti-myc antibody and immunoblotted with an anti-Gβ1 antibody.

PhLP2 proteins bind CCT as well as PhLP1

PhLP2 is known to interact with the CCT holocomplex in yeast (*58, 97, 98*), so it was hypothesized that PhLP2 might act as a co-chaperone with CCT in protein folding akin to PhLP1. To investigate this hypothesis in human cells, PhLP2's ability

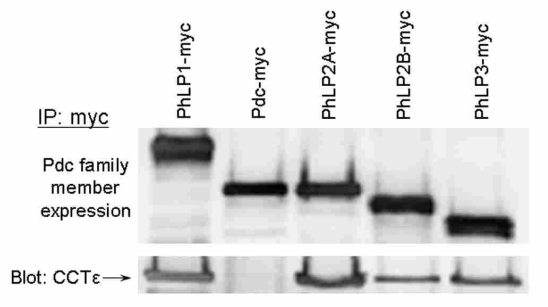

Figure 4-2. All Pdc family proteins, except Pdc, bind CCT.
HEK 293T cells were transfected with 1 μg of each indicated myc-tagged Pdc family genes in pcDNA3.1 B+. After 48 hours, cell lysates were immunoprecipitated with an anti-myc antibody and immunoblotted with either an anti-CCTε antibody or an anti-myc antibody .

to co-immunoprecipitate CCTε was tested. Pdc, PhLP1, PhLP2A, PhLP2B, or PhLP3 were separately expressed with a C-terminal myc tag in HEK 293T cells. Each Pdc family protein was immunoprecipitated with an anti-myc antibody and the immunoprecipitates were blotted with either the anti-myc or a monoclonal anti-CCTε antibody. It was clearly shown (Fig. 4-2) that all Pdc family members, with the exception of Pdc, bind CCT with PhLP1 and PhLP2 binding equally well. This data suggests that all human Pdc family proteins, except Pdc itself, act as co-chaperones with CCT in protein folding.

A proteomics search for PhLP2A binding partners

To facilitate the identification of PhLP2A folding substrates, an immunoprecipitation coupled with mass spectrometry strategy was employed. Pdc-TEV, PhLP1-TEV, PhLP2A-TEV, each with a C-terminal myc tag, or an empty vector control, were expressed in HEK 293T cells. Each Pdc family member was immunoprecipitated with an antibody against the myc tag and the samples were incubated with TEV protease. This procedure freed the PhLP proteins and any interacting partners from the antibody and protein A/G beads, removing these contaminants from the mass spec analysis. The proteins were reduced, alkylated,

acetone precipitated, and then digested with trypsin. The resulting peptides were analyzed by LCMSMS and protein identifications assigned using the MASCOT software found at www.matrixscience.com. The proteins listed in Table 4-1 were found to interact with either the empty vector control, Pdc, PhLP1 or PhLP2A. Proteins found in the PhLP2A sample that were also found in the Pdc or empty vector controls were treated as false-positive identifications, except for 14-3-3ε which is a known Pdc binding partner (*109, 110*). Several proteins, including elongation factor 1α (eEF1α), NADH-quinone reductase, and S-adenosylmethionine decarboxylase proenzyme 1 were found to interact with PhLP1 and PhLP2A. Six of eight CCT subunits were found in the PhLP2A sample, indicating that PhLP2A interacts with the entire CCT holocomplex and not only with individual CCT subunits. Three proteins, α-tubulin, 14-3-3γ, and ribosomal protein L3, were found to interact specifically with PhLP2A, and not with the positive and negative controls.

PhLP2A and CCT both bind 14-3-3 epsilon

The PhLP2A-14-3-3 interaction identified by mass spec was further substantiated by immunoprecipitation. Flag-tagged 14-3-3ε and myc-tagged PhLP2A were co-expressed in HEK 293T cells and each protein was able to immunoprecipitate the other (Figure 4-3A). Clearly, 14-3-3 and PhLP2A were able to associate despite the fact that PhLP2A does not contain a consensus 14-3-3 binding site. This observation led to the belief that 14-3-3 might also associate with CCT. To test this hypothesis, Flag-tagged 14-3-3ε or an empty vector control were expressed separately in HEK 293T cells. In each sample, endogenous CCTε was immunoprecipitated, and 14-3-3ε was found in the CCT co-immunoprecipitate

Identified Protein	*Bait Protein*			
Contaminants	**vector**	**Pdc**	**PhLP1**	**PhLP2A**
Bovine albumin	244	132	90	112
TEV protease	99	117		118
Trypsin	54			
Non-specific interactors				
β-actin		78	44	78
α-actinin 1		80		79
ATP synthase β subunit		96		83
Cobalamin synthesis protein		50		50
HSP 60		90	111	66
HSP 70		125	40	62
PhLP1 and 2A interactors				
CCTα			76	64
CCTγ			64	80
CCTη	40	29	99	196
Elongation factor 1α			67	65
NADH-quinone reductase			44	39
S-adenosylmet. decarboxylase			45	37
PhLP2A specific interactors				
CCTβ				83
CCTδ				32
CCTθ				60
14-3-3ε		164		59
14-3-3γ				60
α-tubulin				45
Ribosomal protein L3				46

Table 4-1. Pdc family binding partners identified in a mass spec analysis.
HEK 293 cells were transfected with an empty vector control, Pdc-TEV, PhLP1-TEV, or PhLP2A-TEV all with a C-terminal myc tag in pcDNA 3.1 B+. After 48 hours, cells were lysed and immunoprecipitated with an anti-myc antibody. PhLP2A and co-immunoprecipitating proteins were cleaved from Protein A/G beads using a TEV protease. Proteins were then reduced, alkylated, precipitated with acetone, and digested with trypsin. LCMSMS was performed on each sample and each spectra sent to MASCOT. Each protein is listed with its assigned MOWSE (molecular weight search) score which is a weighted probability score based on peptide masses and fragment ions (theoretical values vs. experimental data). Higher MOWSE scores indicate greater confidence in the protein identification. Only those scores with p values <0.05 are listed.

(Figure 4-3B). These findings indicate that 14-3-3 is able to associate with both PhLP2A and CCT in human cells.

PhLP2A phosphorylation site identification

In order to learn more about PhLP2A, phosphorylation site identification (PSI) via mass spectrometry was used. PhLP2A was cloned into pETDuet-1 bacterial expression vector in frame with the vector's N-terminal His tag. The protein was expressed in *E. coli*, and purified over a nickel chelate column. The purified His-PhLP2A protein was divided into two samples and the first sample was CK2 phosphorylated while the other was dephosphorylated with calf intestinal alkaline phosphatase to act as a non-phosphorylated control. Both protein samples were digested with trypsin and the phosphorylated sample was enriched for

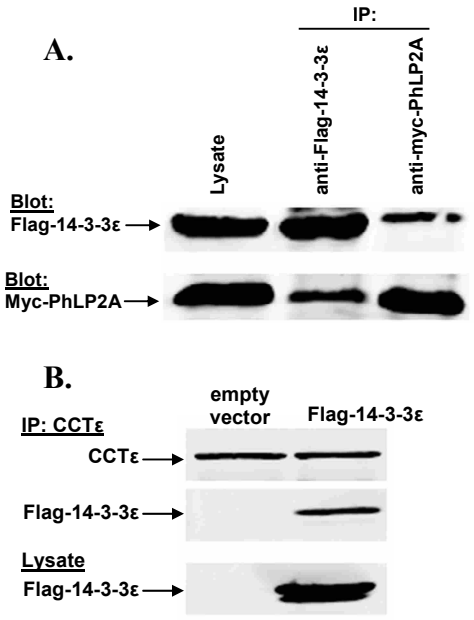

Figure 4-3. PhLP2A and CCT bind 14-3-3ε.
HEK 293T cells were treated as follows. A) Cells were transfected with 1 μg of each Flag-14-3-3ε and PhLP2A-myc in pcDNA3.1(+)/myc-His. After 48 hours, the cell lysate was divided in half. One half was immunoprecipitated with an anti-Flag antibody and the other half was immunoprecipitated with an anti-myc antibody. Each immunoprecipitation was blotted with either the anti-Flag antibody for 14-3-3ε or the anti-myc antibody for PhLP2A. B) Cells were transfected with 1μg of either Flag-14-3-3ε in pcDNA3.1(+)/myc-His or the empty vector control. After 48 hours, the cells were lysed, immunoprecipitated with an anti-CCTε antibody, and then immunoblotted with the anti-CCTε antibody or an anti-Flag antibody for 14-3-3ε. Ten micrograms of total cell lysate was blotted with an anti-Flag antibody for 14-3-3ε.

phosphopeptides using a TiO_2 microtip. The TiO_2 microtip is positively charged and attracts the negatively charged phosphate groups yielding an eluant which contains a higher percentage of phosphopeptides, thereby increasing the likelihood of phosphorylation site identification. Each sample was analyzed by LCMSMS and peptide identities were assigned by MASCOT. When the phosphorylated sample spectra were sent to MASCOT, the program indicated that T52 on tryptic peptide 8 was phosphorylated. The monoisotopic masses of peptide 8 were 2996.1 and 2916.1 for the phosphorylated and non-phosphorylated peptide, respectively (Fig. 4-4 A and B). This mass difference of 80 Da indicated that this peptide was singly phosphorylated in this analysis. The y-series in the MSMS spectra for both samples was the same until T52 which indicated that T52 was the phosphorylated amino acid. The same tryptic peptide was identified in a subsequent LCMSMS run with evidence

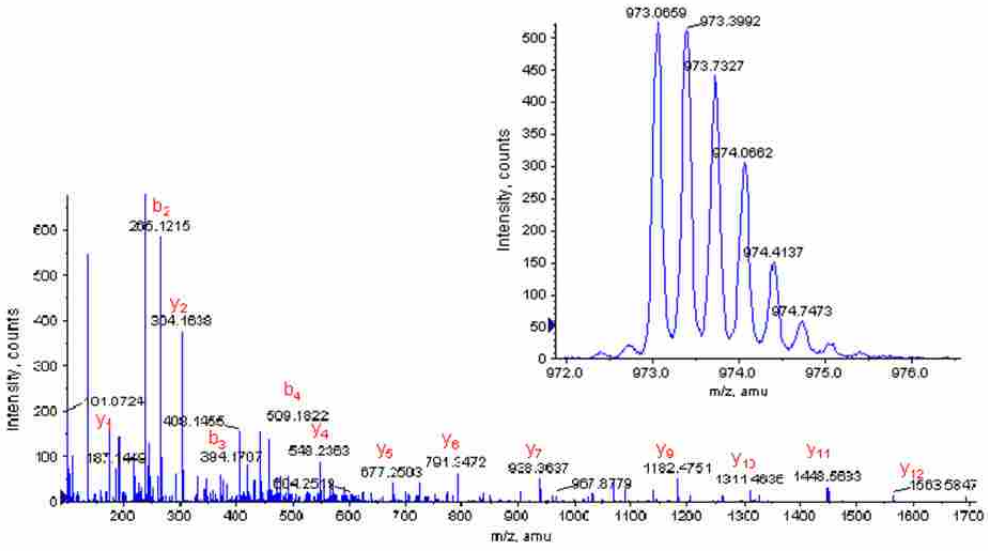

Figure 4-4A. MS and MSMS spectra from non-phosphorylated PhLP2A . MS spectrum shows tryptic peptide 8, T8, (m/z = 973.4, +3 charge state) which had a monoisotoptic mass of 2916.1 and eluted from time 17.175 to 17.857 minutes. MSMS spectrum shows ions from the b and y series.

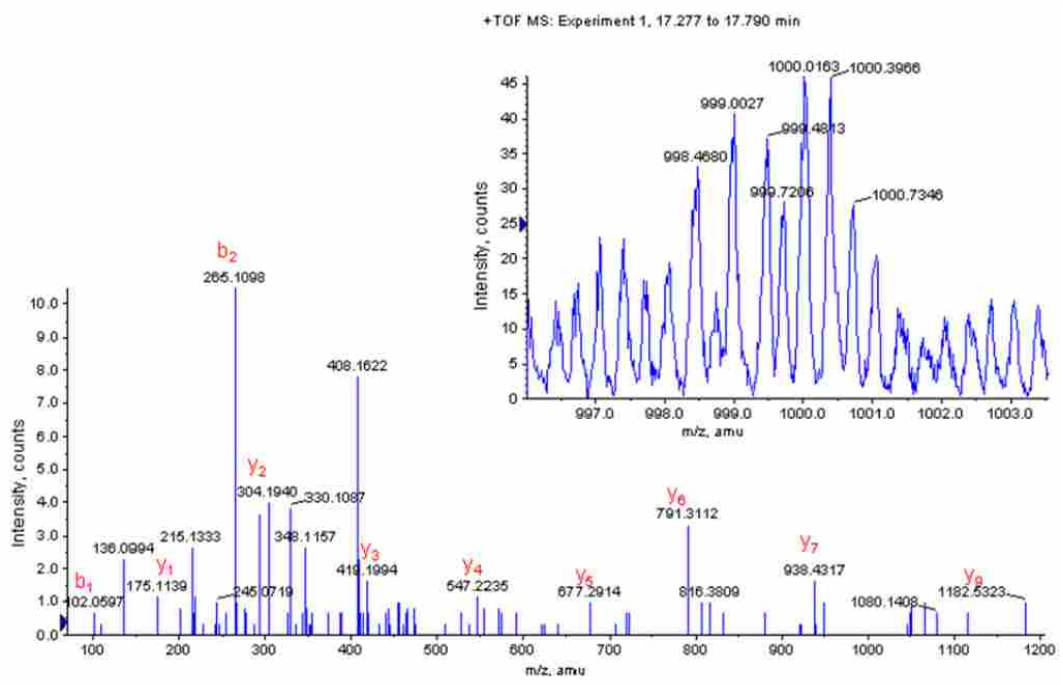

T8 = T_{47}YEDM$\underline{T}_{52}$LEELEDHEDEFNEEDER$_{69}$

Figure 4-4B. MS and MSMS spectra from T52 phosphorylated PhLP2A. MS spectrum shows tryptic peptide 8, T8, (m/z = 1000.0, +3 charge state) which had a monoisotopic mass of 2996.11 and eluted at time 17.62 minutes. MSMS spectrum shows ions from the b and y series. The phosphorylated peptide's mass is 80 Da greater than the non-phosphorylated peptide indicating to a singly phosphorylated peptide. The y series ions matches the non-phosphorylated y ions up until T52 which MASCOT identified as a phosphothreonine.

of a single phosphorylation site at T47. The MSMS spectra showed a neutral loss of phosphoric acid in the b-ion series, starting at b1, in the phosphorylated sample indicating that T47 had been phosphorylated before collision induced dissociation fragmentation (Fig 4-4C). MS data could not be obtained for all tryptic peptides, but a good percentage, 75%, of the amino acids in PhLP2A were covered in the phosphorylated sample. Unfortunately, no MS data was gathered for the most C-terminal peptide, DSDSEGD, in the phosphorylated sample so no phosphorylation data was obtained for these two serines that were phosphorylated in the mouse screen. The MASCOT search for both samples showed that *E. coli* elongation factor Tu (EF-

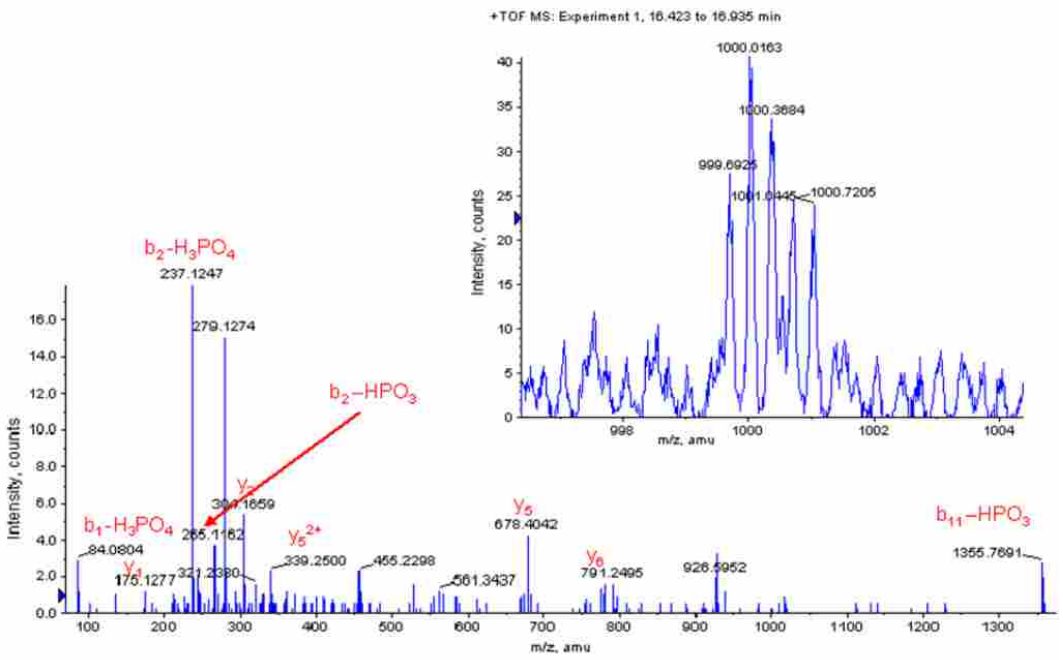

T8 = $\underline{T}_{47}$YEDMTLEELEDHEDEFNEEDER$_{69}$

Figure 4-4C. MS and MSMS spectra from T47 phosphorylated PhLP2A . MS spectrum shows tryptic peptide 8, T8, (m/z = 1000.0, +3 charge state) which had a monoisotoptic mass of 2996.11 and eluted at time 16.64 minutes. MSMS spectrum shows ions from the b and y series. The phosphorylated peptide's mass is 80 Da greater than the non-phosphorylated peptide indicating a singly phosphorylated peptide. The b series indicates the loss of a phosphate group at T47.

Tu) was present in the nickel-purified PhLP2A samples and was assigned a MOWSE score of 1302 in the nonphosphorylated sample and 876 in the phosphorylated sample when a score of 60 was significant with $p<0.05$. Consequently, both scores were highly significant indicating that EF-Tu purified with His-PhLP2A. Since bacterial EF-Tu and eukaryotic eEF1α are homologous proteins, this identification is consistent with the eEF1α identified in mammalian cells.

Discussion

This data proved that human PhLP2A and PhLP2B were not able to bind endogenous Gβ1 in mammalian cells; an observation in agreement with that seen in

yeast where the PhLP2-Gβγ interaction was extremely weak (*29*). Together, these findings expand the thinking about the functions of Pdc family proteins and leads to a belief that Pdc family members participate in functions other than G protein signaling. A more unifying Pdc family attribute is the ability to act as cochaperones with CCT in protein folding. The data herein established that human PhLP2A was able to associate with CCT to the same extent as PhLP1 lending much credibility to the hypothesis that PhLP2 acts as a CCT co-chaperone.

In previous studies, loss of optimal PhLP2A or CCT function due to temperature sensitive mutants or protein knockdown led to some overlapping consequences such as actin, tubulin, and cell cycle defects. Recently, the list of possible CCT substrates has grown to include proteins involved in DNA replication, mitosis, meiosis, RNA processing, transcription, translation, and signal transduction (*48, 90*). Since both PhLP2 and CCT temperature sensitive mutants stall in the G1-S phase transition, their folding functions must be required to promote entry into S phase. During G1, the cell must dramatically increase its mass and volume via protein synthesis to prepare for entry into S phase. In order to support the high level of protein synthesis, elevated amounts of proteins and RNA involved in translation, ribosome synthesis, and tRNA metabolism/charging are present (*111*). In fact, downregulation of 270 out of 773 essential yeast genes (35%) caused a delay in G1-S transition with nearly all of these genes playing some role in protein synthesis (*111*). Logically, the need for protein folding and assembly increases directly with increased translation. The model that PhLP2 and CCT work together in protein folding makes sense given that *phlp2-ts* mutants or CCT knockdown cause a delay at the G1-S

transition. However, a model in which PhLP2 *only* assists CCT in actin and tubulin folding is too limited given that the prefoldin complex, which acts as a cochaperone with CCT in the folding of actin and tubulin, is not an essential protein complex. Loss of prefoldin function in yeast only led to a reduction in actin and tubulin folding efficiency and a phenotype which exhibited slowed growth (*51, 112*). Since loss of PhLP2 leads to cell death instead of merely slowed growth, it is hypothesized that PhLP2A plays a key role with CCT in folding essential proteins necessary for the G1-S transition that cannot be fully compensated by other chaperones.

Consequently, the identified PhLP2A interactions with 14-3-3ε, 14-3-3γ, ribosomal protein L3, elongation factor 1α (eEF1α), and EF-Tu may be important for entry into S phase because each of these proteins is known to play some role in the cell cycle. The other identified interaction between PhLP2A and α-tubulin further demonstrates that PhLP2A may play a role in tubulin folding and proves that PhLP2A and α-tubulin interact *in vivo*. Even though these mass spec identifications were not able lead to a specific PhLP2A function, they provide some clues that may lead to that discovery.

14-3-3 proteins are highly conserved essential proteins found in all eukaryotes which modulate many processes including cell cycle control and apoptosis. On the molecular level, 14-3-3 proteins bind to specific phosphorylated sequences on many proteins to induce conformational changes or manipulate protein-protein interactions (*113*). Two 14-3-3 isoforms were found in association with PhLP2A, but oddly, PhLP2A does not contain any consensus 14-3-3 binding sites. A small percentage of non-phosphorylated proteins are able to bind 14-3-3s (*114*), but perhaps rather than

binding to PhLP2A alone, 14-3-3 proteins bind to the PhLP2A-CCT complex to be folded, dimerize, or modulate the folding of other proteins.

Two homologous proteins known to participate in translational elongation, bacterial elongation factor Tu (EF-Tu) and mammalian elongation factor 1α (eEF1α), were found as PhLP2A binding partners. During elongation, the GTP-bound form of eEF1α transports aminoacyl-tRNAs to the empty ribosomal A site. Upon GTP hydrolysis, eEF1α is released from the ribosome, the nascent polypeptide is transferred from the P site to the A site aminoacyl-tRNA, and an amino acid is added to the polypeptide (*115*). Next, the mRNA translocates along the ribosome with the assistance of elongation factor 2 (eEF2) so that a new codon is present in the A site (*116*). Elongation factor binding and release from the ribosome is coordinated by ribosomal protein L3 which binds separately to eEF1α and eEF2 and assists in their sequential ribosome binding (*117*). The structure of eEF1α is predicted to be similar to EF-Tu which consists of a GTPase domain and two β-barrel domains. As well, the structure of eEF2 is comparable to the eEF1α-tRNA structure and consists of a six domains including a GTPase domain and a β-barrel domain analogous to those of eEF1α. Whereas this study found eEF1α and ribosomal protein L3 bound to PhLP2A *in vivo*, Yam and colleagues determined that eEF2 interacted with CCT *in vitro* (*48*). Both elongation factors contain at least one β-barrel domain which may be aggregation prone due to its high β-sheet content. Perhaps the folding of these elongation factors and assembly with ribosomal protein L3 is mediated by PhLP2A and CCT. Elongation factors and ribosomal proteins are essential in protein synthesis so their loss or misfolding would be congruent with G1-S arrest.

The exact folding function of PhLP2A is not yet known, but it is probably regulated by phosphorylation given the essential role of CK2 phosphorylation of PhLP1 in Gβ folding and assembly with Gγ (*36*). Two phosphothreonine residues were identified, T52 and T47. Both phosphorylation sites were identified on tryptic peptide #8, T*YEDMT*LEELEDHEDEFNEEDER. There are probably other CK2 phosphorylation sites within human PhLP2A, especially at its C-terminus, but they were not identified by this method. The reason for that may be because TiO_2 microtips tend to bind negatively charged phosphorylated peptides as well as acidic peptides. Both T52 and T47 were found on an acidic peptide with 13 acidic residues out of 23 total residues. The additional phosphate group as well as the acidic nature of the peptide may have led to this peptide's preferential binding to the TiO_2 column and therefore this peptide may have been enriched to a greater degree than other peptides. In the future, a different, but complementary phosphopeptide enrichment technique may be used in order to enrich the sample for other phosphopeptides.

In conclusion, this work suggests that PhLP2A is a co-chaperone with CCT in the folding of a possible subset of cytoskeletal and G1-S promoting proteins. In the future, it will be interesting to positively identify the essential folding function of the PhLP2A-CCT interaction.

REFERENCES

1. Rockman, H. A., Koch, W. J., and Lefkowitz, R. J. (2002) Seven-transmembrane-spanning receptors and heart function, *Nature 415*, 206-212.
2. Gainetdinov, R. R., Premont, R. T., Bohn, L. M., Lefkowitz, R. J., and Caron, M. G. (2004) Desensitization of G protein-coupled receptors and neuronal functions, *Annu Rev Neurosci 27*, 107-144.
3. Arshavsky, V. Y., Lamb, T. D., and Pugh, E. N., Jr. (2002) G proteins and phototransduction, *Annu Rev Physiol 64*, 153-187.
4. Foord, S. M., Bonner, T. I., Neubig, R. R., Rosser, E. M., Pin, J. P., Davenport, A. P., Spedding, M., and Harmar, A. J. (2005) International Union of Pharmacology. XLVI. G protein-coupled receptor list, *Pharmacol Rev 57*, 279-288.
5. Simonds, W. F. (2003) G protein-regulated signaling dysfunction in human disease, *J Investig Med 51*, 194-214.
6. Schoneberg, T., Schulz, A., Biebermann, H., Hermsdorf, T., Rompler, H., and Sangkuhl, K. (2004) Mutant G-protein-coupled receptors as a cause of human diseases, *Pharmacol Ther 104*, 173-206.
7. Cabrera-Vera, T. M., Vanhauwe, J., Thomas, T. O., Medkova, M., Preininger, A., Mazzoni, M. R., and Hamm, H. E. (2003) Insights into G protein structure, function, and regulation, *Endocr Rev 24*, 765-781.
8. Neubig, R. R., and Siderovski, D. P. (2002) Regulators of G-protein signalling as new central nervous system drug targets, *Nat Rev Drug Discov 1*, 187-197.
9. DeWire, S. M., Ahn, S., Lefkowitz, R. J., and Shenoy, S. K. (2007) Beta-arrestins and cell signaling, *Annu Rev Physiol 69*, 483-510.
10. Ross, E. M., and Wilkie, T. M. (2000) GTPase-activating proteins for heterotrimeric G proteins: regulators of G protein signaling (RGS) and RGS-like proteins, *Annu Rev Biochem 69*, 795-827.
11. Krispel, C. M., Chen, D., Melling, N., Chen, Y. J., Martemyanov, K. A., Quillinan, N., Arshavsky, V. Y., Wensel, T. G., Chen, C. K., and Burns, M. E. (2006) RGS expression rate-limits recovery of rod photoresponses, *Neuron 51*, 409-416.
12. Bauer, P. H., Muller, S., Puzicha, M., Pippig, S., Obermaier, B., Helmreich, E. J., and Lohse, M. J. (1992) Phosducin is a protein kinase A-regulated G-protein regulator, *Nature 358*, 73-76.
13. Lee, R. H., Lieberman, B. S., and Lolley, R. N. (1987) A novel complex from bovine visual cells of a 33,000-dalton phosphoprotein with beta- and gamma-transducin: purification and subunit structure, *Biochemistry 26*, 3983-3990.
14. Lee, R. H., Ting, T. D., Lieberman, B. S., Tobias, D. E., Lolley, R. N., and Ho, Y. K. (1992) Regulation of retinal cGMP cascade by phosducin in bovine rod photoreceptor cells. Interaction of phosducin and transducin, *J Biol Chem 267*, 25104-25112.
15. Yoshida, T., Willardson, B. M., Wilkins, J. F., Jensen, G. J., Thornton, B. D., and Bitensky, M. W. (1994) The phosphorylation state of phosducin

determines its ability to block transducin subunit interactions and inhibit transducin binding to activated rhodopsin, *J Biol Chem 269*, 24050-24057.
16. Barhite, S., Thibault, C., and Miles, M. F. (1998) Phosducin-like protein (PhLP), a regulator of G beta gamma function, interacts with the proteasomal protein SUG1, *Biochim Biophys Acta 1402*, 95-101.
17. McLaughlin, J. N., Thulin, C. D., Bray, S. M., Martin, M. M., Elton, T. S., and Willardson, B. M. (2002) Regulation of angiotensin II-induced G protein signaling by phosducin-like protein, *J Biol Chem 277*, 34885-34895.
18. Humrich, J., Bermel, C., Bunemann, M., Harmark, L., Frost, R., Quitterer, U., and Lohse, M. J. (2005) Phosducin-like protein regulates G-protein betagamma folding by interaction with tailless complex polypeptide-1alpha: dephosphorylation or splicing of PhLP turns the switch toward regulation of Gbetagamma folding, *J Biol Chem 280*, 20042-20050.
19. Lukov, G. L., Hu, T., McLaughlin, J. N., Hamm, H. E., and Willardson, B. M. (2005) Phosducin-like protein acts as a molecular chaperone for G protein betagamma dimer assembly, *EMBO J 24*, 1965-1975.
20. Sokolov, M., Strissel, K. J., Leskov, I. B., Michaud, N. A., Govardovskii, V. I., and Arshavsky, V. Y. (2004) Phosducin facilitates light-driven transducin translocation in rod photoreceptors. Evidence from the phosducin knockout mouse, *J Biol Chem 279*, 19149-19156.
21. Blaauw, M., Knol, J. C., Kortholt, A., Roelofs, J., Ruchira, Postma, M., Visser, A. J., and van Haastert, P. J. (2003) Phosducin-like proteins in Dictyostelium discoideum: implications for the phosducin family of proteins, *EMBO J 22*, 5047-5057.
22. Savage, J. R., McLaughlin, J. N., Skiba, N. P., Hamm, H. E., and Willardson, B. M. (2000) Functional roles of the two domains of phosducin and phosducin-like protein, *J Biol Chem 275*, 30399-30407.
23. Thibault, C., Sganga, M. W., and Miles, M. F. (1997) Interaction of phosducin-like protein with G protein betagamma subunits, *J Biol Chem 272*, 12253-12256.
24. Reig, J. A., Yu, L., and Klein, D. C. (1990) Pineal transduction. Adrenergic----cyclic AMP-dependent phosphorylation of cytoplasmic 33-kDa protein (MEKA) which binds beta gamma-complex of transducin, *J Biol Chem 265*, 5816-5824.
25. Miles, M. F., Barhite, S., Sganga, M., and Elliott, M. (1993) Phosducin-like protein: an ethanol-responsive potential modulator of guanine nucleotide-binding protein function, *Proc Natl Acad Sci U S A 90*, 10831-10835.
26. Schroder, S., and Lohse, M. J. (2000) Quantification of the tissue levels and function of the G-protein regulator phosducin-like protein (PhlP), *Naunyn Schmiedebergs Arch Pharmacol 362*, 435-439.
27. Lopez, P., Yaman, R., Lopez-Fernandez, L. A., Vidal, F., Puel, D., Clertant, P., Cuzin, F., and Rassoulzadegan, M. (2003) A novel germ line-specific gene of the phosducin-like protein (PhLP) family. A meiotic function conserved from yeast to mice, *J Biol Chem 278*, 1751-1757.
28. Wilkinson, J. C., Richter, B. W., Wilkinson, A. S., Burstein, E., Rumble, J. M., Balliu, B., and Duckett, C. S. (2004) VIAF, a conserved inhibitor of

apoptosis (IAP)-interacting factor that modulates caspase activation, *J Biol Chem 279*, 51091-51099.
29. Flanary, P. L., DiBello, P. R., Estrada, P., and Dohlman, H. G. (2000) Functional analysis of Plp1 and Plp2, two homologues of phosducin in yeast, *J Biol Chem 275*, 18462-18469.
30. Lacefield, S., and Solomon, F. (2003) A novel step in beta-tubulin folding is important for heterodimer formation in Saccharomyces cerevisiae, *Genetics 165*, 531-541.
31. Stirling, P. C., Cuellar, J., Alfaro, G. A., El Khadali, F., Beh, C. T., Valpuesta, J. M., Melki, R., and Leroux, M. R. (2006) PhLP3 modulates CCT-mediated actin and tubulin folding via ternary complexes with substrates, *J Biol Chem 281*, 7012-7021.
32. Gaudet, R., Bohm, A., and Sigler, P. B. (1996) Crystal structure at 2.4 angstroms resolution of the complex of transducin betagamma and its regulator, phosducin, *Cell 87*, 577-588.
33. Schroder, S., and Lohse, M. J. (1996) Inhibition of G-protein betagamma-subunit functions by phosducin-like protein, *Proc Natl Acad Sci U S A 93*, 2100-2104.
34. Garzon, J., Rodriguez-Diaz, M., Lopez-Fando, A., Garcia-Espana, A., and Sanchez-Blazquez, P. (2002) Glycosylated phosducin-like protein long regulates opioid receptor function in mouse brain, *Neuropharmacology 42*, 813-828.
35. Thulin, C. D., Howes, K., Driscoll, C. D., Savage, J. R., Rand, T. A., Baehr, W., and Willardson, B. M. (1999) The immunolocalization and divergent roles of phosducin and phosducin-like protein in the retina, *Mol Vis 5*, 40.
36. Lukov, G. L., Baker, C. M., Ludtke, P. J., Hu, T., Carter, M. D., Hackett, R. A., Thulin, C. D., and Willardson, B. M. (2006) Mechanism of assembly of G protein betagamma subunits by protein kinase CK2-phosphorylated phosducin-like protein and the cytosolic chaperonin complex, *J Biol Chem 281*, 22261-22274.
37. Kasahara, S., Wang, P., and Nuss, D. L. (2000) Identification of bdm-1, a gene involved in G protein beta-subunit function and alpha-subunit accumulation, *Proc Natl Acad Sci U S A 97*, 412-417.
38. McLaughlin, J. N., Thulin, C. D., Hart, S. J., Resing, K. A., Ahn, N. G., and Willardson, B. M. (2002) Regulatory interaction of phosducin-like protein with the cytosolic chaperonin complex, *Proc Natl Acad Sci U S A 99*, 7962-7967.
39. Gavin, A. C., Bosche, M., Krause, R., Grandi, P., Marzioch, M., Bauer, A., Schultz, J., Rick, J. M., Michon, A. M., Cruciat, C. M., Remor, M., Hofert, C., Schelder, M., Brajenovic, M., Ruffner, H., Merino, A., Klein, K., Hudak, M., Dickson, D., Rudi, T., Gnau, V., Bauch, A., Bastuck, S., Huhse, B., Leutwein, C., Heurtier, M. A., Copley, R. R., Edelmann, A., Querfurth, E., Rybin, V., Drewes, G., Raida, M., Bouwmeester, T., Bork, P., Seraphin, B., Kuster, B., Neubauer, G., and Superti-Furga, G. (2002) Functional organization of the yeast proteome by systematic analysis of protein complexes, *Nature 415*, 141-147.

40. Ho, Y., Gruhler, A., Heilbut, A., Bader, G. D., Moore, L., Adams, S. L., Millar, A., Taylor, P., Bennett, K., Boutilier, K., Yang, L., Wolting, C., Donaldson, I., Schandorff, S., Shewnarane, J., Vo, M., Taggart, J., Goudreault, M., Muskat, B., Alfarano, C., Dewar, D., Lin, Z., Michalickova, K., Willems, A. R., Sassi, H., Nielsen, P. A., Rasmussen, K. J., Andersen, J. R., Johansen, L. E., Hansen, L. H., Jespersen, H., Podtelejnikov, A., Nielsen, E., Crawford, J., Poulsen, V., Sorensen, B. D., Matthiesen, J., Hendrickson, R. C., Gleeson, F., Pawson, T., Moran, M. F., Durocher, D., Mann, M., Hogue, C. W., Figeys, D., and Tyers, M. (2002) Systematic identification of protein complexes in Saccharomyces cerevisiae by mass spectrometry, *Nature 415*, 180-183.
41. Leroux, M. R., and Hartl, F. U. (2000) Protein folding: versatility of the cytosolic chaperonin TRiC/CCT, *Curr Biol 10*, R260-264.
42. Valpuesta, J. M., Martin-Benito, J., Gomez-Puertas, P., Carrascosa, J. L., and Willison, K. R. (2002) Structure and function of a protein folding machine: the eukaryotic cytosolic chaperonin CCT, *FEBS Lett 529*, 11-16.
43. Llorca, O., McCormack, E. A., Hynes, G., Grantham, J., Cordell, J., Carrascosa, J. L., Willison, K. R., Fernandez, J. J., and Valpuesta, J. M. (1999) Eukaryotic type II chaperonin CCT interacts with actin through specific subunits, *Nature 402*, 693-696.
44. Hynes, G. M., and Willison, K. R. (2000) Individual subunits of the eukaryotic cytosolic chaperonin mediate interactions with binding sites located on subdomains of beta-actin, *J Biol Chem 275*, 18985-18994.
45. Llorca, O., Martin-Benito, J., Grantham, J., Ritco-Vonsovici, M., Willison, K. R., Carrascosa, J. L., and Valpuesta, J. M. (2001) The 'sequential allosteric ring' mechanism in the eukaryotic chaperonin-assisted folding of actin and tubulin, *EMBO J 20*, 4065-4075.
46. Melki, R., Batelier, G., Soulie, S., and Williams, R. C., Jr. (1997) Cytoplasmic chaperonin containing TCP-1: structural and functional characterization, *Biochemistry 36*, 5817-5826.
47. Thulasiraman, V., Yang, C. F., and Frydman, J. (1999) In vivo newly translated polypeptides are sequestered in a protected folding environment, *EMBO J 18*, 85-95.
48. Yam, A. Y., Xia, Y., Lin, H. T., Burlingame, A., Gerstein, M., and Frydman, J. (2008) Defining the TRiC/CCT interactome links chaperonin function to stabilization of newly made proteins with complex topologies, *Nat Struct Mol Biol 15*, 1255-1262.
49. Farr, G. W., Scharl, E. C., Schumacher, R. J., Sondek, S., and Horwich, A. L. (1997) Chaperonin-mediated folding in the eukaryotic cytosol proceeds through rounds of release of native and nonnative forms, *Cell 89*, 927-937.
50. Camasses, A., Bogdanova, A., Shevchenko, A., and Zachariae, W. (2003) The CCT chaperonin promotes activation of the anaphase-promoting complex through the generation of functional Cdc20, *Mol Cell 12*, 87-100.
51. Siegers, K., Bolter, B., Schwarz, J. P., Bottcher, U. M., Guha, S., and Hartl, F. U. (2003) TRiC/CCT cooperates with different upstream chaperones in the folding of distinct protein classes, *EMBO J 22*, 5230-5240.

52. Martin-Benito, J., Bertrand, S., Hu, T., Ludtke, P. J., McLaughlin, J. N., Willardson, B. M., Carrascosa, J. L., and Valpuesta, J. M. (2004) Structure of the complex between the cytosolic chaperonin CCT and phosducin-like protein, *Proc Natl Acad Sci U S A 101*, 17410-17415.
53. Martin-Benito, J., Boskovic, J., Gomez-Puertas, P., Carrascosa, J. L., Simons, C. T., Lewis, S. A., Bartolini, F., Cowan, N. J., and Valpuesta, J. M. (2002) Structure of eukaryotic prefoldin and of its complexes with unfolded actin and the cytosolic chaperonin CCT, *EMBO J 21*, 6377-6386.
54. Knol, J. C., Engel, R., Blaauw, M., Visser, A. J., and van Haastert, P. J. (2005) The phosducin-like protein PhLP1 is essential for G{beta}{gamma} dimer formation in Dictyostelium discoideum, *Mol Cell Biol 25*, 8393-8400.
55. Wells, C. A., Dingus, J., and Hildebrandt, J. D. (2006) Role of the chaperonin CCT/TRiC complex in G protein betagamma-dimer assembly, *J Biol Chem 281*, 20221-20232.
56. Humrich, J., Bermel, C., Grubel, T., Quitterer, U., and Lohse, M. J. (2003) Regulation of phosducin-like protein by casein kinase 2 and N-terminal splicing, *J Biol Chem 278*, 4474-4481.
57. Dupre, D. J., Robitaille, M., Richer, M., Ethier, N., Mamarbachi, A. M., and Hebert, T. E. (2007) Dopamine receptor-interacting protein 78 acts as a molecular chaperone for Ggamma subunits before assembly with Gbeta, *J Biol Chem 282*, 13703-13715.
58. Stirling, P. C., Srayko, M., Takhar, K. S., Pozniakovsky, A., Hyman, A. A., and Leroux, M. R. (2007) Functional interaction between phosducin-like protein 2 and cytosolic chaperonin is essential for cytoskeletal protein function and cell cycle progression, *Mol Biol Cell 18*, 2336-2345.
59. Ogawa, S., Matsubayashi, Y., and Nishida, E. (2004) An evolutionarily conserved gene required for proper microtubule architecture in Caenorhabditis elegans, *Genes Cells 9*, 83-93.
60. Wettschureck, N., and Offermanns, S. (2005) Mammalian G proteins and their cell type specific functions, *Physiol Rev 85*, 1159-1204.
61. Farrens, D. L., Altenbach, C., Yang, K., Hubbell, W. L., and Khorana, H. G. (1996) Requirement of rigid-body motion of transmembrane helices for light activation of rhodopsin, *Science 274*, 768-770.
62. Li, J., Edwards, P. C., Burghammer, M., Villa, C., and Schertler, G. F. (2004) Structure of bovine rhodopsin in a trigonal crystal form, *J Mol Biol 343*, 1409-1438.
63. Palczewski, K., Kumasaka, T., Hori, T., Behnke, C. A., Motoshima, H., Fox, B. A., Le Trong, I., Teller, D. C., Okada, T., Stenkamp, R. E., Yamamoto, M., and Miyano, M. (2000) Crystal structure of rhodopsin: A G protein-coupled receptor, *Science 289*, 739-745.
64. Reiter, E., and Lefkowitz, R. J. (2006) GRKs and beta-arrestins: roles in receptor silencing, trafficking and signaling, *Trends Endocrinol Metab 17*, 159-165.
65. Willars, G. B. (2006) Mammalian RGS proteins: multifunctional regulators of cellular signalling, *Semin Cell Dev Biol 17*, 363-376.

66. Marrari, Y., Crouthamel, M., Irannejad, R., and Wedegaertner, P. B. (2007) Assembly and trafficking of heterotrimeric G proteins, *Biochemistry 46*, 7665-7677.
67. Kubota, S., Kubota, H., and Nagata, K. (2006) Cytosolic chaperonin protects folding intermediates of Gbeta from aggregation by recognizing hydrophobic beta-strands, *Proc Natl Acad Sci U S A 103*, 8360-8365.
68. Gautam, N., Downes, G. B., Yan, K., and Kisselev, O. (1998) The G-protein betagamma complex, *Cell Signal 10*, 447-455.
69. Robishaw, J. D., and Berlot, C. H. (2004) Translating G protein subunit diversity into functional specificity, *Curr Opin Cell Biol 16*, 206-209.
70. Watson, A. J., Katz, A., and Simon, M. I. (1994) A fifth member of the mammalian G-protein beta-subunit family. Expression in brain and activation of the beta 2 isotype of phospholipase C, *J Biol Chem 269*, 22150-22156.
71. Downes, G. B., and Gautam, N. (1999) The G protein subunit gene families, *Genomics 62*, 544-552.
72. Myung, C. S., Lim, W. K., DeFilippo, J. M., Yasuda, H., Neubig, R. R., and Garrison, J. C. (2006) Regions in the G protein gamma subunit important for interaction with receptors and effectors, *Mol Pharmacol 69*, 877-887.
73. Ray, K., Hansen, C. A., and Robishaw, J. D. (1996) Gbetagamma-Mediated Signaling in the Heart: Implications of beta and gamma Subunit Heterogeneity, *Trends Cardiovasc Med. 6*, 115-121.
74. Jones, M. B., Siderovski, D. P., and Hooks, S. B. (2004) The G{beta}{gamma} DIMER as a NOVEL SOURCE of SELECTIVITY in G-Protein Signaling: GGL-ing AT CONVENTION, *Mol Interv 4*, 200-214.
75. Dingus, J., Wells, C. A., Campbell, L., Cleator, J. H., Robinson, K., and Hildebrandt, J. D. (2005) G Protein betagamma dimer formation: Gbeta and Ggamma differentially determine efficiency of in vitro dimer formation, *Biochemistry 44*, 11882-11890.
76. Carter, M. D., Southwick, K., Lukov, G., Willardson, B. M., and Thulin, C. D. (2004) Identification of phosphorylation sites on phosducin-like protein by QTOF mass spectrometry, *J Biomol Tech 15*, 257-264.
77. Arshavsky, V. Y., and Pugh, E. N., Jr. (1998) Lifetime regulation of G protein-effector complex: emerging importance of RGS proteins, *Neuron 20*, 11-14.
78. Dohlman, H. G., Song, J., Ma, D., Courchesne, W. E., and Thorner, J. (1996) Sst2, a negative regulator of pheromone signaling in the yeast Saccharomyces cerevisiae: expression, localization, and genetic interaction and physical association with Gpa1 (the G-protein alpha subunit), *Mol Cell Biol 16*, 5194-5209.
79. Siderovski, D. P., Hessel, A., Chung, S., Mak, T. W., and Tyers, M. (1996) A new family of regulators of G-protein-coupled receptors?, *Curr Biol 6*, 211-212.
80. Siderovski, D. P., and Willard, F. S. (2005) The GAPs, GEFs, and GDIs of heterotrimeric G-protein alpha subunits, *Int J Biol Sci 1*, 51-66.
81. Natochin, M., and Artemyev, N. O. (2000) Mutational analysis of functional interfaces of transducin, *Methods Enzymol 315*, 539-554.

82. Tesmer, J. J., Berman, D. M., Gilman, A. G., and Sprang, S. R. (1997) Structure of RGS4 bound to AlF4--activated G(i alpha1): stabilization of the transition state for GTP hydrolysis, *Cell 89*, 251-261.
83. Hu, G., and Wensel, T. G. (2002) R9AP, a membrane anchor for the photoreceptor GTPase accelerating protein, RGS9-1, *Proc Natl Acad Sci U S A 99*, 9755-9760.
84. Martemyanov, K. A., Yoo, P. J., Skiba, N. P., and Arshavsky, V. Y. (2005) R7BP, a novel neuronal protein interacting with RGS proteins of the R7 family, *J Biol Chem 280*, 5133-5136.
85. Witherow, D. S., and Slepak, V. Z. (2003) A novel kind of G protein heterodimer: the G beta5-RGS complex, *Receptors Channels 9*, 205-212.
86. Chen, C. K., Burns, M. E., He, W., Wensel, T. G., Baylor, D. A., and Simon, M. I. (2000) Slowed recovery of rod photoresponse in mice lacking the GTPase accelerating protein RGS9-1, *Nature 403*, 557-560.
87. Nishiguchi, K. M., Sandberg, M. A., Kooijman, A. C., Martemyanov, K. A., Pott, J. W., Hagstrom, S. A., Arshavsky, V. Y., Berson, E. L., and Dryja, T. P. (2004) Defects in RGS9 or its anchor protein R9AP in patients with slow photoreceptor deactivation, *Nature 427*, 75-78.
88. Zachariou, V., Georgescu, D., Sanchez, N., Rahman, Z., DiLeone, R., Berton, O., Neve, R. L., Sim-Selley, L. J., Selley, D. E., Gold, S. J., and Nestler, E. J. (2003) Essential role for RGS9 in opiate action, *Proc Natl Acad Sci U S A 100*, 13656-13661.
89. Cheever, M. L., Snyder, J. T., Gershburg, S., Siderovski, D. P., Harden, T. K., and Sondek, J. (2008) Crystal structure of the multifunctional Gbeta5-RGS9 complex, *Nat Struct Mol Biol 15*, 155-162.
90. Grantham, J., Brackley, K. I., and Willison, K. R. (2006) Substantial CCT activity is required for cell cycle progression and cytoskeletal organization in mammalian cells, *Exp Cell Res 312*, 2309-2324.
91. Kisselev, O., and Gautam, N. (1993) Specific interaction with rhodopsin is dependent on the gamma subunit type in a G protein, *J Biol Chem 268*, 24519-24522.
92. Fletcher, J. E., Lindorfer, M. A., DeFilippo, J. M., Yasuda, H., Guilmard, M., and Garrison, J. C. (1998) The G protein beta5 subunit interacts selectively with the Gq alpha subunit, *J Biol Chem 273*, 636-644.
93. He, W., Lu, L., Zhang, X., El-Hodiri, H. M., Chen, C. K., Slep, K. C., Simon, M. I., Jamrich, M., and Wensel, T. G. (2000) Modules in the photoreceptor RGS9-1.Gbeta 5L GTPase-accelerating protein complex control effector coupling, GTPase acceleration, protein folding, and stability, *J Biol Chem 275*, 37093-37100.
94. Jones, M. B., and Garrison, J. C. (1999) Instability of the G-protein beta5 subunit in detergent, *Anal Biochem 268*, 126-133.
95. Kunisawa, J., and Shastri, N. (2003) The group II chaperonin TRiC protects proteolytic intermediates from degradation in the MHC class I antigen processing pathway, *Mol Cell 12*, 565-576.
96. Wang, Y., and Dohlman, H. G. (2004) Pheromone signaling mechanisms in yeast: a prototypical sex machine, *Science 306*, 1508-1509.

97. Collins, S. R., Kemmeren, P., Zhao, X. C., Greenblatt, J. F., Spencer, F., Holstege, F. C., Weissman, J. S., and Krogan, N. J. (2007) Toward a comprehensive atlas of the physical interactome of Saccharomyces cerevisiae, *Mol Cell Proteomics 6*, 439-450.
98. Gavin, A. C., Aloy, P., Grandi, P., Krause, R., Boesche, M., Marzioch, M., Rau, C., Jensen, L. J., Bastuck, S., Dumpelfeld, B., Edelmann, A., Heurtier, M. A., Hoffman, V., Hoefert, C., Klein, K., Hudak, M., Michon, A. M., Schelder, M., Schirle, M., Remor, M., Rudi, T., Hooper, S., Bauer, A., Bouwmeester, T., Casari, G., Drewes, G., Neubauer, G., Rick, J. M., Kuster, B., Bork, P., Russell, R. B., and Superti-Furga, G. (2006) Proteome survey reveals modularity of the yeast cell machinery, *Nature 440*, 631-636.
99. Spiess, C., Meyer, A. S., Reissmann, S., and Frydman, J. (2004) Mechanism of the eukaryotic chaperonin: protein folding in the chamber of secrets, *Trends Cell Biol 14*, 598-604.
100. Ghaemmaghami, S., Huh, W. K., Bower, K., Howson, R. W., Belle, A., Dephoure, N., O'Shea, E. K., and Weissman, J. S. (2003) Global analysis of protein expression in yeast, *Nature 425*, 737-741.
101. McMillan, J. N., Sia, R. A., and Lew, D. J. (1998) A morphogenesis checkpoint monitors the actin cytoskeleton in yeast, *J Cell Biol 142*, 1487-1499.
102. Ito, T., Chiba, T., Ozawa, R., Yoshida, M., Hattori, M., and Sakaki, Y. (2001) A comprehensive two-hybrid analysis to explore the yeast protein interactome, *Proc Natl Acad Sci U S A 98*, 4569-4574.
103. Wysocka, M., Rytka, J., and Kurlandzka, A. (2004) Saccharomyces cerevisiae CSM1 gene encoding a protein influencing chromosome segregation in meiosis I interacts with elements of the DNA replication complex, *Exp Cell Res 294*, 592-602.
104. Stoldt, V., Rademacher, F., Kehren, V., Ernst, J. F., Pearce, D. A., and Sherman, F. (1996) Review: the Cct eukaryotic chaperonin subunits of Saccharomyces cerevisiae and other yeasts, *Yeast 12*, 523-529.
105. Yokota, S., Yanagi, H., Yura, T., and Kubota, H. (1999) Cytosolic chaperonin is up-regulated during cell growth. Preferential expression and binding to tubulin at G(1)/S transition through early S phase, *J Biol Chem 274*, 37070-37078.
106. Yaffe, M. B., Rittinger, K., Volinia, S., Caron, P. R., Aitken, A., Leffers, H., Gamblin, S. J., Smerdon, S. J., and Cantley, L. C. (1997) The structural basis for 14-3-3:phosphopeptide binding specificity, *Cell 91*, 961-971.
107. Willardson, B. M., and Howlett, A. C. (2007) Function of phosducin-like proteins in G protein signaling and chaperone-assisted protein folding, *Cell Signal*.
108. Gygi, S. (2008) Personal communication between Barry M. Willardson and Steven Gygi, (Willardson, B. M., Ed.).
109. Nakano, K., Chen, J., Tarr, G. E., Yoshida, T., Flynn, J. M., and Bitensky, M. W. (2001) Rethinking the role of phosducin: light-regulated binding of phosducin to 14-3-3 in rod inner segments, *Proc Natl Acad Sci U S A 98*, 4693-4698.

110. Thulin, C. D., Savage, J. R., McLaughlin, J. N., Truscott, S. M., Old, W. M., Ahn, N. G., Resing, K. A., Hamm, H. E., Bitensky, M. W., and Willardson, B. M. (2001) Modulation of the G protein regulator phosducin by Ca2+/calmodulin-dependent protein kinase II phosphorylation and 14-3-3 protein binding, *J Biol Chem 276*, 23805-23815.
111. Yu, L., Pena Castillo, L., Mnaimneh, S., Hughes, T. R., and Brown, G. W. (2006) A survey of essential gene function in the yeast cell division cycle, *Mol Biol Cell 17*, 4736-4747.
112. Siegers, K., Waldmann, T., Leroux, M. R., Grein, K., Shevchenko, A., Schiebel, E., and Hartl, F. U. (1999) Compartmentation of protein folding in vivo: sequestration of non-native polypeptide by the chaperonin-GimC system, *EMBO J 18*, 75-84.
113. Bridges, D., and Moorhead, G. B. (2004) 14-3-3 proteins: a number of functions for a numbered protein, *Sci STKE 2004*, re10.
114. Mackintosh, C. (2004) Dynamic interactions between 14-3-3 proteins and phosphoproteins regulate diverse cellular processes, *Biochem J 381*, 329-342.
115. Noble, C. G., and Song, H. (2008) Structural studies of elongation and release factors, *Cell Mol Life Sci 65*, 1335-1346.
116. Nelson, D. L., and Cox, M. M., (Eds.) (2000) *Lehninger Principles of Biochemistry*, 3 ed., Worth Publishers, New York, New York.
117. Meskauskas, A., and Dinman, J. D. (2008) Ribosomal protein L3 functions as a 'rocker switch' to aid in coordinating of large subunit-associated functions in eukaryotes and Archaea, *Nucleic Acids Res 36*, 6175-6186.